Functional insights into *Plasmodium berghei* rhoptry associated protein- RON6 (*Pb*RON6)

Thesis submitted to University of Hyderabad for the award of

Doctor of Philosophy

In Department of Animal Biology



By Veeda Narahari 17LAPH07

Department of Animal Biology
School of Life Sciences
University of Hyderabad
Hyderabad - 500 046
India

2024



University of Hyderabad A central University by an act of Parliament Department of Animal Biology School of Life Science P.O. Central University, Gachibowli, Hyderabad-500046.



CERTIFICATE

This is to certify that the thesis entitled "Functional insights into *Plasmodium berghei* rhoptry associated protein- RON6 (*Pb*RON6)" submitted by Veeda Narahari bearing registration number 17LAPH07 in partial fulfilment of the requirements for award of Doctor of Philosophy in the School of Life sciences is bona fide work carried out by him under my supervision and guidance.

This thesis is free from plagiarism and has not been submitted previously in part or in full to this or any other University or Institute for award of any degree or diploma.

A. Published in the following journal:

1. Molecular Microbiology. 2022 Mar 8. doi: 10.1111/mmi.14894.

B. Presented in the following conferences:

- International Conference on Molecular Signaling (ICMS) & 9th Annual meeting of Society for Molecular Signaling (SMS). Organized by School of Life Science, UoH. From 1st to 3rd February 2024.
- 2. XVIII BioMalPar: biology and Pathology Organized by the European Molecular Biology Laboratory. Heidelberg, Germany. From 23rd to 25th May 2022.
- 3. SBC (Society of Biological Chemist). Jointly organized by Bose institute, CSIR-IICB, NIBMG and SNU. Kolkata. From 08th to 11th December 2022.

Further, the student has passed the following courses towards fulfillment of coursework requirement for Ph.D.

S. No.	Course code	Name of Course	Credits	Pass/Fail
1	AS801	Research Methodology/ Analytical Techniques	4	Pass
2	AS802	Research Ethics, Biosafety, Data Analysis and	3	Pass
		Biostatistics		
3	AS803	Scientific writing and Research proposal	5	Pass

Dr. KOTA ARUN KUMAR

upervisor

Professor
Department of Animal Biology
School of Life Sciences
University of Hyderabad
Ocentral University, Gachibowli

University of Hyderabad
P.O. Central University, Gachibowli,
Hyderabad-500 046. Telangana. INDIA

Head of Department

जंतु जीवका विभाग Department of Animal Biology Dean Dean

संकाय अध्यक्ष / Dean जीव विज्ञान संकाय / School of Life Sciences हैदराबाद विश्वविद्यालय / University of Hyderabad हैदराबाद / Hyderabad-500 046.



University of Hyderabad

Department of Animal Biology School of Life Sciences University of Hyderabad Hyderabad-500 046

DECLARATION

I hereby declare that the results of the study incorporated in the thesis entitled "Functional insights into *Plasmodium berghei* rhoptry associated protein- RON6 (*Pb*RON6)" has been carried out by me under the supervision of **Prof. Kota Arun Kumar** and this work has not been submitted for any degree or diploma of any other university earlier.

Date: 15/10/2024 Veeda Narahari 17LAPH07

SDG (good health and well-being)

The United Nations established the Sustainable Development Goals (SDGs) as a comprehensive framework to address various social, economic, and environmental issues on a global scale. The challenges against malaria are included in the third Sustainable Development Goal, which focusses on ensuring good health and well-being. The goal includes a specific target to eradicate the epidemics like AIDS, tuberculosis, malaria, and neglected tropical diseases by 2030. This objective embodies the worldwide effort to eradicate malaria as a significant public health concern.

In line with the above SDG the current thesis work focusses on identifying and validating novel pre-erythrocytic vaccine candidates. In the current work we demonstrate the role of *Plasmodium berghei* RON6 in maintaining parasite virulence and infectivity. Our studies show the possibility of targeting sporozoite expressed RON6 in neutralizing the parasite infectivity. This has implication for developing RON6 based sporozoite vaccine as a probable preventive therapy for curtailing malaria.

Acknowledgement

First and foremost, I am deeply grateful to my supervisor, **Prof. Kota Arun Kumar,** for his continuous support, insight, and patience. Without his constant encouragement, unique guidance, and precious suggestions, I could not have completed this thesis. I am indebted for his expertise, keen interest, and for giving me complete freedom to design and execute my doctoral work. I thank him for always pushing me a little bit further.

My sincere thanks to doctoral committee members Prof. Suresh Yenugu and Prof. Sharmista Banerjee for their critical comments and invaluable suggestions during the course of my Ph.D.

I thank Present and former Deans of SLS, Prof. Anand Kondapi, Prof. Siva Kumar, Prof. Dayananda Siddavattam, Prof. Ramaiah, Prof. M.N.V Prasad, Prof. Pallu Reddanna for providing central facilities at school of life sciences.

I thank present and former HOD's of Animal Biology Department, Prof. Kota Arun Kumar, Prof. Srinivasulu Kurukuti, Prof. Anita Jagota, and Prof. Jagan Pongubala for providing departmental facilities.

I thank all the faculty of School of Life Sciences, for their guidance and providing the research facilities in their labs and common facilities.

I thank all the non-teaching office staffs of Department of Animal Biology for their constant service and help.

I express my heartfelt thanks to my former lab seniors for their vast support and guidance. I thank them for teaching me all the tricks, techniques, and troubleshoots in the lab and sharing their knowledge with me regarding *Plasmodium* biology. I am particularly grateful to Dr. Surendra Kumar Kolli for his unwavering inspiration and extensive knowledge of molecular biology, cloning, and infection biology. The transfection vectors he designed for the lab have been a crucial part of our investigations, and we will always appreciate his efforts. I am deeply grateful to Dr. Maruthi Malaka for generously providing me with antibodies and sharing his expertise in conducting experiments with limited resources. His guidance and knowledge have been invaluable throughout my Ph.D. studies.

Special thanks to Dr. Sandeep Dey for his unwavering support and kindness throughout this journey, from late-night discussions to moments of doubt, his guidance and encouragement have been invaluable. I am also thankful to Dr. Dipti Singh for sharing scientific knowledge and friendly environment to work in.

I would like to express my deepest gratitude to Ms. Smita for her unwavering support during the course of my PhD. Her invaluable assistance in conducting experiments, as well as her dedication and expertise have greatly contributed to the progress of my work, and I am truly thankful for her constant support. Many thanks to Ms. Sneha for always being so supportive and helping during my stay in the lab.

A special thanks to all my juniors in the lab Ms. Anusha for her constant encouragement and kindness. I am grateful for all the times you've been there to lend a helping hand. Mr. Chandan for always being supportive and sharing his scientific knowledge. Ms. Bharati, Ms. Yamini, and Ms. Minal, your support and enthusiasm have made my PhD journey easy. I greatly appreciate your encouragement and the sense of community you've fostered. Thank you for being such amazing colleagues and adding a touch of coolness to our everyday work.

I extend my deepest gratitude to Dr. Pallabhi Mitra, DST Inspire Faculty, for her invaluable support and guidance throughout my Ph.D. I am especially thankful for the resources she provided, which were crucial for completing my LC/MS experiment. Her encouragement and feedback have greatly contributed to my research and the achievement of my research objective.

I thank to Dr. Anand Srivastava (Scientist-E) and Vijay from NIAB for their efforts in immuno-Electron microscopy.

I thank UGC for the financial support in the form of *JRF* and *SRF* fellowships. I thank to all the funding bodies, DST-SERB, CSIR, DBT, ICMR, UGC for funding the lab. I am thankful to DST-FIST, DBT-CREBB and UGC-SAP for funding Department of Animal Biology and School of Life Sciences.

I wish to express my deepest gratitude and admiration to my parents, who have sacrificed every comfort to provide me with a better life and have shown remarkable patience in allowing me to pursue the career of my choice. I am also immensely grateful to my brother Nagaraju, for his unwavering support of our family in my absence, and to my sister Bhavani for her unconditional love and encouragement.

Above the all, I owe my thanks to Almighty, for giving me patience to wade through the ebbs and tides of my research.

Narahari...

Dedicated to My Beloved Parents

For their endless love, support and encouragement

Table of contents

	Page No.
Abbreviations	i
Chapter I: Review of Literature	
1.1 Introduction	2
1.2 History of Malaria	2
1.3 Epidemiology of malaria	2
1.4 Overview of <i>Plasmodium</i> lifecycle	4
1.5 Details of the mammalians host's Plasmodium life cycle	5
1.5.1 Sporozoite motility inside the host dermis	5
1.5.2 Exo-erythrocytic stage development	7
1.5.3 Erythrocytic stage development	12
1.5.4 Sexual differentiation and Gametogenesis	15
1.5.5 Fertilization, development of ookinete and oocyst formation	17
1.5.6 Sporozoite egress and release into mosquito hemocoel	20
1.5.7 Sporozoite attachment and invasion of salivary gland	20
1.6 Clinical manifestation	22
1.7 Malaria control measures	23
1.8 Diagnosis	23
1.9 Treatment	24
1.10 Plasmodium berghei as a model organism	25
1.11 Ongoing challenges to malaria	26
1.12 Research objective	27

Chapter II. Functional characterization of *Plasmodium berghei* rhoptry associated protein- RON6 (*PBANKA_0311700*)

Anti-Plagiarism report	118
Publications	
References	103
2.4 Discussion	98
2.3 Results	61
2.2 Materials and methods	35
2.1 Introduction	28

Abbreviations

ACT Artemisinin combination therapy

AMA Apical membrane antigen

bp Base pairs

BSA Bovine serum albumin

CD Cluster of differentiation

CDPK Cyclin dependent protein kinase

cDNA Complementary DNA

CELTOS Cell traversal protein for ookinetes and sporozoites

CSP Circumsporozoite Protein

Ct Cycle threshold

DAPI 4', 6' diamidino-2 phenyl indole

DIC Differential interference contrast

DMEM Dulbecco's modified Eagle's medium

DMSO Dimethylsulfoxide

DNA Deoxy ribonucleic acid

dNTP Deoxyribonucleoside triphosphate

DOZI Development of zygote inhibited

EBL Erythrocyte binding like

ECP Egress cysteine protease

EDTA Ethylene diamine tetra acetic acid

EEF Exo-erythrocytic form

EMP Erythrocyte Membrane Protein

ETRAM Early transcribed membrane protein

EXP Exported protein

FBS Fetal bovine serum

FLP Flippase

FP Forward primer

FRT Flippase recognition target site

GAP Genetically attenuated parasite

GAPDH Glyceraldehyde 3-phosphate dehydrogenase

GPI Glycosylphosphatidylinositol

HA Hemagglutinin

HepG2 Hepatoma cell line

hDHFR Human Dihydrofolate reductase

HEPES 4-(2-hydroxyethyl)-1-piperazineethanesulfonic acid

HGF Hepatocyte growth factor

HSPG Heparin sulfate proteoglycan

IP immunoprecipitation

i.p. intraperitoneal

i.v. intravenous

IFN Interferon

IMC Inner membrane complex

iRBC Infected red blood cell

ITN Insecticide treated net

Kb Kilobase pairs

KO Knockout

LB broth Luria-Bertani broth

LC/MS liquid chromatography-mass spectrometry

LISP Liver specific protein

LS Liver stage

MCS Multiple cloning sites

MG Mid-gut

MJ Moving junction

mRNA messenger RNA

MSP Merozoite surface protein

MTIP Myosin tail interacting protein

ng nanogram

NIMA Never in mitosis Aspergillus

⁰C Degrees Celsius

OD Optical density

ORF Open reading frame

P. falciparum Plasmodium falciparum

P. knowlesi Plasmodium knowlesi

P. malariae Plasmodium malariae

P. ovale Plasmodium ovale

P. vivax Plasmodium vivax

Pb or P. berghei Plasmodium berghei

PBS Phosphate buffer saline

PEXEL Plasmodium export element

PhL-IP Photosensitized INA-labelled protein-interacting protein

PL Phospholipase

PTEX Plasmodium translocon of exported proteins

PV Parasitophorous vacuole

PVM Parasitophorous vacuolar membrane

RAMA Rhoptry-associated membrane antigen

RBC Red blood cell

RH Relative humidity

RNA Ribonucleic acid

rRNA ribosomal RNA

RON Rhoptry neck protein

RP Reverse primer

RPM Revolutions per minute

RPMI Roswel Park Memorial Institute medium

SAP Sporozoite asparagine rich protein

SAP Sporozoite asparagine rich protein

SBP Skeletal binding protein

SERA Serine repeat antigen

SG Salivary gland

SIAP Sporozoite invasion associated protein

SIMP Structural Integrity Maintenance Protein

SPECT Sporozoite protein essential for cell traversal

SUB Subtilisin like protease

TAE Tris acetate EDTA

TBS Tris buffer saline

TE Tris EDTA

TMHMM Transmembrane prediction using Hidden Markov Models

TRAP Thrombospondin related anonymous protein

TRSP Thrombospondin related sporozoite protein

UIS Up-regulated in infected salivary glands

UOS Upregulated in oocyst sporozoites

UTR Untranslated region

v/v Volume per volume

VTS Vacuolar translocation signal

w/v Weight per volume

WHO World health organization

WT Wild type

XA Xanthurinic acid

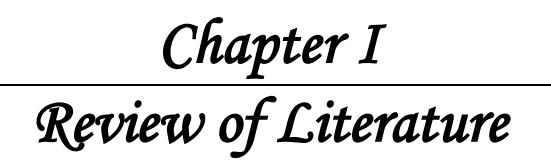
yFCU Cytosine deaminase-uracil phosphoribosyl transferase

μg Microgram(s)

μL Microliter(s)

μm Micrometer(s)

μM Micromolar(s)



1.1 Introduction

Malaria is mosquito borne infectious disease of humans and other animals. It is caused by protozoan parasite that belongs to *Plasmodium* genus. Malaria is a major threat to the health and welfare of the world's population. It is mostly found in regions within the tropical or subtropical climates[1]. It has been reported that children and expectant mothers are the most vulnerable to malaria infections. The disease causes substantial loss, with several million fatalities reported annually[2].

1.2 History of Malaria

Malaria is an age-old disease, and evidence of its presence was recorded in Chinese documents around 2700 BC, and in ancient Egypt medical texts around 1500 BC. Furthermore, descriptions of the malaria disease date back to the 6th century BC in ancient Hindu scripture Hippocrates described malaria as an intermittent fever in the 4th century BC. In 1885, Marchiafava and Celli introduced the genus *Plasmodium*. In 1880, Charles Alphonse Laveran, a surgeon in the French Army, discovered the specific organism responsible for causing malaria, which has been identified from patient blood who was suffering from the disease, and he reported it as *Oscillaria malariae*. In 1897, Sir Ronald Ross, a British medical practitioner, conclusively proved that mosquitoes serve as carriers for spreading malaria [3]. In 1902 and 1907, respectively, Sir Ronald Ross and Charles Louis Alphonse Laveran received Nobel prizes for their contributions to the discovery of *Plasmodium* life cycle stages. [4]. The word malaria is derived from the Italian mal'aria, which means "bad air." During the Middle Ages, it is believed that swamps and marshy land spread malaria. In Greek, malaria means "the disease of the wetland." Horace Walpole introduced the word malaria to England. However, the first English scientific publication used the word "malaria" in 1827 [5].

1.3 Epidemiology

Historically, malaria is one of the oldest and most lethal infectious diseases, and it remains a major threat to global health. The complex nature of malaria focuses on several factors, such as geographical region, socioeconomic status, environmental condition and health care infrastructure. The World health organization (WHO) estimated nearly 249 million cases were recorded in 2022 from 85 malaria endemic countries and approximately 11.7 million fatalities were recorded globally. Nearly 5 million cases were increased in 2021 as compared between 2000 to 2014. Most of the

increased cases over past five years were recorded in African regions. Recently, in October 2023 WHO recommended R21/Matrix-M (R21) as second malaria vaccine after RTS,S/AS01 vaccine, to prevent malaria in children living in endemic area [6].

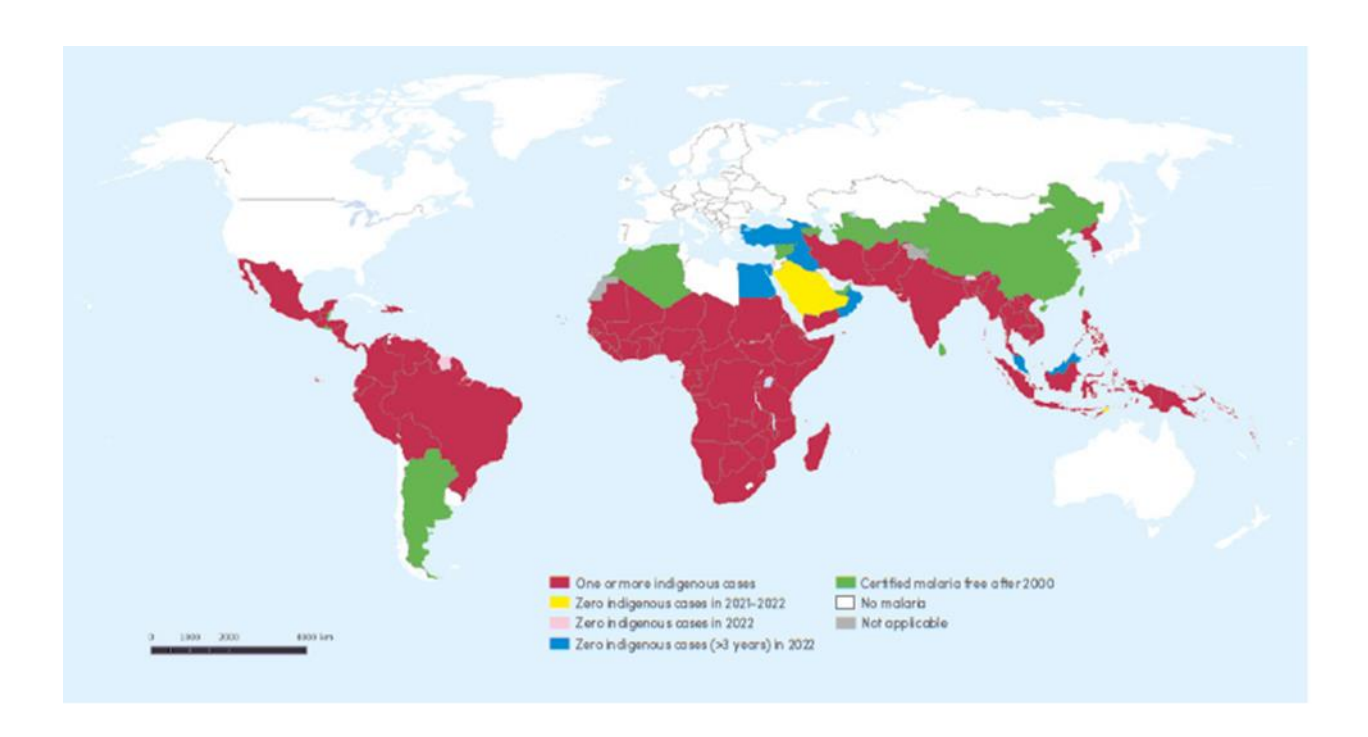


Fig 1: Global distribution and indigenous malaria cases in 2000 as well as their status by 2022. The several countries in the Africa, North Latin America, Mexico, South Asian countries and Middle East countries (dark red), have more malaria cases. China, Argentina and Algeria (green) were recognized as malaria free countries in 2000. Zero malaria cases were reported in South Asian countries and Egypt (Blue) in the year 2022. Few countries currently report being malaria-free, but if proper control measures are not implemented, there could be a chance of reintroduction (WHO 2023).

Plasmodium is a protozoan parasite that belongs to the phylum Apicomplexa. The human population is affected by a quintet of distinct Plasmodium species, namely Plasmodium falciparum, Plasmodium malariae, Plasmodium vivax, Plasmodium knowlesi, and Plasmodium ovale. Plasmodium falciparum has been identified as the most formidable and lethal pathogen among all Plasmodium species and responsible for the vast majority of fatalities associated with malaria. P. vivax is the second common etiological species responsible for malaria. Unlike P. falciparum, it has distinctive ability to produce hypnozoites, which are latent liver stages that can induce malaria relapse after months or even years following primary infection. It is difficult to effectively control and eliminate

malaria due to the presence of this distinctive feature. The geographical distribution of *P. vivax* includes Asia, Latin America, Middle East Asia, and many countries in Africa [7].

1.4 Overview of *Plasmodium* Life cycle

The *Plasmodium* life cycle is complex and digenetic, requiring two hosts to complete the life cycle. The definitive host is a female Anopheles mosquito and mammals serve as intermediate host [8]. The life cycle begins following inoculation of the sporozoites into host dermis, when the female mosquitoes are taking a blood meal. The sporozoites migrate actively in the dermis and travel via circulation and subsequently invade the liver hepatocytes. The liver stage development is clinically silent. To establish successful infection sporozoites must cross multiple cellular barriers including, the dermal layer of skin cells, endothelial cells lining of blood vessels, sinusoidal lumen, Kupffer cells, and several hepatocytes. Inside the hepatocytes sporozoites develop into Exo-erythrocytic forms (EEFs) and eventually form thousands of hepatic merozoites [9]. Upon rupture of infected hepatocytes, the hepatic merozoites are released into blood circulation, where they invade RBC and initiate blood-stage infection. With in RBC, the parasites transform into distinct stages, viz., the ring stage, an actively feeding trophozoite stage and a multi nucleated schizonts with 16-32 merozoites. The schizonts rupture and release daughter merozoites into blood circulation, where some merozoites invade new RBC and continue asexual propagation, while others differentiate into male and female gametocytes [10]. The mature gametocytes were ingested by female *Anopheles* mosquito. Inside the mid-gut xanthurenic acid, low pH and low temperature collectively triggers the emergence of female and male gametes from respective gametocytes. After fertilization, a zygote is formed that further transforms into a motile ookinete. The invasive form of ookinetes breaches mid-gut epithelium and differentiates into oocyst towards the hemocoel side. Sporulation occurs inside the oocyst, and subsequent egress releases these forms into the hemocoel, which migrate and colonize the salivary gland. Sporozoites undergo a sequential invasion, allowing them to migrate from the salivary gland basal lamina to ducts, where they reside until the mosquito takes the next blood meal to transmit sporozoites to a new mammalian host, thus continuing the parasite life cycle [11].

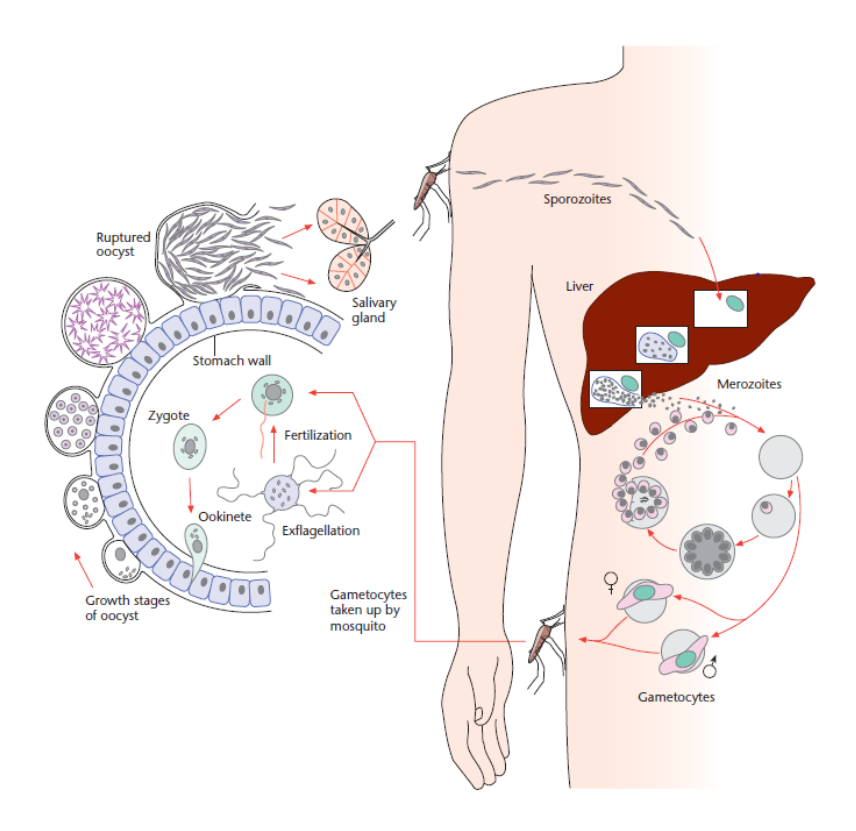


Fig 2: The *Plasmodium* life cycle begins after delivering the sporozoites into vertebrate host. These Sporozoites actively glide through the host dermal cells to find the blood vessels. Through the circulation, they reach the liver and infect hepatocytes. Inside the hepatocytes, sporozoites transform into EEFs (Exo-erythrocytic forms) and upon maturation release hepatic merozoites that infect RBC. Within RBC, the parasites transform into rings, trophozoites, multinucleated schizonts and gametocytes- the terminal stages of *Plasmodium* in mammalian host. Upon ingestion by mosquitoes, the gametocytes produce gametes that undergo fertilization and produce zygote and motile ookinete that migrate through the mid-gut epithelium and reside on the basal lamina of the midgut epithelium. Here they transform into oocyst and sporulation within oocyst produces thousands of sporozoites which eventually egress into hemocoel and colonize the salivary gland lobes. The salivary gland sporozoites freshly infect new host during blood feed [12].

1.5 Detail of the mammalian host's *Plasmodium* life cycle

1.5.1 Sporozoite motility inside the host dermis

During the blood-meal, an infected female *Anopheles* mosquito inject saliva containing sporozoites, vasodilators and anti-coagulants into the dermis [13]. A successful inoculum does not always result in an infection because epidermal fibroblasts, leukocytes, and capillary endothelial cells act as physical and cellular barriers, limiting the successful transit of sporozoites into the circulation and therefore to the liver [14]. To migrate away from the inoculation site, the sporozoite relies on a substrate-dependent motility called "gliding motility" [15]. Motile sporozoites in the dermis exhibit

a mean gliding velocity of 1-2 μ m/s, significantly higher than the 0.1 μ m/s observed in salivary ducts [9]. The sporozoites migrate through the dermis until they a reach blood vessel and penetrate into the circulatory system, which enable them to swiftly arrive in hepatocytes [9, 16]. Another alternative journey of sporozoites to reach liver is through lymphatic system, likely transported inside the leukocytes, which are reported to be more infectious than delivered by intravenous inoculation. An intravital microscopy observations revealed that, the *P. berghei* sporozoites inoculated into avascular dermis tissue actively migrate by using gliding motility and reach dermal vessel which takes approximately 30 minutes [17].

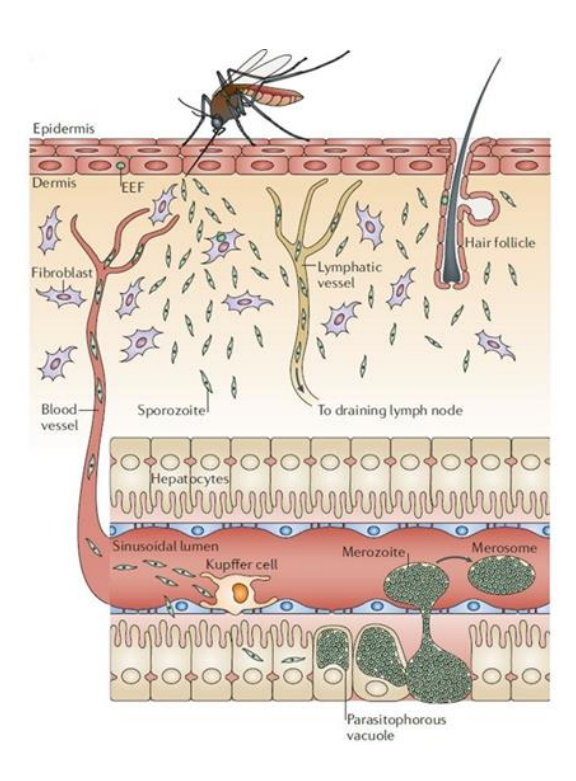


Fig 3: The journey of sporozoites from the inoculation site to the liver. A female *Anopheles* mosquito injects motile sporozoites into the host skin during the blood meal. These sporozoites migrate away from the inoculation site and enter a blood or lymphatic vessel. Lymphatic vessels may transport sporozoites to the proximal lymph node, where they can penetrate host cells. Sporozoites, which are released into the bloodstream from the inoculation site, directly reach to the liver. The sporozoites actively glide in sinusoids which are lined by endothelial and Kupffer cells. The sporozoites enter through the Kupffer cells prior to invading hepatocytes. The invasion into hepatocytes leads to the parasitophorous vacuole formation, the sporozoites develop into EEF, and upon complete maturation produce hepatic merozoites [18].

The penetration of the biological barriers by *Plasmodium* parasites is propelled by the gliding motility [19]. The intravital microscopy observations demonstrated that sporozoites actively migrate through skin cells towards dermal blood vessels, which is facilitated by actomyosin motor complex located under the parasite plasma membrane [16]. Sporozoite surface and transmembrane proteins are the core components of the parasite cellular machinery, function as critical mediators between actin-myosin motor complex and extracellular environment. TRAP (thrombospondin related anonymous protein), is one of the sporozoite surface protein, that is essential for motility and enabling sporozoites to cross several cellular barriers. Notably, TRAP displays functional efficiency over the whole trajectory of the parasite, from the oocyst stage to the mammalian liver [20]. The circumsporozoite protein (CSP) is another prominent surface protein which is required for the sporozoite motility, while TRAP servers as a major motor protein [20, 21]. In addition, SPECT (sporozoite microneme protein essential for cell traversal), perforin-like protein 1 (PLP1), cell traversal protein for ookinetes and sporozoites (CelTOS), TRAP-like protein (TLP) is also involved in sporozoite cell traversal and initiate liver stage infection. However, the deletion of both SPECT1 and SPECT2 genes resulted in a developmental arrest in the liver stage, and delayed prepatancy [22-24]. The phospholipase (PbPL) is also a surface protein, wwhich required for the breaching host cell membrane while migrating in the skin. The deletion of PbPL resulted in a phenotype where the sporozoites were impaired in crossing epithelial cell monolayers and a significant reduction in transmission after mosquito bite [25].

1.5.2 Exo-erythrocytic stage development

Sporozoites display remarkable motility and cell traversal activity prior to hepatocyte invasion. The motility of sporozoites through the bloodstream from a dermal capillary to the hepatic sinusoids, and breaching of the endothelial barriers to invade the liver parenchyma, ensure successful establishment of infection. During and post-invasion, sporozoites release the contents of micronemes and rhoptries, a specialised organelles housing proteins that mediate host-parasite interactions [26, 27].

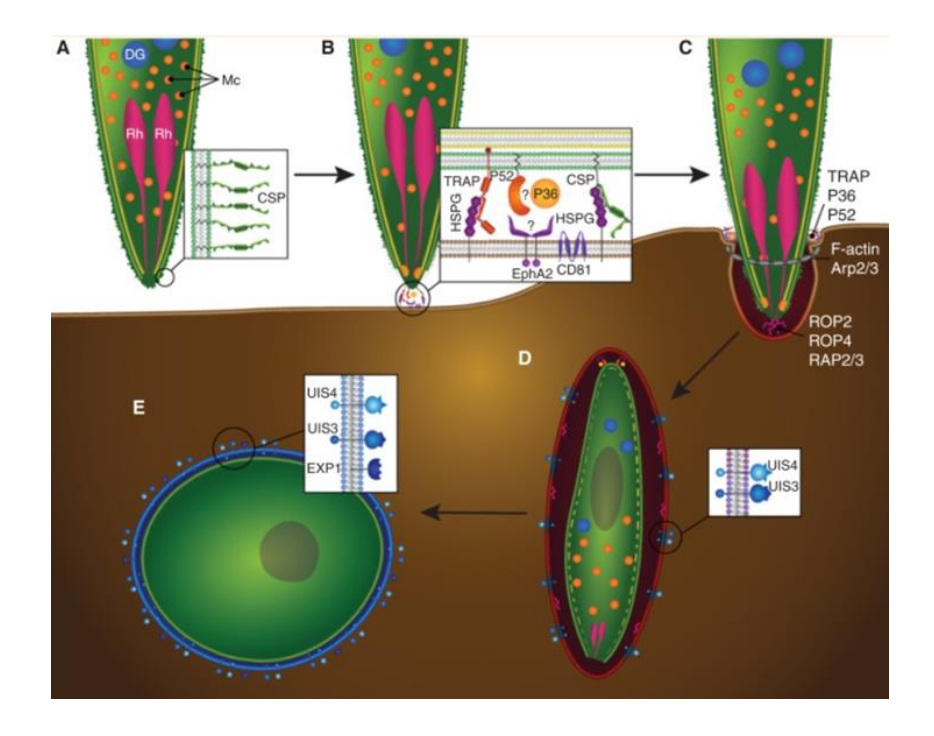


Fig 4: The diagrammatic representation of the sequential stages of sporozoite invasion of hepatocytes. **(A)** The outer surface of sporozoite is covered by circumsporozoite protein (CSP), that interacts with HSPGs (heparin sulfate proteoglycans) of host hepatocytes. The sporozoite apical end comprises rhoptry, micronemes, and dense granules. **(B, C)** Upon activation of CSP, it causes the release of TRAP, which binds to the HSPG of hepatocytes. P52 and P36 are the two microneme proteins, that interact with the hepatocyte receptor Ephrin A2. The P36/P52/Ephrin A2 axis is essential for the parasitophorous vacuole (PV) formation. **(D)** The parasite induces significant modifications in Parasitophorous Vacuole Membrane (PVM), resulting in the release and trafficking of putative dense granule proteins UIS3 and UIS4, as well as EXP-1, towards the PVM. **(E)** The liver stage trophozoite is found to be localised within a parasitophorous vacuole (PV), exhibiting its distinct parasite plasma membrane that remains coated by circumsporozoite protein indicated a green hue. This trophozoite is further enveloped into a parasitophorous vacuole membrane (PVM), depicted in blue [27].

CSP is a prominent surface protein found on sporozoites, which is crucial for facilitating the interaction between the sporozoites and the host cell during their migration to the liver and subsequent infection of hepatocytes. The CSP contains a species-specific central repeat region, and flanked by a conserved amino-terminal region I and a carboxy-terminal motif referred to as the type I thrombospondin repeat (TSR). The carboxy terminal motif is essential for the hepatocyte adhesion, is masked by the amino-terminal region I until the sporozoite reaches the liver, where cleavage uncovers the TSR, allowing for hepatocyte invasion [28]. The TRAP protein is classified as a type I transmembrane protein, sharing similarities with the CSP protein. TRAP contain a TSR domain, similar to CSP, and additionally harbors an integrin-like domain. The crucial event involves the binding of the carboxy terminal domain of TRAP to the actin-myosin motor located on the sporozoite

surface. Additionally, the extracellular domain of TRAP also binds to heparan sulfate proteoglycans. These interactions play a significant role in the invasion process and contribute to the successful establishment of the parasite within the host [29]. The 6-cys domain proteins such as P52, P36 and TRAP have been identified as vital components of micronemes, and they are known to possess significant importance in the complex cellular machinery [27]. The process of hepatocyte invasion is contingent upon a limited number of well-documented parasite proteins, which interact with host receptors situated on the surface of hepatocytes. P36 and P52 protein complexes facilitated the successful invasion of the sporozoites into hepatocytes. The depletion of P36 and P52 proteins in P. falciparum proved parasites could not develop after invading hepatocytes [30]. The recent investigation revealed that, the hepatocyte receptor known as Ephrin A2 (EphA2) interacts with these protein complex. The transmembrane EphA2 belongs to the Eph receptor tyrosine kinase family and is expressed on the surface of hepatocytes. EphA2 is crucial for both rodent and human malaria sporozoites to invade hepatocytes and subsequently form the parasitophorous vacuole (PVM). Antibodies against EphA2 prevent sporozoite infection. Interestingly, EphrinA1, the natural ligand of EphA2, shares structural similarities with the 6-cys fold protein family. Moreover, strong evidence suggests a direct interaction between EphA2 and the parasite protein P36, establishing the first known host receptor-parasite ligand pair essential for hepatocyte infection [31]. Other hepatocyte surface protein known as CD81 (a tetraspanin membrane protein) is required for the invasion and PVM formation in *P. falciparum* and *P yellii*, but its role in *P. berghei* seemed dispensable. Although the antibodies against CD81 inhibit P. yoelii and P. falciparum sporozoite infection in vitro and CD81deficient mice are resistant to P. yoelii infection, a sporozoite ligand for CD81 remains unidentified. Cholesterol-dependent formation of CD81 rich microdomains on hepatocyte surface is crucial for sporozoite infection, suggesting that microdomain organization, rather than direct CD81 interaction, facilitates successful hepatocyte invasion [32, 33]. Scavenger receptor BI (SR-BI), a hepatocyte membrane receptor, is involved in the specific absorption of cholesteryl esters from low-density and high-density lipoproteins. This receptor has an indirect role in hepatocyte infection. The SR-BI depletion leads to reduced CD81 expression on the surface of hepatocytes [34].

UIS3 and UIS4, associated with the parasitophorous vacuole membrane in the liver stage, are encoded by up-regulated in sporozoites (UIS) genes. The transcriptional activity of these genes is significantly up-regulated in salivary gland sporozoites. UIS3 and UIS4 have been identified as crucial

for the initial stages of liver stage development. Early liver-stage developmental arrest is observed upon deleting either the UIS3 or UIS4 genes [35]. The carboxyl terminal of UIS3 and UIS4 are orientated towards the cytoplasmic region of hepatocytes and amino-terminal towards the PV, suggesting that these proteins play a crucial role in the interactions between the parasite and hepatocytes. UIS3 directly interacts with liver fatty acid protein (L-FABP) [36]. Membrane associated ATP-binding cassette or ABC transporters facilitate lipid transfer between host and parasite. ABCC2 is also a transporter known as MRP2, is found in both P. berghei and P. falciparum liver stages. The deletion of ABCC2 in both parasites impaired liver-stage development [37]. Few proteins exports into the host cytosol during liver stage development. The export proteins contain a characteristic motif called PEXEL/HTS (Plasmodium export element/host targeting signal), which is a pentameric amino acid sequence consisting of RxLxE/Q/D [38, 39]. The PEXEL motif is found in both membrane-bound and soluble proteins. Plasmepsin V, an enzyme belonging to the aspartyl protease family, cleaves the PEXEL motif at the conserved leucin residues (RxL \downarrow xE/D/Q) towards c-terminal region [40, 41]. After the cleavage, the protein undergoes N-acetylation. PTEX (Plasmodium Translocon of Exported Proteins) is crucial for transportation of malarial effector proteins across PVM. The core complex of PTEX consists of EXP2, PTEX150, and HSP101 [42]. These proteins are translocated into the cytoplasm through PETEX after unfolding within the PV. following which, they are refolded by cytosolic HSPs. Some of the proteins do not contain a PEXEL motif, those exported by an PEXEL independent export system [43]. CSP was the first protein to be identified within infected hepatocyte containing two PEXEL motifs [44]. Apart from the CSP, few other exported proteins have been characterized, such as IBIS1, a transmembrane protein exported into the host during liver stage and blood stage, a tryptophan enriched protein- SLTRiP exported early in liver stage infection, and LISP2 [45, 46]. During the late liver stage development, LISP1 and LISP2 proteins expression was shown to be associated with parasitophorous vacuole membrane (PVM). The LISP1 is essential for the breakdown of PVM, followed by subsequent release of merozoites, whereas LISP2 contains modified 6-cys domain, transported to the host cell cytoplasm. The deletion of LISP2 impairs merozoite formation [47].

Once the sporozoite successfully invades the hepatocytes, it differentiates into liver trophozoites [35], and few organelles like ER, apicoplast and mitochondria are retained during this process, while there is a breakdown of cellular and molecular components associated with motility [48]. During

schizogony, the parasite's DNA undergoes a multiplication for 104-105 times, coupled with the replication of cell organelles, followed by cytokinesis resulting in the formation of daughter merozoites [49]. The formation of individual exoerythrocytic merozoites occurs when the plasma membrane of the parasite expands and folds inward to make a structure called cytomeres. The process of synchronised division of both the nucleus and organelles ensures that the emerging merozoites are evenly divided [38]. The merozoites are released into the host cytosol by rupturing parasitophorous vacuole membrane. The breakdown of parasitophorous vacuole membrane is facilitated by Plasmodium derived cysteine proteases, such as SERA (Serine repeat antigen) are known as cystine proteases. These proteases conserved among the *Plasmodium* species and play a crucial role during the merozoite egress from erythrocytes as well as release of sporozoites from the midgut oocyst [50]. SERA1 and 2 are the part of SERA protein family which are upregulated in late liver stage development, and the deletion of these two proteins does not show any significant delay in parasite life cycle. Nonetheless, in these mutants, the SERA3 was shown to be upregulated during late liver stage development indicating that these protein family may functionally replace with other proteins [51]. Another protease known as subtilisin-like protease (SUB1) is also a conserved serine protease found in *Plasmodium*, which is crucial for the release of merozoites in the liver stage and blood stage [52, 53]. The increased levels of calcium inside the cell [52], and the activation of cGMPdependent protein kinase (PKG) [54, 55], stimulate the release of SUB1 into PV from exonemes. SUB1 protease cleaves and triggers the activation of SERA proteases, as SERA serves as substrates for SUB1, which leads to the activation of series of proteases that are essential for the egress process [56, 57].

After the PVM breakdown, several merozoites are packaged in a membranous structure derived from the host cell. This structure referred to as merosomes, is eventually extruded into the liver sinusoid [49, 58]. The merosome membrane is crucial for evading the immune response of host cells such as liver phagocytic cells known as Kupffer cells, found in the found in the liver sinusoid. These hepatic merozome extrude into liver blood stream where merozome membrane will rupture and release hepatic merozoites. The released merozoites can infect RBC and proceed for further erythrocytic cycle [49].

1.5.3 Erythrocytic stage development

The Exo-erythrocytic stages of malaria are metabolically active but asymptomatic. Merozoites proliferate and invade RBC during the subsequent erythrocytic cycle, which results in the appearance of disease symptoms. Upon the rupture of merosomes, approximately ten thousand to thirty thousand merozoites were released into the blood circulation, thereby initiates infection cycle [59]. Merozoites are small, elliptical parasites measuring approximately 1-2 µm in length and width [60]. Their apical end is distinguished by a prominent protrusion housing polar rings and essential secretory organelles such as micronemes, rhoptries, and dense granules. Merozoite surface is coated with GPI (glycosylphosphatidylinositol) anchored proteins [61].

The merozoite invasion follows a sequential pattern. The interaction between host RBC and merozoite initially its weak and reversible binding, followed by a stronger interaction that causes the RBC to change shape and wrap around the merozoite [62]. MSP1 is a predominant glycophosphatidylinositol (GPI)-anchored protein on the surface of merozoites and acts as a structural scaffold for protein complexes. The initial merozoite binding to the RBC is facilitated by MSP1, which interact with band3 on RBC membrane [63], and subsequent reorientation of merozoite is facilitated by AMA1 towards RBC [64]. The merozoite surface proteins and actomyosin motor complex is crucial for the completion of merozoite invasion [62]. Inhibitors against actomyosin motor complex prevents the merozoite invasion [65]. The merozoites are equipped with adhesins, that are released during the merozoite invasion and daughter cell formation [60]. The affinity between the parasite ligands and host receptors is facilitated by the formation of tight-Junction [66]. The tight junction formation is majorly regulated by Duffy binding proteins also known as EBL (erythrocyte binding proteins) [67]. In addition, the reticulocyte proteins (Rhs) are require for the merozoite invasion, particularly *Pf*Rh5, that facilitates the attachment of the merozoite to the RBC through its interaction with the basigin protein receptor [68].

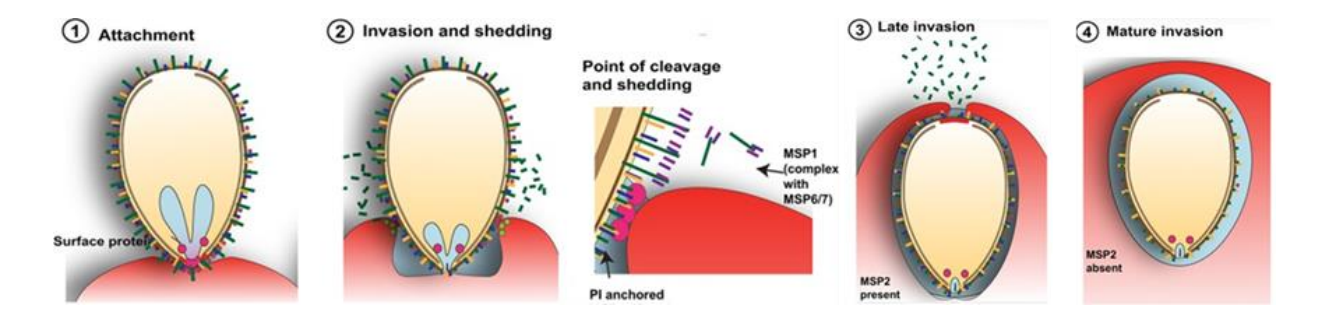


Fig 5: The merozoite invasion involves a sequential and coordinated cleavage of surface proteins. The merozoite surface coat comprises a multitude of proteins. During the process of invasion, it has been observed that a subset of merozoite proteins undergo cleavage and subsequent shedding, although not all proteins exhibit this behavior. (1) MSP1 is the major surface protein, which is ubiquitously present within a multi-component framework alongside other antigens (shown in green and purple). The color blue denotes the protein MSP2, whereas the color yellow denotes the protein MSP4. The proteins AMA1 and the tight junction are visually depicted as pink circular entities in the present illustration. (2) Shedding of proteins involves a significant portion of the MSP1 complex, wherein MSP1-19 is moved into the RBC along with MSP3. The proteins MSP2 and MSP4 exhibit distinct behavior about their cleavage and shedding processes, deviating from the anticipated mechanism occurring at the tight junction. Rather than being cleaved and shed at the tight junction, these proteins are transported into the RBC compartment. The process of shedding persists as the merozoite successfully infiltrates the RBC (3). During the transition from late invasion to mature invasion, it has been observed that the MSP2 protein undergoes loss. On the other hand, the MSP4 and MSP1-19 proteins stay in place during the early stages of intra-erythrocytic development [69].

Following a successful invasion, the merozoites proceed to form a parasitophorous vacuole. Nutrient acquisition such as purines, lipids, and proteins, from host blood plasma is facilitated by a tubulovesicular network (TVN), that connects parasiitophorous vacuole membrane to erythrocyte membrane [70]. Similar to Exo-erythrocytic stages, the *Plasmodium* parasites transport several proteins into the cytosol of the host organism, which is mediated by a specific export motif PEXEL or vacuolar translocation signal (VTS), and this motif is involved in protein trafficking, suggesting its potential role in sustaining the virulence and survival of the parasite [71]. Several proteins do not contain PEXEL motifs, that referred PEXEL-negative exported proteins (PNEPs). Examples of PNEPs include skeletal binding protein (SBP1), *P. falciparum* erythrocyte membrane protein 1 (*Pf*EMP1), and Exported Proteins 1 and 2 (REX1 and 2) [72]. The var genes are crucial for antigenic variation and critical for evading immune response in the host. Family of *Pf*EMP1 encoding of nearly 60 var genes. The two var genes viz., STEVOR and RIFIN have been investigated in greater detail due to their remarkable ability to exhibit antigenic variation within the parasite [73], in addition to their expression on gametocyte surface. Due to shift in gene expression of these two genes, parasite will

evade the host immune response [74]. In addition, the PfEMP1 also involving in the cytoadherence regulation in *P. falciparum* infected RBCs, facilitating the sequestration of iRBCs in brain capillaries and placental tissues [75]. Within the confines of the erythrocyte, the *Plasmodium* parasite undergoes significant structural transformations, resulting in the formation of a vacuole that envelops a membrane delimited cytoplasm containing a nucleus and many internal organelles. During the subsequent phase, the organism undergoes transition into a metabolically active trophozoite stage [76]. During the blood stage development, the parasite effectively utilizes hemoglobin as a primary nutrient source, simultaneously generate heme as a by-product. Notably, heme is a toxic substance, that significantly impairs the parasite survival. The parasite converts the heme into hemozoin, which is devoid of toxicity and is stored inside the food vacuole [77]. A wide range of anti-malarial drugs including chloroquine and mefloquine identified as effective drugs that inhibit the enzymes that are involved in the conversion of heme into hemozoin [78]. The trophozoite undergo erythrocytic schizogony, in which several rounds of nuclear division results in the formation of 16-32 multi nucleated schizonts. The subsequent generation of individual merozoites is facilitated by the distinctive cytokinesis known as segmentation, leading to the formation individual merozoites [79]. The mechanism of merozoite egress form the infected RBC is facilitated by SERA proteases and SERA5 and SERA6, that play a crucial role during blood stage propagation [80, 81]. The *Plasmodium* SUB2 is crucial for the merozoite egress from infected RBC, as well in merozoite surface proteins shedding [82]. The segmented schizont undergoes a dramatic transformation before egress, from an asymmetrical structure form with the merozoites scattered around to one in which they are organized symmetrically around the vacuole at its center. The PV will enlarge, and the host cell appears to shrink during this phase, known as "flower formation" or "rounding up." [83]. Upon release into the bloodstream, merozoites proceed to infect fresh RBCs, thereby sustaining their life cycle. However, it is significant that a subset of these merozoites undergo a distinct development and ultimately giving rise to sexual forms known as gametocytes. These gametocytes exhibit differentiation into female and male parallels, thereby facilitating the sexual reproduction phase in parasite [84].

1.5.4 Sexual differentiation and Gametogenesis

The blood stage parasites undergo sexual differentiation to generate gametocytes, that are precursor cells for gamete production. In each asexual cycle, approximately 5-25% of blood-stage parasites become gametocytes.

The mechanism behind gametocytogenesis in Plasmodium biology remains poorly understood. The sexual commitment of a merozoite occurs prior to schizogony. The *P. falciparum* genes reported as genes implicated in gametocytogenesis (Pfgig), which reduced the gametocyte production upon silencing and restore the gametocyte specific genes upregulation after the complementation [85]. AP2-G is a member of the ApiAP2 that belong DNA-binding protein family, has been identified as a key regulator of gametogenesis in P. berghei, P. falciparum, and P. yoelii. AP2-G is normally required for gametogenesis and depleting its expression leads sustained arrest in asexual stages. In P. falciparum, AP2-G expression is regulated by epigenetic modification, particularly H3K9me3 mediated silencing. Recent studies have shown that this silencing is regulated by HP1 (heterochromatin protein 1) and Hda2 (histone deacetylase 2) across the *Plasmodium* species. The depletion of ap2-g leads to impair in the formation of gametocytogenesis. As a result, several transcripts were down regulated in early gametocytes [86, 87]. AP2-G specifically binds to the GTAC motif in DNA found upstream of various genes specific to gametocytes, including pfs16, pfg27, pfg14.774, etc., and established through gel shift assays. The presence of the GTAC motif in the promoter region that found to drive the expression of the reporter, providing further confirmation of the AP2-G specific DNA motif. However, when the motif was mutated, the expression was blocked [86, 88]. Plasmodium protein specific for gametocyte development 1 (GDV1) played a crucial role in facilitating the enhancement of gametocyte production. The interaction between GDV1 and HP1 critical for the activation of ap2-g. The deletion of both GDV1 and ap2-g reduced gametocyte formation, resulting in a reduction in gametocytogenesis [89]. The inner membrane complex (IMC) has a significant role in the transformation of gametocytes. GAP40 and GAP45 are the proteins of the IMC that are interacting with the spectrin-ankyrin network of RBC [90]. The expression of multigene STEVOR is significantly upregulated and involved in stabilizing the membrane during gametocyte elongation [91]. The translational regulators of P. berghei, such as DOZI (development of zygote inhibited) and CITH (CAR-I and fly trailer hitch), were found to be in a suppressed state in female gametocytes, which are essential for the fertilization of gametocytes in the mosquito midgut [92].

Gametocytes have a vital role in the *Plasmodium* life cycle since they are crucial to its transmission to mosquitoes and eventual infection of vertebrate hosts. Investigating gametocyte biology is crucial to blocking the malaria transmission to mosquitoes, ultimately eradicating the disease. The antimalarial drugs such as chloroquine and ACT (Artimisinin-based combination therapy) do not effectively target mature gametocytes, and primaquine clinically approved antimalarial drug has gametocidal activity against *Plasmodium*, including *Plasmodium falciparum* [93].

The malaria infection depends on the developmental stages of the parasites within the mosquito midgut, which commences upon the activation of the intra-erythrocytic gametocytes shortly after ingestion, resulting in the traversal of the mid-gut epithelium by the invasive ookinetes within a time frame of less than 24 hours [94]. The gametocyte development in *P. falciparum* requires approximately ten days. During this period, the gametocytes undergo a series of five distinct morphological stages, represented as stages I to V [95]. After transforming the mature gametocytes into mosquito midgut undergo a series of events inside the midgut in response to environmental stimuli. The formation of gamete is facilitated by low pH, reduced temperature and xanthurenic acid (XA) a byproduct of tryptophan catabolism in the mosquito [96-98]. Calcium-dependent signaling regulates several functions in the Plasmodium, the increased intracellular Ca2+ activates the phospholipase C and guanylyl cyclase, which is responsible for the formation of second messenger cGMP leads to the synchronized development of gametocytes in P. berghei was observed [99]. The impairment of gametogenesis was observed in *P falciparum* upon deletion of $GC\alpha$ (guanylyl cyclase) and ookinete motility was impaired [100]. CDPK4 (calcium dependent protein kinase-4) in P. berghei is required for the increasing intracellular calcium, which also activates XA [101]. The P48/45 proteins belong to a highly conserved 6-cys protein family. These proteins have been recognized as markers for male gametocytes. The absence of these genes has been reported to cause a significant decrease in the ability of male gametocytes to fertilize [102]. P47 is a paralogous protein of P48/45, expressed in female gametocytes. The depletion of the P47 gene impairs female gametogenesis [100]. The product of male development gene-1 (MDV1) is identified in osmiophilic bodies of mature male and female gametes, which is crucial for egress from host RBC [103]. MARK2 is a multifunctional protein kinase that is crucial for the development of male gametes in *Plasmodium berghei* [104]. Inside the mosquito midgut, the female gametocyte transform into macrogamete and are released from the RBC, that eventually fuse with male gamete. Actin II, pf16, hap2/gcs1 proteins are expressed

in male gametocytes which are essential for the motility and fertilization [105]. The Actin II is specific to male gamete and the deletion of Actin II leads to the impaired exflagellation in male gamete was observed [106].

1.5.5 Fertilization, development of ookinete and oocyst formation

Fertilization involves the fusion of the plasma membranes of the male and female gametes. The precise identification of the proteins responsible for the initial binding of male and female gametes remains elusive. However, the fusion of gametes is facilitated by a protein known as GCS1 (generative cell-specific 1), referred to as HAP2. Deletion of the corresponding gene in *P. berghei* resulting in the sterility in male, which led to the impairment of fertilization [107]. After the fertilization the gametes convert into zygote, which is the diploid stage throughout the life cycle of *Plasmodium*. The diploid stage zygote converts into tetraploid after the meiosis [108]. Few proteins related to Never in meiosis Aspergillus such as NEK-2 and NEK-4 are crucial for the zygote development and ookinete conversion [109, 110]. The zygote transforms into a motile ookinete approximately 18 to 22 hours after the fusion of gametes. The initially spherical zygote transforms into a banana- shaped structure. Two crucial acetylated IMC proteins, ISP I and III, play a significant role in connecting the subpellicular microtubule (SPM) and IMC, hence contributing to the maintenance of the pellicular structure as a whole, and the absence of both proteins resulted in a reduced rate of ookinete formation from the zygote [96, 111]. Notably, the absence of these proteins correlates with a decreased ookinete formation rate. The glideosome is stabilized and propelled forward by its attachment to IMC. The parasite secretes chitinase, which breaks down the peritrophic matrix in the mosquito's midgut, allowing the ookinete to breach through the epithelium [112].

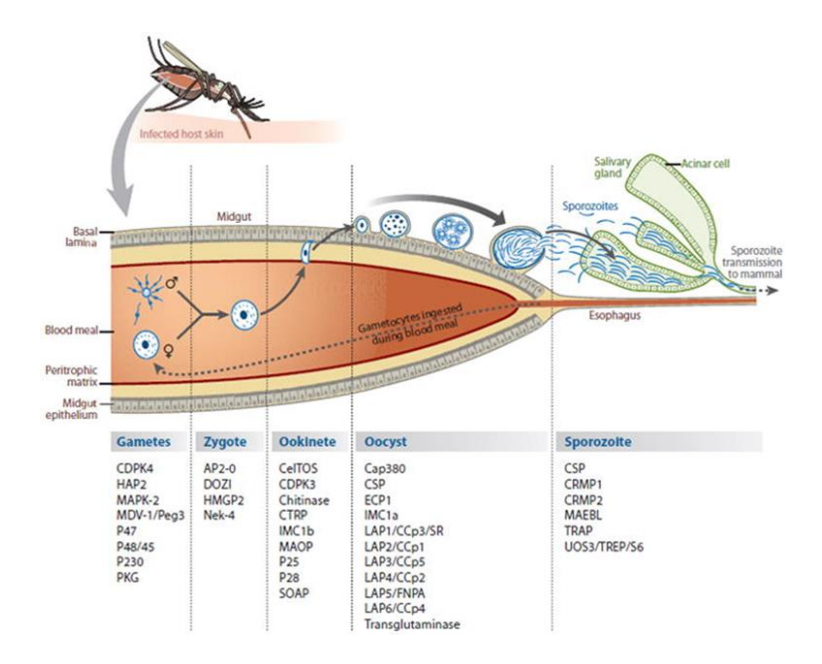


Fig 6: The female *Anopheles* mosquito ingest gametocuyes during the blood fed, which subsequently transform into gametes. After the fertilization of gametes results in the formation of a zygote, and eventually transform into the ookinete. The ookinete penetrates into peritrophic matrix of midgut epithelium. Subsequently, it traverses many layers of midgut epithelium, and resides on basal lamina of the mid-gut epithelium and differentiate into oocyst. Inside the oocyst, sporulation occurs and form thousands of sporozoites. In *P. berghei*, the sporozoites egress into hemocoel after 14 days of post infection. These sporozoites eventually colonise the salivary gland and wait for transmission to a new host upon mosquito bite [11].

P25 and P28 proteins contain an epidermal growth factor (EGF) domain and a glycosylphosphatidylinositol (GPI) anchor. These structural elements provide the ookinete with a defensive mechanism against the proteolytic activity present in the gut lumen of mosquitoes [113]. CSP, CTRAP, and CDPK3 are crucial for the ookinete and oocyst development. The depletion of CTRAP and CSP impairs respectively the formation of ookinetes and oocyst colonization [18, 114]. Nonmotile ookinetes were generated as a result of the CDPK3 deletion [115, 116]. The ookinete motility was also impaired by the deletion of two inner membrane complex (IMC) proteins, IMC1b and ALV5, which subsequently reduced the number of oocysts colonising the midgut. The transition of ookinete to oocyst is accompanied by the concomitant loss of the IMC [90, 117, 118]. The oocysts represents longest phase in the life cycle of *Plasmodium* with 10 to 14 days maturation time [96], which are essential for the ookinete-to-oocyst transformation. The interaction of SOAP with the laminin protein in mosquito midgut was observed in the *P. berghei*. The disruption of SOAP leads to the decreased in invasion ability to the mid-gut epithelium and oocyst transformation, CTRAP binds to laminin during

the invasion of midgut epithelium [119, 120]. Following the oocyst formation, the parasite forms a capsule or wall around the oocyst, which separates the parasite from mosquito tissue. It is likely that the acquisition of nutrients from the host hemolymph via the basal lamina. The precise mechanism of nutrient transport into the oocyst remains unknown. It is widely believed that the oocyst capsule or wall plays a crucial role in obtaining nutrients. The bipartite oocyst capsule structure consisting of a robust outer layer primarily composed of laminin and the inner membrane of the oocyst. The capsule consists of parasite specific transglutaminase [121, 122].

CSP (Circumsporozoite protein) expression has been observed after few days of oocyst formation [123], and is crucial for formation of sporozoites. The CSP contains signal sequence at Nterminal and GPI transfer sequence at C-terminal. The N-terminal is associated with the membrane of parasite via the GPI anchor [124]. The early developmental stages of sporozoite, the plasma membrane of the oocyst undergoes a retraction process facilitated by internal invaginations. This retraction leads to the formation of cytoplasmic lobes, within which the nuclei undergo final rounds of mitotic divisions [125, 126]. These lobes are referred to as sporoblasts. The sporoblast has the characteristic of having CSP present on its membrane, as well as the daughter nuclei being localized to its perimeter [123]. The presence of CSP is crucial in facilitating the development of sporoblasts, thus leading to the production of sporozoites [127]. The microtubule organizing centers (MTOCs) reside just below the membrane of sporoblast. MTOCs is crucial for initiating the apical complex development and subsequently positioning the nuclei into newly formed daughter sporozoites. The mechanism behind MTOCs' development and positioning under the sporoblast plasma membrane is still unknown. However, it has been suggested that the CSP plays a significant role influence on this mechanism [123]. Following the formation of the apical ring, subpellicular microtubule assembly, polymerization, and association with IMC occur. Sporozoites undergo asynchronous budding, emerging from the membrane of the sporoblast consecutively [128, 129]. IMC1, located inside the IMC, is a crucial protein responsible for determining sporozoite shape and crucial for motility. IMC1a depletion in *Plasmodium berghei* leads to the disruption in membrane integrity and impaired motility [130]. After successfully emerging from the sporoblasts, mature sporozoites bear a crescent shape. IMC1 is crucial for the inner membrane complex, and targeted deletion showed that it is essential for maintaining the crescentic shape and its critical role in sporozoite motility [126]. After completion of the sporozoite development inside the oocyst, they egress and release into hemolymph.

1.5.6 Sporozoite egress and release into mosquito hemocoel

Before egressing from the oocyst, the sporozoites become motile, but this motility is incomplete and less vigorous than mature salivary gliding sporozoite motility, and it does not directly cause the release of sporozoites from the oocyst. Instead, it is believed that the oocyst rupture is due to a passive expansion and accumulation of thousands of sporozoites. [20, 131]. The oocyst capsule contains pores that facilitate the release of sporozoites into the hemocoel. ECP1 (egress cysteine protease 1), a cysteine protease is essential for the sporozoite egress [132]. The deletion of ecp1 in *P. berghei* resulted in fully mature oocysts with sporulation, however, sporozoites were unable to egress from the oocyst. A similar phenotype was observed when mutations were introduced in positively charged region II of CSP [133]. When the uncharged alanine was substituted at the position of positively charged domain II of CSP resulted in the normal oocyst sporulation was observed but the sporozoites were unable to exit, which suggests the direct or indirect involvement of ECP1 processing of the oocyst expressing CSP, thereby playing a crucial role in the subsequent release of sporozoites [134]. This indicates that the release of sporozoites is an active mechanism that relies on several proteins and is not just a mechanical force that results in the fully developed oocyst.

1.5.7 Sporozoite attachment and invasion of salivary gland

Following the release of sporozoites into the hemocoel, they migrate through hemolymph, and ultimately invade the salivary glands in mosquitoes. During this process, parasites interact with the distinct receptors thereby facilitating the attachment to the salivary gland basal lamina. These sporozoites successfully penetrate the basal lamina and then migrate through the basal plasma membrane to invade salivary gland secretory acinar cells. For the initial binding of sporozoites to the salivary glands, several parasitic ligands are required. Several studies have reported that few proteins play a crucial role in the sporozoite attachment to the basal lamina of the salivary gland. The CSP region I have shown in the sporozoite attachment to the salivary gland [135]. Antibodies against CSP protein inhibits the salivary gland invasion [136-138]. Additionally, the invasion of sporozoite is mediated by thrombospondin-related anonymous protein (TRAP) [139]. The deletion of the TRAP in *Plasmodium berghei* generated viable parasites that have accumulated in hemocoel with loss of motility and impaired salivary gland invasion [20]. The TRAP has two functional domains, the thrombospondin repeat domain and the conserved extracellular adhesive domain. Notably, these

domains are also implicated in the invasion of hepatocytes [19]. The cytoplasmic carboxy terminal domain harbor tryptophan residue. The deletion of these domain including tryptophan residue significantly inhibits the gliding and invasion of sporozoites [29]. Moreover, saglin, a receptor expressed on the distal lobe surface of the mosquito salivary gland, binds with TRAP and antibodies that target saglin decreases the invasion of sporozoites into the salivary glands [140]. Another protein that resembles TRAP known as UOS3 (Upregulated in oocyst sporozoite 3) also facilitates the salivary gland invasion. UOS3 is also referred to as TREP (TRAP-related protein) and S6 [141, 142]. The deletion of UOS3 in P. yoelii and P. berghei produced viable sporozoites which accumulated in the hemocoel but impairment of salivary gland invasion was observed. However, the initial investigations reveal defect in sporozoite motility in absence of UOS3 as a likely reason for inhibition of salivary gland invasion [141, 143]. The cysteine repeats modular proteins (CRMPs) such as CRMP-1 and 2, have a distinct function in the invasion of salivary glands. The disruption of both CRMP-1 and CRMP-2 proteins demonstrated their involvement in the salivary invasion [144]. Another protein known as MAEBL is also required for the salivary gland invasion and is expressed in distinctive stages such as oocysts, hemocoel, and salivary gland sporozoites. The MAEBL deletion in P. berghei results in defect in sporozoite attachment to the salivary gland basal lamina [145]. Moreover, the hemocoel sporozoites motility was displayed normal and actively infect mammalian host. Differential alternative splicing and posttranslational modifications of MAEBL have been observed across various life cycle stages [146-148]. These findings suggest that various forms of MAEBL could play distinct roles at different stages of parasite life cycle [149]. During the blood meal, the sporozoites within the salivary glands undergo transcriptional changes to achieve enhanced infectivity and successful transmission to the human host. Transcriptomic investigations have uniquely upregulated 30 genes in salivary gland sporozoites, which we have designated as UIS genes (upregulated in infectious sporozoites) [150]. UIS1 is crucial for the negative regulation of eukaryotic initiation factor- 2α (eIF-2α). This regulation is carried out by phosphorylation, resulting in the inhibition of mRNA translation that is stored in the form of granules. The deletion of *uis1* leads to the transforming the sporozoites into EEFs prematurely resulting in the loss of their infectivity [151]. Eventually, the UIS3 and UIS4 are required for the development of the liver stage. The *uis3* and *uis4* deletion led to the block during initial hepatocyte stage development [35]. SAP1 (sporozoite asparagine-rich protein 1) is characterized by its low complexity, exhibits a specific subcellular localization within the cytoplasm of sporozoites. Its pivotal role involves the regulation of sporozoite infectivity. The disruption of SAP1 resulted in its inability to initiate liver stage development, though it shows intact cell traversal activity

and hepatocyte invasion [152]. Interestingly, mice immunised with *uis3* and *uis4* knockout sporozoites, generated immune effectors comparable to radiation attenuated sporozoites (RAS) [153]. Identifying and characterizing crucial proteins implicated in the invasion of hepatocytes by sporozoites holds significant importance in developing genetically attenuated sporozoites (GAS) capable of inducing sterile immunity.

1.6 Clinical manifestation

Malaria symptoms appear when parasitemia in the erythrocytic cycle exceeds a threshold of around 100 parasites per microliter. The period of incubation varies depending on the parasitic species. For example, the incubation period for *P. falciparum*, *P. knowlesi*, *P. ovale*, and *P. malariae* spans between 10 and 14 days. However, some strains of P. vivax have been observed to have an extended incubation period of 3 to 6 months. Periodic fever may be noticed at regular intervals corresponding to the duration of the blood stage cycle in the infected species, which typically ranges from 48 to 72 hours [154]. Pregnant women are vulnerable to placental malaria, which is caused by the malaria parasite's sequestration in the intervillous space. This condition may lead to adverse complications, including anemia, preterm labor, low birth weight, and an increased risk of miscarriage. Malaria often exhibits several symptoms, such as anemia, intravascular hemolysis, bone marrow suppression, and dyserythropoiesis. Common symptoms of this disease may include vomiting, moderate diarrhea, abdominal distress, myalgia, vertigo, lethargy, and nausea. Furthermore, other symptoms such as jaundice, hypotension, hepatomegaly, tachycardia, orthostatic, pallor, and splenomegaly may also be observed [155]. Acute pulmonary complications and cerebral malaria are frequently observed as evidence of severe malaria, which results in the development of acute respiratory distress syndrome.

1.7 Malaria control measures

An integrated strategy is needed to effectively control malaria, which is a major public health issue. This strategy should have preventive measures, including the usage of insecticide-treated bed nets and indoor residual spraying, as well as effective antimalarial drugs. Implementing preventative measures is crucial for successfully managing and controlling disease outbreaks. This method

represents an innovative and comprehensive strategy on a worldwide scale within the realm of public health [156]. Currently, the primary focus of research and intervention efforts is on disease vector control. Different approaches are followed to reduce the transmission of disease, including insecticidal nets, repellents, larvicides, and pesticides. These approaches are likely to benefit primarily the high-risk groups, such as pregnant women and infants, to reduce the spread of the disease [157]. A larvivorous fish known as Gambusia is a natural biological control for mosquito populations by preying on larvae. The IRS (indoor residual spraying) used as a vector control strategy, specifically DDT (dichloro diphenyl trichloroethane), effectively kills mosquitoes by operating Na+ channels in the neuron [158, 159]. Environmental factors have a significant impact on malaria transmission. In a geographical region where malaria is prevalent, information about environmental management techniques, vector control, and an understanding of the parasite biology is essential to control the transmission.

1.8 Diagnosis

One of the most important strategies for disease treatment is an accurate and timely diagnosis of malaria, especially in populations that are sensitive to sickness and have low immunity. Light microscopy and RDT (rapid diagnostic tests) are the two most commonly used methods of diagnosis. RDT facilitate the identification of parasite-specific antigens, enabling the differentiation of several *Plasmodium* species. The microscopic detection methods are simple and more costeffective than RDTs. This approach is applicable in cases when the patient exhibits a high parasite burden. However, the use of microscopic detection methods requires the expertise of trained personnel to accurately identify parasite stages. Additionally, it is essential to ensure the proper maintenance of the instruments and to have a reliable and uninterrupted power supply [160, 161]. Although RDTs are expensive, they exhibit sensitivity and specificity in comparison to other methods for confirming detection. However, an accurate diagnosis may still be made by utilizing RDTs due to their ability to identify *P. falciparum* Histidine-Rich Protein 2 (*Pf*HRP2). The lactate dehydrogenase enzyme is detected by rapid diagnostic tests (RDTs) in asexual and sexual stages of the parasite [162].

1.9 Treatment

Drug resistance in *Plasmodium* significantly affects the effective management and control the disease. Protective vaccines are considered a more efficient for controlling risk factors and reducing the transmission of diseases.

The expression of polymorphic antigens across various phases of complex life cycle of *Plasmodium* poses many challenges. Antigens expressed in different phases of the life cycle can be tested for their efficacy to serve as a probable vaccine candidate [163]. Pre-erythrocytic vaccines, specifically sporozoite and liver-stage targeting vaccines, have been identified as effective for preventing malaria. These vaccines are designed to either neutralize the infectivity of extracellular sporozoites or stimulate cell-mediated immunity against liver-stage antigens. By targeting these critical stages of malaria parasite's life cycle, these vaccines aim to prevent the establishment of infection and subsequent progression to the blood stage [164]. The RTS-S/AS01 vaccine is remarkably efficacious immunogen against sporozoites, specifically designed to target the CSP, a prominent protein of sporozoite surface [165]. The *Plasmodium* sporozoites, subjected to radiationinduced attenuation, causes arrest in liver, and fail to cause blood stage infection. Genetically attenuated parasites (GAP) exhibit variable rates of attenuation at various liver stage time points, from early to late liver stage, and also mimic RAS in their inability to cause clinical malaria. As previously described, the uis 3 and uis 4 KOs parasites manifest an early developmental arrest in liver and hence trigger a CD8+ T cell-mediated immune response [153, 166]. The erythrocytic vaccines mainly inhibits the invasion and propagation of parasites, by inducing high titer of antibodies. The most prominently expressed merozoite surface proteins include merozoite surface proteins (MSP1/2/3), EBL-175 (erythrocyte binding protein), AMA-1 (Apical membrane antigen 1), Glutamate rich protein (GLURP), and SERA-5. Each of these proteins has the potential to be effective blood stage vaccine [167]. Transmission-blocking vaccines aim at preventing disease transmission in a given population. These vaccines inhibit the development of *Plasmodium* sexual stages by targeting surface proteins like Pfs25 and Pfs28 present on the surface of zygote and ookinetes, Pfs48/45 and Pfs230 has shown the expression on gametocyte surface. The initial phase of clinical testing for Pvs25 did not yield appreciable immunogenicity [168, 169]. Another essential component of the malaria treatment is chemotherapy. Chloroquine is derived from a parent drug called quinine, is an extract of cinchona plant and used as the primary alternative for treating malaria [170]. In the same way,

primaquine works well against the hypnozoites of *P. vivax*. It is used with other antimalarial drugs as part of a combination treatment plan. Artemisinin, a sesquiterpene lactone, is obtained through the extraction and isolation process from the Artemisia annua plant. Due to its inherent properties as a natural inhibitor of malaria, this compound has been used in Chinese traditional medicine. Artemisinin combination therapy (ACT) has emerged as a primary pharmacological intervention for malaria treatment, often employed in conjunction with other classes of antimalarial drugs [171]. The World Health Organisation (WHO) is advocating for the use of artemisinin-based combination therapies (ACTs) as a more effective treatment option for malaria, given the prevalent resistance seen toward other currently available antimalarial drugs [172]. Multiple antibiotics have demonstrated to have an impact on the metabolic pathways that operate within the Plasmodium mitochondria or apicoplast, likely due to their bacterial ancestry. Doxycycline and tetracycline impede the process of protein translation within the mitochondrion. Clindamycin is a highly efficacious inhibitor of protein translation within the apicoplast [173, 174].

1.10 Plasmodium berghei as a model organism

Investigating the biology of human *Plasmodium spp.* poses several challenges, including obtaining mosquito stages and the liver stages. Non-human malaria models -like avian, simian and rodent are valuable alternatives, owing to the feasibility of cycling the parasites to obtain both the mosquito as well as asexual stages, as well as being able to perform challenge experiments. In particular, rodent malaria models exhibit characteristics similar to those of the human species [39], and their gene models are comparable to *P. falciparum*. The rodent malaria models include the *P.* yoelii, P. berghei, P. vinckei, and P. chabaudi, of which P. berghei was isolated from the thicket rats residing in the Central African region. Subsequently, these species acclimated to laboratory mice and rats for experimental purposes [175]. Plasmodium berghei, has demonstrated significant utility in understanding comprehensively the parasite biology as well as in exploration of host-parasite interactions. Plasmodium berghei exhibits notable resemblances to human malaria species related to its morphological characteristics, physiological attributes, and life cycle. These similarities, albeit with minor divergences, render *P. berghei* an invaluable model organism. Nearly 85% (about 4,500) of the expressed P. falciparum genes out of 5,300 have been shown to possess an orthologue in at least one of the rodent malaria parasites, that likely constitute the fundamental set of *Plasmodium* genes [176]. Genome comparisons between *P. falciparum* and *P. berghei* reveal the identity of the protein is 62.9%, the identity of the nucleotide is 70.3%, and there are 3,890 orthologous genes in the former parasite. The size of the *P. berghei* genome is 18–20 MB and includes 14 chromosomes [177]. Standard recombinant methods allow for facile genome modification of *P. berghei*, providing a way for detailed life-cycle analysis of parasites *in vivo* and *in vitro*. Because of this, *P. berghei* has become the popular model for studying *Plasmodium* gene functions [178]. Studying the parasite biology and gene functions is greatly facilitated by the fact that the whole parasite life cycle can be replicated in the lab with minimal effort [179].

1.11 Ongoing challenges to malaria

The successful control and elimination of malaria constitute a major challenge, that is exacerbated by the ongoing evolution of resistance in parasites and vectors against antimalarial drugs and insecticides, respectively. The emergence of resistance to pyrimethamine and sulfadoxine in parasites is due to mutations occurring in the dihydrofolate reductase (DHFR) gene [180]. The emergence of artemisinin-resistant parasites was initially documented in 2008 [181]. Artemisininbased combination therapy (ACT) is now the only effective drug used for treatment under the prevailing circumstances. The primary cause of artemisinin resistance is the presence of mutations in the Pfkelch13 propeller gene, often referred to as K13[182]. P. falciparum and P. vivax parasite infections may be diagnosed quickly with the RDTs, which detect the presence of histidine-rich proteins 2 and 3 (Pfhrp2 and Pfhrp3). Natural deletion of Pfhrp2/3 has emerged as a major obstacle to malaria detection and treatment [183]. The Anopheles mosquito serves as a principal carrier for the transmission of P. falciparum and P. vivax, and insecticidal resistance has brought significant challenges to the effectiveness of eradication strategies [184]. A prompt surveillance of illness plays a crucial role in the plan for eradicating malaria. In Asian, African, and Southern American nations, the issue of inadequate surveillance has emerged as a significant concern, characterized by several deficiencies in illness monitoring and reporting [185, 186].

1.12 Research objective

The eradication of malaria presents multiple challenges, such as complex life cycle, blood stage antigenic variation, resistance to the currently available drugs and emergence of insecticide resistance mosquitos. Given this scenario, a comprehensive understanding of *Plasmodium* gene functions, expressed in different stages, may help discover novel vaccine and drug targets that can curb malaria. P. berghei genome is highly amenable to genetic modifications and therefore are used for generating mutants and tagged parasite lines. The feasibility of cycling the mutants through mice and mosquito further enables investigation of the stage specific functions of the candidate gene in question. The Plasmodium zoites are characterised by having a distinct apical end with three important secretory organelles- the micronemes, dense granules, and rhoptry organelles. These three organelles release proteins are crucial for parasite invasion, infection, and survival inside the host, and these, a complement of proteins residing inside the rhoptry organelles are called as rhoptry neck proteins and rhoptry bulb proteins. The role of RONs and ROPs are increasingly being shown in formation of a complex called moving junction that propels the entry of zoites into the host cell and for facilitates establishment of intracellular infections. Owing to their critical role in host cell invasion, targeting RONs may have a profound influence in modulating the infectivity and virulence of the parasites. In line with this idea, we have performed functional investigation of P. berghei RON6 (PbRON6), owing to the indispensable nature of P. falciparum RON6 locus. The current work investigates the localization and stage specific functions of *P. berghei* RON6 using genetic approaches.



Functional characterization of Plasmodium berghei rhoptry associated protein (RON6)

2.1 Introduction

Rhoptries are the largest membrane-bound secretory organelles within the Apicomplexan species, exhibiting variability in size, contents, and number across the phylum. These organelles assume a club-shaped structure due to their lower bulb region that tapers into a narrow neck. The proteins present in the neck region are known as rhoptry neck proteins (RONs), which are secreted during parasite invasion and facilitate initial interaction between host and parasite. The proteins secreted from bulb region are known as rhoptry bulb proteins (ROPs) and these are essential for host cell remodeling and creation of an intracellular niche called as Parasitophorous Vacuole (PV), that harbours the parasite. The composition of the bulb includes different lipids viz., cholesterol, phospholipids, and phosphatidylcholine [187, 188], that make up the PV [189]. In Plasmodium life cycle, the parasite produces various zoites forms that infect different cell types. For example, the sporozoites infect mammalian hepatocytes, whereas merozoites infect erythrocytes. Interestingly, both invasive forms contain rhoptry organelles. The third invasive form, called the ookinetes that breach the mosquito midgut epithelium, are though zoite forms, they lack rhoptry organelles [190]. Other apicomplexan parasites such as *Theileria parva* contain six rhoptries in the merozoites stage [191], while Cryptosporidium contains only single rhoptry organelle [192]. Rhoptries have also been well studied in Toxoplasma gondii, another model apicomplexan parasite. The fast growing tachyzoites of Toxoplasma contains 10 to 12 rhoptries while the intracellular quiescent bradyzoites, responsible for chronic infections contain only one to three rhoptries [193].

2.1.1 Rhoptry Biogenesis

Although rhoptries are essential for the survival and invasion of apicomplexan parasites, their biogenesis is poorly understood. Though classical secretory pathways are considered to be responsible for the formation of rhoptry organelles through the Golgi-derived vesicles fusion [194], the process remains elusive [195, 196]. The sortilin-like receptor (SRTLR) is critical for transporting secreted protein from the Golgi to the endosomal compartment. The Golgi cis region specifically localizes a substantial SRLTR region, where it interacts with GPI-anchored RAMA and serves as a chaperon for cargoing proteins like RAP1, RAP2, and RhopH3 [197, 198]. An adaptor protein 1 (AP1) also plays a significant role during the transportation of microneme and rhoptry proteins after processing in the Golgi complex. Specifically, AP1 participates in the maturation of the pre-rhoptry

compartment, which results in the formation of fully mature organelles that anchored apically [199]. The rhoptries undergo discernible differentiation during their maturation, which ultimately results in the formation of two distinct regions viz., rhoptry neck and bulb [195].

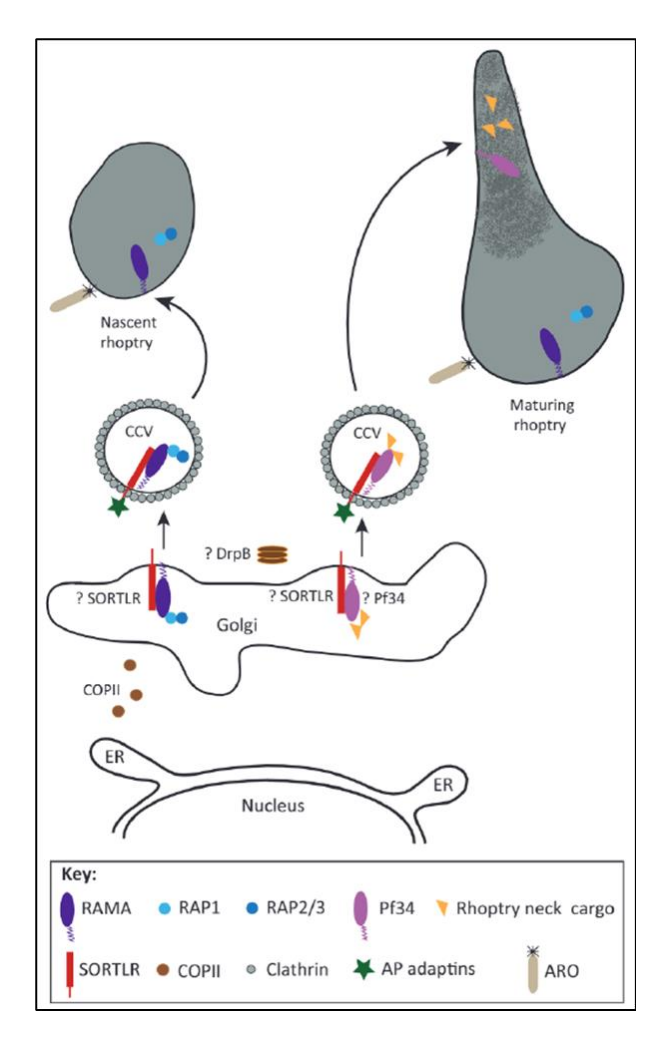


Figure 6: Schematic showing protein sorting in the rhoptries of *Plasmodium.* COPII-coated vesicles carry the proteins to the Golgi. The GPI anchored protein RAMA inside the Golgi, clusters with other cargo proteins from the rhoptry bulb, including the RAP complex. SORTLR acts as a rhoptry escort, assisting in cytosolic trafficking machinery and adapter proteins. Eventually, membrane clusters resistant to detergent divide to form clathrin-coated vesicles (CCV). The cargo is released into the growing rhoptries by merging CCVs with the target membrane. Here the rhoptry cargo is released through proteolytic digestion. The RAP complex bulb reorientation stops the cargo from spreading throughout the whole rhoptry as it matures. The *Pf34* a GPI anchored protein could serve similarly to RAMA. The role of DrpB and ARO during the rhoptry biogenesis and trafficking is still unknown [196].

The rhoptry-resident proteins undergo proteolytic processing by aspartic proteases. Plasmepsin IX is an aspartyl protease that plays a crucial role in rhoptry protein processing, and Plasmepsin X is essential for the processing of microneme proteins [200, 201]. Despite the existence of several secretory compartments within the parasite, the specific mechanism by which parasite proteins selectively target the rhoptries, particularly the neck or bulb region, remains unclear. The potential transfer of rhoptry cargo to the Golgi apparatus and its subsequent packaging into trafficking vesicles is a possibility that needs further experimental validation. In parasites, the formation of secretory pathway vesicles depends on dynamin like GTPase known as DrpB [202].

2.1.2 Molecular basis of *Plasmodium* ligands interaction for host cell invasion:

During the erythrocyte invasion, the initial interaction is mediated by two major protein families, such as reticulocyte binding proteins (Rh) and Duffy binding like proteins (DBL) also known as erythrocyte binding like proteins [67]. The Rh family proteins was first discovered in *P. vivax* [203]. Reticulocyte-binding homologs (Rh) are the most well characterized ligands involved in merozoite invasion of RBC. There are many subcategories within the Rh which includes Rh1, Rh2a, Rh2b, Rh4, and Rh5. These adhesin proteins interact with the receptor present on the host cell, that facilitates the parasite invasion. Recently an avidity-based extracellular interaction screen (AVEXIS) identified basigin as the specific erythrocyte receptor for Rh [68]. AVEXIS is a highly sensitive approach for identifying scalable transient extracellular protein-protein interactions with the lowest false positives [204]. Studies have shown that antibodies specifically targeting the Rh5 protein significantly inhibit the growth and development of various laboratory strains including *P. falciparum* [205]. Rh5 has an affinity for RBC, and importantly, antibodies targeting Rh5 prevent the RBC invasion. Rh5 is a crucial ligand for merozoite invasion of RBC. Given its vital role in merozoite invasion, it is a considerable potential candidate for a future anti-malarial vaccine [206].

In addition to Rh protein, several additional rhoptry neck proteins are crucial for the parasite invasion. RONs play crucial role for the host cell adhesion prior to and during invasion [207]. The interaction between RON protein complex and AMA1 is crucial for *Plasmodium* parasite invasion. The super-resolution microscopy studies reported that the formation of tight junctions involves the interaction of specific proteins, namely RON2, RON4, and RON5, with a micronemal protein called

AMA1 [208, 209]. RON2 is highly conserved across various apicomplexan protozoan parasites, including Plasmodium, Toxoplasma, Theileria, Babesia, Eimeria, and Neospora. The interaction between RON2 and AMA1 is a crucial in the invasion of target cells by *Plasmodium* merozoites. The expression and localization of RON2 has been identified in sporozoites, which is also essential for the salivary gland invasion and transmission to host hepatocytes [210]. The molecular basis of interaction between AMA1 and RON2 was studied by co-crystallization in both P. falciparum and T. gondi. These studies have also provided insights into how antibodies against AMA1 and inhibitory peptide R1 can effectively hinder the interaction with RON2 [211, 212]. A promoter-swapping strategy was adapted to investigate the functional role of RON2 in sporozoites, restricting its expression only to the asexual stage. This strategy resulted in a conditional knockdown of RON2 in sporozoites, resulting in reduced capacity of sporozoite invasion of salivary glands. This reduction is likely due to decreased adhesion to the substrate and reduced hepatocyte infectivity. These seminal studies revealed the role of RON2 for the first time in the salivary gland invasion [210]. RON3 is another rhoptry protein that forms a complex by interacting with RAMA (Rhoptry-associated membrane antigen), as proven by a co-immunoprecipitation assay and LC/MS analysis in P. falciparum [213]. RON3 is required for the transportation of glucose from RBC cytoplasm to parasite and the functioning of PTEX, present in the outer membrane of PVM, which facilitates the transportation of proteins into erythrocyte membrane. Parasites depleted of RON3 were unable to develop beyond the ring stage, and manifested significantly reduced glucose intake. However, the specific role of RON3 in PTEX function remains to be elucidated [214]. In addition, the other known apical protein complexes were also identified by LC/MS analysis, including a high molecular weight protein complex called RhopH1/Clag, RhopH2, and RhopH3, as well as a low molecular weight protein complex known as rhoptry associated protein complex RAP1 and RAP2, which are essential for merozoite invasion[213].

More recently, the role of RONs has also been implicated in sporozoite motility for colonizing salivary glands as well as for committing to mammalian hepatocytes. For example, RON4 was shown to be essential for transmission of *Plasmodium* sporozoites to mosquito salivary gland invasion and transition from mosquitoes to mammalian hepatocytes [215]. The promoter-swapping strategy for the RON4 conditional knockdown revealed that RON4 plays a crucial role in the adhesion and gliding motility of sporozoites [216]. The conditional depletion of RON4 using Flp-FRT recombination or

DiCre excision-inducible systems provided evidence that RON4 is required for *in vitro* hepatocyte infection [217]. RON4 secretion was detected during hepatocyte infection [218]. Furthermore, the neutralization of RON4 significantly delays the infection of hepatocytes by sporozoites [216]. The specific function of rhoptry proteins in sporozoite attachment and motility has yet to be fully understood.

As previously described the infective forms of *Plasmodium* such as sporozoites and merozoites displayed apical structure which contain rhoptries and micronemes. During the target host cell invasion, parasite secretes proteins from both compartments, that form a complex. For example, the merozoite invasion of RBC is marked by micronemal secretion of AMA-1 and rhoptry section of RON2. This complex is further reinforced by addition of RON4 and RON5- that form a moving junction. Recent studies reiterate that similar complex also form during sporozoite invasion of salivary glands. The formation of a complex between RON2, RON4, and RON5 in oocyst-derived sporozoites was substantiated by immunoprecipitation assay using anti-RON4 C-terminal antibody and further confirmed by RON2 N-terminal antibody [219, 220]. The conditional depletion of RON4 and RON5 results in decreased sporozoites adhering to the surface of salivary glands. These phenotypes bear a striking resemblance to RON2 conditional knockdown sporozoites. These studies show that RON2, RON4, and RON5 cooperatively function in sporozoites prior to or during salivary gland invasion [210, 215].

Rhoptry neck protein 11, a conserved protein of Apicomplexans, possesses seven transmembrane domains and a C-terminal region containing two EF-hand motifs for calcium binding [221]. An ultrastructural expansion microscopy identified an altered rhoptry biogenesis, following conditional depletion of *Pf*RON11, where the merozoites exhibited only a single rhoptry with no structural differentiation into neck and bulb regions. The orientation of a single rhoptry was properly positioned at the merozoite apical end, as it is characterized by the apical ring. The single rhoptry merozoites successfully adhered to host RBC, but were unable to invade. The continuous adhering of merozoite to the RBC results in echinocytosis which is caused by releasing proteins from a single rhoptry into host RBC. These findings suggest that, RON11 is required for de novo rhoptry biogenesis and RBC invasion [222]. Other findings from the *Pb*RON11 study indicated its essential role in

sporozoite invasion of the salivary gland. Conditional knockdown of PbRON11 significantly impaired the adhesion and gliding motility of sporozoites. Moreover, PbRON11 is crucial for sporozoite infectivity to mammalian hepatocytes. The expression of RON11 was detected in the rhoptries of both sporozoites and merozoites [221]. RON12 is a novel rhoptry neck protein present only in *Plasmodium* species and is highly conserved among the genus. Unlike other RON proteins, RON12 is completely soluble and does not have any tight membrane interactions, which distinguishes it from other RONs. RON12 is majorly identified in the rhoptry neck and is released into the nascent parasitophorous vacuole (PV) during the invasion. A significant portion of RON12 is transferred into the PV of ringstage parasites, which remains as a soluble protein throughout the blood-stage cycle. The knockout studies of RON12 in both P. falciparum and P. berghei revealed that, RON12 is not essential for the parasite survival but it requires for the parasite proliferation. The RON12 mutant parasites exhibited a significant reduction in invasion and growth compared to wild type, confirming that RON12 is not essential for the survival but critical for optimal growth and proliferation [223]. RON6 is a novel rhoptry protein characterized by the presence of cysteine-rich domain at c-terminal region in P. falciparum. This domain may be required for the receptor-ligand interaction or may be required for the protein trafficking. The expression and localization of PfRON6 was detected in apical end of schizonts, which may suggest its role in asexual propagation [224], In a recent investigation, PfRON6 conditional depletion lead to highly compromised asexual propagation [225].

Currently, we have investigated the role of RON6 throughout the *P. berghei* life cycle, by reverse genetic approach. *Pb*RON6 is a putative ortholog of *Pf*RON6. The endogenous tagging of HA inframe with C-terminus of *Pb*RON6 allowed characterizing the cellular localization in all the stages of parasite life cycle which includes blood stage, gametocyte stage, oocyst and importantly in salivary gland sporozoites and liver stages. We observed the localization of RON6 in plasma membrane of sporozoites and further demonstrated the extracellular nature of the C-terminal domain on sporozoite membrane. In addition, the expression of RON6 continued in liver stage and notably was associated with PVM. We successfully generated *Pbron6* KO parasites and the extensively characterised the mutant in all life cycle stages. Our studies show a reduced infectivity associated with the invasive stages, viz., merozoites and sporozoites, however *Pb*RON6 was dispensable in the mosquito stage. Reduced asexual propagation and reduced hepatic schizogony were other important characteristics of the mutant. Further we have observed that chronic infection induced by *Pbron6*

mutants caused hyper-reactive splenomegaly condition in mice. Immunohistochemistry of spleens revealed upregulation of T cell marker (CD3) and downregulation of B cell marker (CD20), pointing to an immunologically altered splenic niche during infection with mutant parasites. Additionally, we have unraveled the novel PbRON6 interacting partners through pull-down and mass spectrometry analysis, that likely form an invasion complex.

2.2 Materials & Methods

2.2.1 Experimental Animals

For the experimental study, male New Zealand rabbit, female C57BL/6, BALB/c and Swiss albino mice were used. All these animals were procured from the Hylasco Bio-Technology (India) Pvt. Ltd., Hyderabad. The experimental animals were housed in a controlled environment at the animal facility of the University of Hyderabad. These animals were maintained at 22°C, with a relative humidity of 50–60%, and in a regular circadian cycle (12 hours light and 12 hours dark). A standard diet, as prescribed for rodents and rabbit, were provided ad libitum. For all experimental studies, mice of 6 to 8 weeks old or 22-25 grams in weight were preferred. The IAEC (Institutional Animal Ethics Committee) of the University of Hyderabad has approved the protocols used in this study.

2.2.2 Parasite Lines

Plasmodium berghei ANKA (P. berghei) is rodent species and well adapted to the laboratory conditions was used in this study. The wild type P. berghei line is highly amenable to genetic modification and was used to as parental line to perform Plasmodium transfections.

2.2.3 Bacteria

The *E. coli* DH10- β competent cells engineered to produce methyl cytosine and methyl adenine were used for effective cloning of genomic DNA sequences. The genotype of DH10- β competent cells, used in the study was F- mcrA Δ (mrr-hsdRMS-mcrBC) ϕ 80lacZ Δ M15 Δ lacX74 recA1 endA1 araD139 Δ (ara-leu)7697 galU galK λ - rpsL (StrR) nuG (Thermo, Cat. no. EC0113). These cells were made chemically competent prior to transformation.

2.2.4 The acquisition of *Pbron6* gene sequences and amino acid sequence

A *Plasmodium* database, hosted by the Sanger Institute referred to as PlasmoDB (www.plasmodb.org), and the gene database (http://www.genedb.org/Homepage/Pberghei), used to retrieve the *Pbron6* gene and amino acid sequences. The retrieval of gene identities and orthologues for other *Plasmodium* species were also from the same database.

Table:1

S.No	Primers used for	Primer's designation	Primer sequence	Expected product size
1	Pbron6- 3XHA transgenic parasite line generation	FP1	GTG <u>CTCGAG</u> CTAATTGTATCATGCTCAATCTG	455bp
2		RP1	CCA <u>AGATCT</u> TTTGTTTGATGGTAACTCAGATT	
3		FP2	GGT <u>GCGGCCGC</u> GAAAAACAATGAGGTATGACCA	507bp
4		RP2	CAC <u>GGCGCGCC</u> TCCCTCTTATACTTTATCGCCA	
5	Pbron6- 3XHA transgenic parasite confirmation	FP3	AATTCCATCTATATGTTTGAAGAT	800 bp
6		RP3	ATATACAACAAAAAGGAGGTACAC	
7		FP4	AAGTTGAAAAATTAAAAAAAAAACATAT	618 bp
8		RP4	CTGCTGCAAAAAATTGACGGC	
9	Pbron6 knockout (KO) construct	FP5	GTG <u>CTCGAG</u> TTTCTATTATTTGCATTTATTCCC	784bp
10		RP5	CCA <u>AAGCTT</u> TTTTGAGAGTAAACACACTTAAC	
11		FP6	GGT <u>GCGGCCGC</u> GAAAAACAATGAGGTATGACCA	800bp
12		RP6	CAC <u>GGCGCGCC</u> TTCAAAAGAGTATATTGATTATGTT	
13	Pbron6 KO integration confirmation	FP7	TATTTTCATGATATTTTCATAATGTT	1.6kb
14		RP7	CAGGTCTTCTTACCCATAATCACC	
15		FP8	TACACACATAAAATGGCTAGTATGA	1.2kb
16		RP8	TACAATGGATGGTCCTATGGC	
17		FP9	ATGGCAACAAAATAAATAGTCAAG	

18	Pbron6 KO clonal confirmation	RP9	CGTCTTCCTTATCTTCGTCAGA	516 bp
19	Pbron6 KO complement ation	FP10	CCA <u>AAGCTT</u> ATGTATTATTATTTTTTTTTTTTT	- 2.5kb
20		RP10	GGT <u>CTGCAG</u> TTATTTGTTTGATGGTAACTCAG	
21	Pbron6 Complement confirmation	FP11	TATTTTCATGATATTTTCATAATGTT	. 1.6kb
22		RP11	CGTTATATCCATCTTCGACAGA	
23		FP12	CATGTTTACTATCGACAAAAAAAT	1.6kb
24		RP12	TACAATGGATGGTCCTATGGC	
29	Pbron6 - qRT PCR	FP15	TAAAGGCGCTGATGAAATGGA	. 136bp
30		RP15	GTCTTCCTTATCTTCGTCAGA	
31	Internal control <i>Pb18S</i> qRT PCR	FP16	AAGCATTAAATAAAGCGAATACATCCTTAC	
32		RP16	GGAGATTGGTTTTGACGTTTATGT	134bp
33	- Pbmsp-1 qRT PCR	FP17	AATGCTGGATGTTTTAGATATGA	- 129bp
34		RP17	ATCACATCCACCATTGTTGTTTCC	
35	Mouse <i>gapdh</i> qRT PCR	FP18	CCTCAACTACATGGTCTACAT	- 122bp
36		RP18	GCTCCTGGAAGATGGTGATG	

2.2.5 In-silico prediction of functional motifs in Plasmodium RON6

The gene sequence of both *P. berghei* RON6 (*Pb*RON6, PBANKA_0311700) and *P. falciparum* RON6 (*Pf*RON6, PF3D7_0214900) were retrieved from the PlasmoDB and analysed using the DTU/Deep TMHMM tool to predict the nature of RON6 protein from both *species*. Similarly, the gene sequence was analysed using the Phobius web server for predicting the cellular distribution of the

protein. Signal P-4.1, was used to analyze the signal sequence or peptide from both *P. berghei* and *P. falciparum* sequences.

2.2.6 Total RNA isolation and cDNA synthesis

The RNA was extracted from different life cycle stages of *P. berghe*. To isolate total RNA from asexual stages, Swiss Albino mice were injected intraperitoneally with stabilites of the WT P. berghei strain. When parasitemia reached around 12-15%, infected RBC was collected by retro orbital and the rbc were lysed with 0.5% saponin, followed by spin at 8000 rpm for 5 min at 4°C. The pellet was further washed with RNAse-free 1X phosphate buffered saline (PBS), pH 7.2 at 8000 rpm for 5 minutes. The total RNA was isolated using an Ambion PureLink RNA mini kit (Cat no. 12183020) following the instructions provided by manufacturers. The parasite pellet was mixed with lysis buffer given in the kit, and for maximal disruption of the cells, the sample was passed in and out through an insulin syringe (BD Ultra-FineTM, U-40, #Cat no. 324902), for 10-15 times. Add equal volume of 70% ethanol to the homogenate and mixed thoroughly. The homogenate was loaded onto a silica membrane column and spun at 12,000 rpm for 1 minute. Then wash the column twice by adding 700μL of wash buffer-I followed by one wash with 500μL of wash buffer-II and spin at 12,000 rpm for 1 minute, discard the flow through. Dry spin the column at 12,000 rpm for 2 minutes. Subsequently, elute the RNA from the column by adding 30µl of DEPC water. Finally, the RNA purity was measured by using a Nanodrop 2000 spectrophotometer (Thermo scientific) at 260nm wavelength, with DEPC treated water serving as a reference blank.

To isolate total RNA from the mosquito stages of *P. berghei*, the mosquitoes were blood fed on infected mice enriched with gametocytes [226] Fourteen and eighteen days post-infective blood meal, mosquito midguts and salivary glands were extracted for the isolation of sporozoites from the midgut oocyst and salivary gland. Both populations of sporozoites were released by disrupting the gut and salivary gland tissues in a 1.5ml eppendorf tube with the help of a small plastic pestle, spin at 800 rpm for 3 minutes at 4°C and. Supernatant having isolated sporozoites were collected and subjected to total RNA isolation as described above. To obtain RNA from developing liver stages, 2X10⁴ sporozoites were added to Hep2 cells (human liver carcinoma cell line), maintained in a CO₂ incubator at 37°C and the cultures were trypsinised at 16 hours, 25 hours, 42 hours, 50 hours, and

65 hours post-addition of sporozoites, and wash the cells twice with RNAse free 1X PBS, pH 7.2. Total RNA was isolated from the pellet obtained from different time points using the Ambion PureLink RNA Mini Kit (Cat no. 12183020), as described above.

The eluted RNA in all the above samples was subjected to DNase I treatment (NEB Cat no. M0303S), to eliminate DNA contamination. The reaction mixture for DNAse treatment contained 1x DNase I buffer (NEB, Cat no. B0303S), $2\mu g$ of total RNA, and 1 Unit DNase I enzyme, made up to 10ml of final reaction volume. The reaction mix was incubated at $37^{\circ}C$ for 30 minutes and the DNase-I was inactivated by adding $5\mu g$ of proteinase-K, followed by incubation at $37^{\circ}C$ for 15 minutes. The cDNA was synthesized from $2\mu g$ of total RNA. The cDNA synthesis was performed using the Takara cDNA kit (Cat. no. 61100A). The final cDNA has been used for the qRT-PCR.

2.2.7 The expression analysis of *Pbron6*

Expression of *Pbron6* across the life cycle stages was analysed by quantitative real time PCR following absolute quantification. Total RNA was isolated from mixed blood stages, midgut sporozoites, salivary gland sporozoites and in vitro liver stages at 13 h, 24 h, 36 h, 47 h, 65 h postinfection and merosomes of *P. berghei* using Ambion PureLink RNA Mini Kit (Thermo Scientific, Cat#12183020) following manufacturer's instructions. Pbron6 gene specific standards were generated by amplifying 136 bp fragment that was ligated into a pTZ57R/T 670 vector (Thermo Scientific, Cat#K1214). Similarly, a 134 bp product of *Pb18S rRNA* ligated into the pTZ57R/T vector was used as an internal control. Primers used for quantitative real time PCR are shown in Table-1. Gene-specific standards were generated in log scale dilution of plasmid copy numbers ranging from 108 to 102. The RNA was subjected to DNase I treatment (NEB, Cat no. M0303S) and cDNA was synthesized from 2 µg of total RNA isolated from different stages of *P. berghei* using the PrimeScript 1st strand cDNA Synthesis Kit (Takara, Cat no. 61100A) following manufacturer's instructions. SYBR Green master mix (TAKARA TB Green® Premix Ex TaqTM II Tli RNase H Plus, Cat no. RR82R) was used for qRT PCR using Eppendorf RealPlex 2 (Cat#2894). Pbron6 absolute transcript numbers were quantified at the selected life cycle stages by quantitative real time PCR using gene specific primers run along with the gene-specific standards and normalized with the absolute transcript numbers of 18s rRNA.

2.2.8 The DH10β competent cells preparation

The DH10 β strain of *E. coli* (Thermo Scientific, Cat no EC0113) was inoculated in a 5 ml volume of Luria-Bertani (LB) broth (HiMedia, Cat no M1245-500G), without antibiotic supplementation, to initiate a primary culture. The culture was maintained overnight at 37°C and 180 rpm in an orbital shaker incubator (Make: Scigenics Orbitek Laboratory Incubator Shaker, India). On the following day, a secondary culture was initiated by adding 1% of an overnight culture inoculum to 100 ml of LB without antibiotic supplementation. The culture was then incubated at 37 °C for 2 to 3 hours with continuous agitation at 180 rpm. The secondary culture was incubated until the optical density (OD) reached a range of 0.35 to 0.56. Subsequently, the cultures were incubated on ice for 30 min. Then spin at 6000 rpm for 10 min at 4°C, after the spin supernatant was discarded, and the pellet was resuspended in 100 mM calcium chloride solution (Sigma, Cat no. C5670). The suspended cells were incubated for 60 minutes on ice, centrifuge at 6000 rpm for 10 minutes. Then discard the supernatant and cell pellet was suspended in 3% glycerol (Invitrogen, Cat. no. 15514-011) prepared in 100 mM CaCl₂ solution. 100µl aliquots were dispensed in a 1.5ml eppendorf tube, immersed in liquid nitrogen, and the aliquots were stored at -80 for long-term use.

2.2.9 Bacterial transformation

Before transformation, the competent cells were thawed on ice, and added 10μ l of ligation mixture to the cells, and incubate at 4° C for 20 minutes. Subsequently, a heat shock treatment was given at 42° C for 90 seconds, followed by a cold shock treatment at 4° C for 5 minutes. Added 1 ml of LB broth (Hi-Media, Cat. no. M1245-500G) to the competent cells, followed by incubation at 37° C for 1 hour with of 180 rpm. Subsequently, the cells were spun at 5000 rpm for 3 minutes and discard the supernatant by leaving behind 50- 100μ l solution. The cells were resuspended in this minimal volume and spread onto LB agar (Hi-Media, Cat. no. M1151-500G) plate containing chloramphenicol (Sigma, Cat no. C0378-25G) antibiotic. The plate was incubated at 37° C overnight in an inverted position to facilitate the growth of transformed colonies.

2.2.10 Generation of Phron6 (PhANKA_0311700) KO construct

The Pbron6 deletion (Pbron6 KO) construct was generated using the plasmid pSKChDHFR::yFCU, which carries a hdhfr::yfcu positive-negative selectable marker under a constitutive Pheef1 α promoter [227]. The Phron6 locus was targeted by the double crossover homologous recombination method. To achieve this, the 5' and 3' untranslated regions (utrs) of Pbron6 were amplified from P. berghei genomic DNA using the primer pairs FP1/RP1 and FP2/RP2 respectively (shown in table 1) and introduced into XhoI/HindIII and NotI/AscI restriction sites respectively to obtain Pbron6 KO construct. Pbron6 KO construct was linearized with XhoI and AscI restriction enzymes and transfected into *P. berghei* parasite line following standard transfection procedure. DNA integrated parasites were selected by providing pyrimethamine in the drinking water of mice resulting in the enrichment of *Pbron6* KO line. The drug-resistant parasites were cloned by limiting dilution and correct integration of *Pbron6* KO construct was confirmed by diagnostic PCR analysis from genomic DNA of the cloned parasite lines. Details of the primers used for genotyping and expected PCR product sizes are listed in Table-1. Two clones that were generated from independent transfections were used for further analysis. The PCR reaction mixture contained the following components: 1x NEB PCR Buffer (Cat No. R72501, Thermo Scientific), 5mM dNTPs (Cat no. 10297-018, Invitrogen), 2.5mM MgCl₂ (NEB, Cat no. B9021S), 0.25μM of primers (forward and reverse), 1.25U of DNA Taq-polymerase (NEB, Cat no. #M0273S), and 50 ng of WT genomic DNA as a template. PCR was performed using thermal cycler (Eppendorf). The program of PCR as adjusted as initial denaturation at 95°C for 2 minutes, followed by denaturation at 95°C for 30 sec, annealing at 56°C for 30 sec and, extension at 68°C for 45 seconds for 35 cycles. Subsequently, the final extension was adjusted at 68°C for 10 minutes. After completion of program, the product was run on 1.5% agarose gel and visualize the amplified product under the UV-transilluminator for the confirmation of product amplification. The PCR product was purified using a DNA clean-up kit (Thermo Scientific, Cat no. K0832), and the purified PCR product was quantified using Nanodrop 2000.

2.2.11 Agarose gel electrophoresis

Agarose gel electrophoresis was used to resolve and analyse the molecular size of the amplified PCR products and DNA fragments subjected to restriction enzyme digestion. The agarose gel as made with 0.8-1% agarose (Lonza, Cat no. 50010) dissolving in 1XTAE buffer (Sigma, Cat no. T9650), heated the solution in microwave oven to solubilise the agarose. After cooling to room temperature, 5µl of 1x (0.3µg/ml concentration) ethidium bromide (EtBr) (Sigma, Cat no. 1239-45-8) was added to this solution. The solution was poured into a gel caster previously fixed with a comb. After solidification of the gel, DNA samples were mixed with 6X DNA loading dye (Thermo Scientific, Cat no. R0611) and loaded into wells, as well as DNA marker (Thermo Scientific, Cat no. SM0333) loaded into the wells used as a reference marker to verify the precise size of resolved DNA fragments within the range of 100 base pairs to 10 kb. The gel was subjected to 100 volts for 1 hour to separate the DNA fragments. Following completion of the gel run, visualized under the UV light and the images were recorded using the E-BOX CX5TS Edge gel documentation system.

2.2.12 Cloning of 5' homologous region of *Pbron6*

The 5' homologous sequence of *Pbron6* was amplified by PCR using primers as described in previous section. The amplified product was purified and quantified using Nanodrop 2000 spectrophotometer. The 5' product carried engineered restriction sites at its termini that were sensitive, respectively to Xho1 and HindIII. For ligation, both the 5' product and vector were double digested using Xho1 (Thermo Scientific, Cat No. FD0691) and HindIII (Thermo Scientific, Cat No. FD0501). The reaction mixture contained 1U of both restriction enzymes, 2μ l of 10X fast digest buffer (Thermo Scientific, Cat no. B64), and 2μ of 5' PCR product and 2μ of vector, and make up to 20μ l with nuclease-free water/NFW (Ambion, Cat no. AM9932). The digestion was performed at 37° C for one hour. After digestion, the PCR product and vector both were purified independently using DNA clean-up kit (Thermo Scientific, Cat no. K0831). The purified products were quantified using a Nanodrop 2000 spectrophotometer. The digested 5' flanking sequence and vector were ligated in a ratio of 1:3. The ligation mixture contained 1μ l of 1X ligation buffer (Thermo Scientific, Cat no. B69), 1000 ligase enzyme (Thermo Scientific, Cat no. EL0014), in a 10μ 1 of final volume using NFW, and ligation was incubated at 22° C for 6 hours.

Approximately 10μl of ligation mixture was transformed in DH10β competent cells (Thermo Scientific, Cat no EC0113), and the recombinants were spread on chloramphenicol (Sigma, Cat no. C0378) containing agar plate, and incubated for 12 hours at 37°C for visualising recombinant colonies. A maximum of 10 colonies were screened to identify the positive clone by colony PCR. The positive clones were further expanded in 10ml of LB broth. On subsequent day, the cloned plasmid was isolated using the commercially available kit (Thermo Scientific, Cat no. K0502). Positive clone was verified by restriction digestion analysis using XhoI and HindIII restriction enzymes, that released the 5′ product from the pSKC:hDHFR-yFCU vector.

2.2.13 Cloning the 3' homology region of Pbron6

The pSKC:hDHFR-yFCU plasmid carrying 5' region in MCS-I was used as a template for cloning the 3' UTR of the *PbRON6* gene in MCS-II. The 3' UTR was amplified by PCR and purified. As described above both the purified products were digested with NotI (Thermo Scientific, Catalogue no. FD0593) and AscI (Thermo Scientific, Catalogue no FD1894). The reaction mixture for restriction enzyme digestion contained 2μ l of 10X digestion buffer (Thermo Scientific, Cat no. B64) and 2μ g of 3' product or 2μ g of vector, incubated separately, in a 20 μ l final volume made up with NFW. After the digestion, both the PCR product and vector were purified and quantified using a Nanodrop spectrophotometer. Ligation and selection of positive clones carrying the 3' region was made as described for the selection of the 5' clone. The positive clone was verified by double digestion with restriction enzymes AscI and NotI that confirmed the presence of a 3' sequence in MSC-II of pSKC:hDHFR-yFCU plasmid carrying 5' region in MCS-I.

2.2.14 The *Pbron6* targeting cassette releasing by restriction digestion

The *Pbron6* KO construct was double digested using XhoI/AscI enzymes, resulting in the release of the hDHFR-yFCU cassette along with the flanking 5' and 3' UTR sequences of *Pbron6*. The size of the targeting cassette was further confirmed on a 0.8% agarose gel. The band was sliced from agarose gel and purified by DNA clean-up kit (Thermo Scientific, Cat no. K0832), and the purified product concentration was measured using a Nanodrop 2000 spectrophotometer. This purified product was used in electroporation of WT *P. berghei* schizonts.

2.2.15 The *P. berghei* ANKA WT parasite propagation in Swiss albino mice

The WT *P. berghei* (*ANKA*) *parasite strain* was aseptically thawed and injected into a Swiss Albino mouse via intraperitoneal route. The parasitemia was assessed through smears done by collecting blood from caudal vein. The smears were dried and fixed using 100% methanol for 5 seconds. Following the fixation, the smears were stained with Giemsa (Sigma, Cat. no. GS489001L), diluted in a 1:4 ratio, and incubated for 7–10 minutes. Subsequently, the slides were washed and dried. A single drop of immersion oil (Sigma, Cat no. 10765-500ml) was placed on stained slide, and the infected RBCs were observed under light microscopy (Lawrence & Mayo XSZ-N107T) equipped with a 100X magnifying lens. The parasitemia was quantified by counting infected rbc per field from 25 random fields.

2.2.16 in vitro culture of P. berghei ANKA asexual stages

P. berghei in vitro culture of asexual blood stages, enrichment of schizont parasites transfection, and subsequent recombinant parasite selection in the presence drug described earlier [228]. For setting up transfection, one BALB/c mouse was infected via intraperitoneal (i.p.,) route with a stabilate of WT *P. berghei ANKA* line. Upon reaching 3–4% parasitemia, the infected blood was collected from donor mouse and subsequently, 109 parasites were inoculated into five recipient mice by i.p., route. After parasitemia reached 3-5% in recipient mice, they were anesthetized, and the infected blood was collected via a cardiac vein puncture using heparinized Pasteur pipette (Fisher brand, Cat no. 13-678-20A). The blood was transferred into a 50ml falcon tube (Tarsons Cat. No. 546041) and gently resuspended in 10 ml of culture media that contained 1X RPMI (Gibco, Cat no. 22400-071), 10% fetal bovine serum (FBS) (Gibco, Cat no. A5256701), and 3.5 ml of 10mg/ml gentamycin (Gibco, 15710064) per 500 ml of media. The sample was spun at 200 g for 8 minutes with an acceleration of 5-9 and a deceleration of 0, using a swinging bucket rotor, in an Eppendorf centrifuge (Model 5810R). After, the spin discarded the supernatant, and resuspended the iRBC pellet in 25 ml of schizont media containing Nunc T75 flask (Thermo, Cat no. 156472). The culture flask was gassed with a mixture containing 5.05% oxygen, 4.96% carbon dioxide, and nitrogen for approximately 3 minutes and further incubated for 16-18 hours at 36.5 °C, with gentle agitation at 37 rpm. After 4 hours of incubation, the cultures were regassed for 3 minutes and placed back in incubator. After 14 hours of incubation, 100 µl of blood was collected from the flask, and transferred

into 1.5ml tube, then short spin for maximum speed for 5 seconds. Discarded the supernatant and resuspended the pellet in in minimal amount of culture media and smeared over a glass slide, stained with 1:4 ration of Giemsa and the cultures were assessed for enriched schizonts under light microscopy.

2.2.17 Density gradient enrichment of schizonts for electroporation

The schizont enrichment was performed by density gradient centrifugation using a 60% Nycodenz (Sigma, cat. no-D2158) solution. The stock solution composition for nycodenz was 27.6g of nycodenz powder in 60ml double-distilled water, and by further adding 500µl of a 5mM Tris-HCl (Sigma, Cat no. T6066), solution, 300µl of a 3mM KCl (Sigma, Cat no. P9541), solution, and 60µl of a 0.5mM EDTA (Sigma, Cat no. E9884) solution to it, and a final volume of 100 ml was adjusted with double distilled water. The autoclaved sterilized solution was stored at 4°C for further use. A 30 ml of overnight schizont culture was transferred into a fresh 50 ml falcon tube. Subsequently, 10ml of a 60% Nycodenz solution (pH of 7.4) was gently released into the bottom of the tube containing the overnight culture without flustering the culture. The culture was spun at 380g for 20 minutes with an acceleration of 5–9 and a declaration of 0, using a swinging bucket rotor, in Eppendorf centrifuge (Model 5810R). After the spin, the brown ring at the interphase of the schizont culture was collected carefully using a pasteur pipette (Fisher Scientific, Cat. no. 13-678). The collected schizonts were washed with schizont media twice and spun at 1500 rpm for 7 minutes at room temperature. The washed schizont pellet is used for the electroporation.

2.2.18 Electroporation of *Pbron6* KO construct

The isolated enriched schizonts were resuspended in 500μ l of schizont culture media. The schizonts were quantified by hemocytometer counting. Approximately 20–30 million schizonts were taken into a 1.5-mL eppendorf tube and short spun at maximum speed (approximately 9000 rpm) for 9 seconds. Prior to transfection, 90μ l of Mouse T-cell Nucleofector reagent (Lonza, Cat. No. VPA-1006) was combined with 10μ l of supplement 2 solution, as provided in the kit and 6–9 μ g of the targeting DNA construct were added to the mixture. The contents were added to the schizont pellet and subsequently, transferred to an electroporation cuvette. Electroporation was performed using an

Amaxa Nucleofector II device, using program U-033. After electroporation, 100μl of culture medium was added to the cuvette. The contents in the cuvette were transferred into an insulin syringe (Cat no. BD Ultra-FineTM, U-40, #Cat no. 324902) and the electroporated parasites were injected intravenously to the tail vein of BALB/c mice.

2.2.19 Selection of recombinant parasites

Following 24-48 hours of transfection, the percentage of parasitemia was scanned in a Giemsa-stained thin blood smear prepared from transfected mouse tail vein blood. When the parasitemia reached 1-2%, the recombined parasites were subjected to anti-malarial pyrimethamine drug selection (Sigma, Cat. No. 46706). The pyrimethamine drug of working concentration 70 ug/ml was prepared in drinking water. As pyrimethamine has limited solubility in water at neutral pH, it was first solubilized in 1 ml of absolute dimethyl sulfoxide (DMSO) (Sigma, Cat no. D8418) and further the volume was made up to 30-40 ml using potable water and the pH was adjusted to 3.5-4.0 using 1N hydrochloric acid (Qualigens, Cat no Q29507), resulting in a final volume of 100 ml. Mice harbouring transfected parasites were administered with drugs, given as a substitute for drinking water. During a 5-6 day selection process, the non-integrant population diminished, with almost undetectable parasitemia. Continued selection further for 2-3 days, resulted in increase in transfected population. The recombined parasites were diagnosed with cassette-specific gene primers, which were listed in Table 1. The drug-resistant parasites were collected when parasitemia reached around 3-4% and cryopreserved. The cryo preservative was prepared by diluting glycerol (Invitrogen, Cat. no. 15514-011) 1;10 with Alsever's solution (Sigma, Cat.no. A3551). The genotyping of drug selected parasite genomic DNA was performed to confirm target specific integration. Two separate transfections were performed and designated as T1 and T2 for each targeting construct. The phenotypic analysis of mutants was conducted using clonal lines derived from two independent transfections

2.2.20 Confirming stable integration of KO cassette at *Pbron6* locus

The drug-resistant parasites were collected from the transfected mouse in 1.5 ml eppendorf tube. 250 U of 1X heparin was added to each tube to avoid blood clot. The blood was spun at 8000 rpm, at room temperature for 5 minutes, and the serum and plasma were discarded. Further, RBC was lysed with 0.5% saponin twice and centrifuged at 6000 rpm for 5 minutes. The parasite pellet was washed twice with 1XPBS pH-7.2 (Gibco, Cat no. 2001207) for 5 minutes at 8000 rpm. The parasite genomic DNA was isolated from the pellet following manufacturer's instructions, using the NucleoSpin Tissue, mini kit (Macherey-Nagel, Cat. No. 740952.250) and was used for genotyping. To confirm stable integration of the KO cassette, integration PCR was performed, by designing primers that read through the cross-over region both at the 5' and 3 'region. Specifically, an FP7 primer was designed 57 bp upstream of the 5' recombination site and RP7 reverse primer was designed 771 bp downstream within the GIMO cassette. Similarly, another set of primers was designed to confirm integration at the 3' end of the target gene. For this, a forward primer, FP8 was designed 300 base pairs upstream of the 3' region of the GIMO cassette and a reverse primer RP8 was designed 138 base pairs downstream of the site of cassette integration.

2.2.21 Limiting dilution of *Pbron6* KO parasites to obtain clonal population

After confirming successful integration, to isolate individual transfected clones of the *Pbron6* KO parasite, a traditional limiting dilution (LD) procedure was performed so that the entire population is genetically homogenous. LD was performed by infecting a mouse with cryopreserved parasites of *PbRON6* KO that contained a mix of both transfected and WT population. When the percentage of parasitemia was around 0.5 to 1 %, 50 ul of tail blood was collected from the mouse and diluted 10^4 times in incomplete RPMI medium and total RBC were counted in a hemocytometer. Following quantification, the stock blood was diluted, such that each microliter contained 1 infected RBC. A group of 20 female Swiss Albino mice were injected with 1 parasite per mouse in a volume $100~\mu l$ of complete RPMI. Blood smears were prepared from day 9, post infection. Approximately 4–5 out of 20 mice became positive for infection. The positive clones without WT contamination were confirmed by diagnostic PCR using specific primers- FP5 and RP5, listed in table 1, that confirmed absence of ORF, in the cloned lines.

2.2.22 Analysis of the *Pbron6* KO phenotype in the mixed blood stages

Cloned lines of *Pbron6* KO were propagated in mice to monitor their asexual propagation rate. Approximately 1x10³ *Pbron6* KO parasites and WT parasites (control) were delivered into two independent groups of 5 Swiss Albino female mice (6–8 weeks old). The growth propagation of parasites was recorded by observing Giemsa-stained thin smears from day 3.5 of post-infection until day 8. The asexual growth of parasites was recorded from 25 fields/mouse on a daily basis, and the average percentage of parasitemia was calculated and represented graphically.

2.2.23 Breeding of Anopheles stephensii

To unravel the developmental growth dynamics of mutant parasites in the mosquito, an Anopheles stephensii colony was maintained. The adult male and female mosquitoes (2-4 days old) were mated immediately after emergence. Post mating, the female mosquitoes were blood fed from anesthetized rabbits. Prior to blood meal, mosquitoes were starved for 4 hours, by keeping them away from sugar-soaked pads. Rabbit was anesthetized using 0.3 ml of xylazine (20 mg/ml) (Indian Immunologicals Limited and 0.6 ml of ketamine (50 mg/ml) (Unijules Life Sciences Ltd). The anesthetized rabbit was placed over the mosquito breeding cage to facilitate optimal uptake of blood meal for 10-15 minutes. Two consecutive blood feedings were given within an interval of 24 hours. A bowl of water was placed inside the breeding cage, to facilitate egg laying by female mosquitoes after 24 hours of second blood meal. Over 3 to 4 consecutive days, the eggs were collected and shifted to a walkin stability chamber maintained at 27°C and a relative humidity of 70–80%. After 48 hours, early larval hatchlings were distributed into trays containing fresh, single-distilled water. The early hatchings subsequently transformed into larvae and pupae. During the developmental period, the larvae were fed on a diet consisting of a mixture of fat-free Kellogg's and wheat germ in a ratio of 60:40. The water in trays harbouring the larvae were refreshed every day by filtering and ensuring an ideal density of larvae. After a week, the larvae developed into pupae which were collected and placed in a cage to facilitate their emergence into adult mosquitoes. The adult mosquitoes were fed on 5% sucrose (Sigma, Cat no. S0389), soaked in cotton pads.

2.2.24 Transmission of *Pbron6* mutant parasites to *Anopheles stephensii*

An infection cage harbouring nearly 150–200 female *Anopheles* mosquitoes was prepared by separating male mosquitoes using vacuum pump. The infection cage with female mosquitoes were placed in a stability chamber, maintained at 20°C and RH of 75–80%. The female mosquitoes were starved for 2-4 hours prior to blood meal, followed by gametocyte-enriched blood meal from anesthetized mice for 15 to 20 minutes. The second consecutive infection blood meal was given after an interval of 24 hours. The infection cage was maintained at 20°C and RH of 75–80% for 18–21 days, to facilitate the development of malaria parasite inside the mosquito. The infected mosquitoes were fed on 5% sucrose, soaked in cotton pads during their maintenance over 21 days.

2.2.25 Analysis of oocyst development inside the mosquito

To study the phenotype of the mutant in mosquito, *Pbron6* KO and WT parasite line were transmitted to mosquitoes. After 14 days of infection blood meal, mid-guts were dissected out from 25 mosquitoes using a dissection light microscope (Lawerence & Mayo, LM-52-3622, NSZ-606). The dissected guts were placed on a clean glass slide with a cover slip over the sample. The slide was observed in higher magnification, to analyse the sporulation pattern inside the oocyst. For quantification of the oocyst sporozoite load, the guts were disrupted in a 1.5ml eppendorf tube (Tarsons, Cat no. 500010) and the supernatant with sporozoite was collected after centrifugation at 800 rpm for 3 min at 4°C. The supernatant containing partially purified sporozoites were collected separately and considered as stock sample. The oocyst sporozoite quantification was done by making a 1:10 dilution of the stock and counted using a hemocytometer.

2.2.26 Isolation of salivary gland sporozoites

To isolate the salivary gland sporozoites, the infected mosquitoes were collected on day 18-21, post infective blood meal and anesthetized by placing them on the ice for 10 minutes. The mosquitoes were washed twice with 50% alcohol for a minute, followed by incomplete RPMI medium. The mosquitoes were additionally washed three times, for 15–20 minutes, with incomplete RPMI medium containing 100X of antibiotic-antimycotic (Gibco, Cat. no. 1524006), $250\mu g/ml$ of fungizone (Gibco, Cat. no. 15290-018), and 10mg/ml of gentamicin (Thermo Fisher, Cat. no. 15750060). For obtaining

salivary glands, the mosquito head was severed and the thorax was compressed with the needle, allowing the release of glands. The glands were isolated in mass, to ensure that the ducts and lobes remained intact. The dissections were performed under dissection microscope (Lawerence & Mayo, LM-52-3622, NSZ-606). The dissected salivary glands were collected and transferred into a 1.5 ml eppendorf tube (Tarson, Cat. no 500010). The salivary glands were disrupted using a small plastic pestle and spun for 3 minutes at 4°C at 800 rpm. The supernatant containing partially purified sporozoites was collected in a fresh 1.5-ml eppendorf tube. For quantification of sporozoite numbers, 1µl from the supernatant was diluted 10 times in incomplete RPMI and placed in a hemocytometer. Sporozoite numbers were recorded from four quadrants. The total number of sporozoites in the stock solution was estimated by using the formula:

Total no. of sporozoites= Total count sporozoites \times 10⁴ (hemocytometor correction factor) \times 10 (dilution factor) per ml

2.2.27 HepG2 cell line maintenance

The HepG2 cell line, was generously shared by Dr. Satish Mishra from the Central Drug Research Institute (CDRI), Lucknow, India. The frozen vial was thawed by immersing it in a water bath maintained at 37°C for 3-5 minutes. The vial was wiped with 70% ethanol to decontaminate the surface. Subsequent procedures were performed under sterile conditions inside the vertical Laminar Air Flow Chamber. The thawed cells were transferred into a 15 ml falcon tube and pre-warmed complete DMEM media (Gibco, Cat. No. 11965-0992), that contained 10% fetal bovine serum (Gibco, Cat. No. 10270-106) and 100X Penicillin-Streptomycin-Neomycin (Gibco, Cat. No. 15640-055) was added to it. The whole solution was centrifuged at 1500 rpm for 3 minutes and cell pellet was collected. Five ml of complete DMEM was added to the cell pellet and transferred into a T25 vented flask (Thermo Fisher Nunc Cat. No. 169900). The flask was maintained at 37°C with 5% CO2 gas supply. The cell growth and change of shape was visualized under an inverted phase contrast microscope after 24 hours of incubation. The media was replaced every 48 hours. 80% confluent cell were detached by 0.25% trypsin-EDTA (Gibco Cat. No. 25200-056) after 3-5 minutes incubation in CO₂ incubator. The trypsinized cells were collected in a 15ml tube and 3 ml of pre-warmed complete DMEM was added to it. The cells were centrifuged for 3 minutes at room temperature at 1500 rpm and the cell pellet was re-suspended in 5 ml of pre-warmed complete DMEM and transferred into a new vented T25 flask.

2.2.28 Assessment of in vitro EEF development

To investigate the developmental progression of the *Pbron6* mutant liver stages, parasite growth was assessed in HepG2 cells. On day 21st post-infection, the *Pbron6* KO sporozoites and *Pb*RON6 3XHA transgenic sporozoites were dissected out from the mosquito salivary glands. Prior to the dissection day, HepG2 cells were seeded at a density of 1 x 10s in a 4-well plate, on collagen (Corning, Cat no. 354236) coated coverslips. Approximately 2X10st sporozoites from both lines were added to HepG2 cells and the well plate was spun at 1500 rpm for 4 minutes, incubated at 37°C in 5% CO₂ supply. The culture was maintained up to 65 hours. Media was replaced every 4–6 hours with fresh, complete DMEM. Subsequently, cells were washed with 1X PBS and fixed at 12 hours, 24 hours, 48 hours, 60 hours and 65 hours by adding 4% paraformaldehyde and stored at 4°C.

2.2.29 Indirect Immunofluorescence Assay (IFA) for analyzing the HA expression in the sporozoite stage

The sporozoites isolated from the mosquito mid-guts and salivary glands were spotted on TEKDON microscope slides (Cat. no. 160-5272 black, TEFLON coated, #5515 plain) and were air dried for 10-15 minutes. The spots were fixed with 4% paraformaldehyde for 20 minutes, and for long-term storage, was placed in 4°C. Following fixation, the slide was washed with 1XPBS (pH 7.4), (Gibco, Cat no. 10010-023) for 5 minutes, followed by permeabilization for 15 minutes in cold acetone and methanol (1:3). The sample was washed with 1X PBS for 5 minutes blocked with 3% BSA dissolved in a 1X PBS solution (pH 7.4) for one and half hours at 37°C. For visualization of HA expression, the blocked sporozoites were stained with anti-mouse HA monoclonal antibody (Abcam, Cat. No. ab18181), and anti-rabbit SIMP polyclonal, that served as a sporozoite marker. Both the primary antibodies were used at a dilution of 1:25 in 3% BSA and incubated at 37°C for one hour. After the primary antibody incubation, the slide was washed three times sequentially with 1XPBS, 1XPBST (containing 0.1% tween 20), and 1XPBS for 15 minutes each at 37°C. Anti-mouse Alexa Fluor 488 secondary antibody (Thermo, Cat.no-A11018) and the anti-rabbit Alexa Fluor 594 secondary antibody (Thermo, Cat.no-A11012) was used at a dilution of 1:1000 in a 3% BSA solution, to reveal respectively the HA and SIMP immunoreactivity. The incubations with secondary antibodies were carried out for 45 minutes at 37°C. To stain parasite nuclei, a stock of 1mg/ml DAPI (Sigma, Cat. No. D9564) was used at a dilution of 1: 1000, along with secondary antibody mixture. The slide was

washed with 1XPBS, 1XPBST, and 1XPBS consecutively for 15 minutes each, at 37°C. Following washes, the slide was air dried, and mounted using ProLong™ gold anti-fade reagent (Invitrogen, Cat. No. P10144). A blue star micro-cover slip (Cat no.#5128789) was placed over the sample and was sealed with transparent nail polish. The slide was visualized under Nikon Eclipse-AR upright fluorescence microscope. The captured images were analysed using the NIS software.

2.2.30 IFA for analyzing the HA expression in developing exo-erythrocytic Forms (EEFs)

To analyze the expression of HA in developing EEFs, partially purified sporozoites were cocultured with HepG2 cells and the cells were fixed at different time points (12h, 26h, 36, 48h 60h, and 65h) in 4% paraformaldehyde. Permeabilization and non-specific blocking was performed as described earlier. For visualization of HA expression, the EEFs were stained with the anti-HA rabbit monoclonal antibody (Abcam, Cat. No. ab236632) and the anti-CSP (3D-11) antibody, that served as an EEF marker. The primary antibody staining was done at 37°C for one hour followed by three washed with 1X PBS, 1X PBST, and 1X PBS for 15 minutes each. Anti-rabbit Alexa Fluor 594 (Thermo Scientific, Cat. No. A11012) and anti-mouse Alexa Fluor 488 (Thermo Scientific, Cat. No. A11018) secondary antibodies (Thermo Scientific, Cat. No. A11012) were used at a dilution of 1:1000 in a 3% BSA solution, to reveal respectively the HA and CSP immunoreactivity. Staining of parasite nuclei, washes after secondary antibody treatment, mounting and visualisation were done as described in previous section.

2.2.31 Analysis of *in vivo* sporozoite infectivity in mice by intravenous injection

To determine the infectivity of *Pbron6* KO line, sporozoites were injected in female C57BL/6 mice by an intravenous route. Two groups containing 6 and 7 mice were exposed to dose of 5X10³ mutant sporozoites. Similar number of mice were used for inoculation of 5X10³ WT sporozoites. The infectivity of the mutant sporozoites were gauged by monitoring the onset of prepatency, which is referred as the time required for initiation of blood stages infection, following exposure of mice to sporozoites. The prepatency of WT *P. berghei* sporozoites was noted around 3.5 days. The delay in

onset of blood-stage infection beyond 3.5 days was considered as reduced infectivity. The prepatency was also monitored by enhancing the dose of sporozoites to 1X10⁴.

2.2.32 Sporozoite inside-out assay

To investigate the efficiency of hepatocyte invasion, 2X10⁴ *Pbron6* KO sporozoites were added HepG2 cells, cultured on 3.2 mg/ml of collagen (Corning, Cat no. 354236) coated coverslips, in 4-well plates (Thermo Fisher #Cat. No. 144444). Similar number of WT *P. berghei* sporozoites were added to another culture plate. The cultures were incubated for 1 hour at 37°C in CO₂ incubator followed by fixing in 4% paraformaldehyde (Sigma, Cat no. HT5012-60ml). Sporozoite invasion was assessed by a dual staining method as described previously[229]. In this assay, after non-specific blocking with 3% BSA, the extracellular sporozoites were first stained, under non-permeabilised condition with 3d11 antibody, that binds to sporozoite membrane and immunoreactivity was revealed with antimouse Alexa Fluor 488 secondary antibody. In next step, the cultures were permeabilized with a 1:3 ratio of chilled acetone methanol solution, followed by non-specific blocking. The permeabilized cultures were stained for second time with 3D11 and immunoreactivity was revealed using an antimouse Alexa Fluor 546 secondary antibody. The number of green and red sporozoites were scored per field. The green and red sporozoites represented respectively the extracellular and total sporozoite per sample. The green and red sporozoites were scored from 20 random fields and the percentage of sporozoite invasion was assessed by following formula:

Red parasites – Green parasites / Red parasites X 100

2.2.33 Sporozoite staining under non-permeabilised condition

In order to confirm the localization of *Pb*RON6 on the surface of the sporozoite, an IFA was performed under non-permeabilized condition. As described previously the sporozoites were blocked with 3% BSA. Two commercially procured anti-HA antibodies viz., anti-HA rabbit monoclonal (Abcam, Cat no. ab236632) and anti-HA rabbit polyclonal (Abcam, Cat. no. ab9110) were used for IFA. 3D11 was used as a positive control, that served as a marker for staining sporozoite membrane. The immunoreactivity of 3D11 and HA was revealed respectively with Alexa Fluor 488 anti-mouse (Thermo Scientific, #Cat.no-A11018) and Alexa Fluor 546 anti-rabbit (Thermo Scientific, #Cat.no-

A11012) secondary antibodies. The immunoreactivity was visualized under Nikon Eclipse AR upright fluorescence microscope.

2.2.34 Sporozoite neutralization assay

The PbRON6-3xHA transgenic sporozoites were isolated from the mosquito salivary gland on day 19 post-infective blood meal. Approximately 25X10³ sporozoites were adjusted in 10µl volume and were placed in five, 1.5ml eppendorf tubes. The sporozoites in each of the five tubes were incubated with 2.5µgm of the following antibodies: 3d11 (positive control), anti-HA rabbit monoclonal (Abcam, Cat no. ab236632), anti-rabbit polyclonal (Abcam, Cat no. ab9110), anti-rabbit purified IgG and without antibody (negative control). The sporozoite incubation was carried out for 35 min at room temperature, followed by diluting the contents of each tube to 1ml with incomplete RPMI. From each tube, nearly 200µl was injected intravenously into each C57BL6 mice, such that each mouse (5 per group), received 5X10³ sporozoites. In a similar experimental setup, 25X10³ sporozoites were incubated with different antibodies as described above, but with 5µgm of antibody concentration. Following 35 min incubation, neutralised sporozoites were injected intravenously, into different groups of mice as described above. The antibody mediated inhibition of sporozoite infectivity was gauged by estimating the prepatency by Giemsa-stained blood smears. Simultaneously, the survival rate of each mouse receiving sporozoites neutralized with 5 µg and 2.5 µg antibody was analyzed by Kaplan-Meier plot.

2.2.35 Quantification of PbRON6-3XHA levels in sporozoite membrane

Freshly dissected *Pb*RON6-3xHA transgenic sporozoites were spotted on a slide (TEKDON microscope slides, #Cat. No. 160-5272 black, TEFLON coated, #5515 plain) and immediately fixed at room temperature, or alternatively, sporozoites were maintained at 37°C for 30 minutes in the presence or absence of host cells. After incubation, cells were fixed with 4% paraformaldehyde, followed by staining with 3D11 (mouse monoclonal) and anti-HA rabbit monoclonal antibody (Abcam, Cat no. ab18181). The immunoreactivity of 3d11 and HA was revealed respectively with Alexa Fluor 488 anti-mouse (Thermo Scientific, #Cat.no-A11018) and Alexa Fluor 546 anti-rabbit (Thermo Scientific, #Cat.no-A11012) secondary antibodies. The sporozoites were visualized under

Nikon Eclipse AR upright fluorescent microscope. The intensity of 3XHA on sporozoite membrane was estimated by using ND2 software.

2.2.36 Preparation of sporozoite lysate

*Pb*RON6-3xHA transgenic sporozoites were isolated from salivary glands and their numbers were estimated as described previously. Approximately 3x10⁵ sporozoites were mixed with 4X SDS PAGE sample buffer composed of 10%SDS (Sigma, Cat no. L3771), 500mM DTT (Sigma, Cat no. D9779), 50% glycerol (Invitrogen, Cat. no. 15514011), 500mM Tris-HCL (Sigma, Cat no T6066), and 0.05% Bromophenol blue dye (Sigma, Cat no. B5525) and boiled at 95°C for 5 minutes. The sporozoite lysate was run on 12% SDS-PAGE immediately or stored at -20°C for later use.

2.2.37 Exocytosis assay for *Pb*RON6

Exocytosis assays were set up to investigate if *Pb*RON6 is secreted by sporozoites. Approximately 5X10⁴ *Pb*RON6-3xHA transgenic sporozoites were suspended in 20μl of complete RPMI medium were placed in two independent 1.5ml eppendorf tubes (Tarsons, Cat no. 500010). Both tubes were incubated at 37°C in CO₂ incubator. One tube was removed after 30 min and other at 60 min of incubation. Both samples were spun for 10 minutes at 12,000 rpm in a refrigerated eppendorf centrifuge (Model# Eppendorf microcentrifuge 5425r). From both tubes, the supernatant and pellet were prepared. The denatured samples in SDS-PAGE sample buffer were resolved on 12% SDS-PAGE gel and immunoblotted. CSP and RON6 levels were analysed in both the supernatant and the pellet by probing the immunoblot with 3d11 and anti-HA rabbit primary antibodies (Abcam, Cat no. ab9110). The immunoreactivity was revealed using anti-mouse and anti-rabbit secondary antibodies conjugated to horse radish peroxidase in the presence of chemiluminescence reagent (G-Biosciences, ECL #786-003) and visualized using ChemiDoc™ Imaging System.

Similarly, 5X10³ *Pb*RON6-3xHA transgenic sporozoites were incubated with 3D11 antibody and anti-HA rabbit monoclonal antibody (Abcam, Cat no. ab236632) for 30 minutes at 37°C. After

incubation sporozoite suspension was placed on the microscopy glass slide (Corning® 2948) and visualized under Nikon Eclipse AR upright right field microscope.

2.2. 38 Sporozoite in vivo invasion efficiency and estimation of parasite burden in liver

Two groups of 6 mice C57BL/6 mice were intravenously infected with 5X10³ sporozoites of *Pbron6* KO or WT *P. berghei*. Three animals from each group were sacrificed and livers were isolated respectively at 12 hours and 48 hours that correspond to early EEF development and hepatic merozoite formation time points. Total RNA isolation from infected livers were performed using acid guanidinium thiocyanate-phenol-chloroform extraction method [230]. cDNA was synthesized from 2µg of total RNA from each liver homogenate sample. Quantitative real-time PCR was performed, and the cycle threshold (Ct) values were determined for *P. berghei* 18S rRNA, *P. berghei* msp-1 and mouse GAPDH respectively for 12 hours and 48 hours isolated livers.

2.2.39 RNA isolation from infected livers

Following isolation of liver tissue from the mice, the samples was homogenized using a tissue homogenizer (Cole-Parmer® HO-200 Series) in the presence of denaturing solution that contained 4 M guanidinium thiocyanate (Sigma, Cat no. 50980), 25 mM sodium citrate, pH 7 (Sigma, S4641-500G), 0.5% sarcosyl (Sigma, Cat no. L9150-250G) and 0.1 M 2-mercaptoethanol (Sigma, Cat no. 3148)]. The homogenate was acidified with 60μ l of 2 M sodium acetate, pH 4 (Sigma Cat no. S7899), followed by addition of 600μ l of buffer saturated phenol (Invitrogen, Cat no. 15513-039), and 0.2 ml of 24:1 ratio of chloroform-isoamyl alcohol (Sigma, Cat no. 25666). The contents were mixed by vortexing for 10 seconds and incubated on ice for 15 minutes. The samples were spun at 13,000 rpm for 20 min at 4 °C. After centrifugation, the upper aqueous layer was transferred into a fresh 1.5-ml eppendorf tube, and 700 μ l of isopropyl alcohol (Sigma, Cat no. I9030-100ML) was added to the aqueous layer and thoroughly mixed. The sample was incubated at -20 °C for at least 1 hour to precipitate RNA. The samples were centrifuged at 13,000 rpm for 20 minutes, and the supernatant was discarded. The pellet was washed with 500 μ l of 75% cold ethyl alcohol (Hayman, Cat no. F204325) by centrifuging at 13,000 rpm for 5 minutes. The supernatant was discarded and the pellet was air dried. The final

RNA pellet was dissolved in DEPC-treated water (Sigma, D5758) and concentration was determined using NanoDrop 2000 spectrophotometer.

2.2.40 Tissue sectioning for analysis of histopathological changes

The isolated spleen tissue was frozen, and optimal cutting temperature compound (OCT compound (Scigen, Cat. No. 23-730-625) was used to embed each sample immediately before to frozen sectioning on a microtome-cryostat. The block was incubated at -80°C for 2–3 hours, and the temperature of the cryostat (LEICA CM 1850 UV-1-1) was adjusted to -20°C for cutting the tissue. After the 3 hours of incubation, the block was placed on the chuck associated with the rotatory microtome of the cryostat, which facilitated tissue sectioning. The sectioned tissues (2mm thick) were transferred onto positively charged microscopy slides (PathnSitu Biotechnologies, Cat. No. PS-011-72).

2.2.41 Hematoxylin and Eosin staining (H&E staining)

Prior to H&E staining, the sections are deparaffinized, by immersing the slide in xylene (concentration 100%, Sigma, Cat no. 296333) for 5 minutes. Series of alcohol washes: 100% alcohol, followed by a 90%, 70%, 50%, and 30% ethanol wash each for 10 minutes was given to dehydrate the sections. Following one additional wash with double distilled water for 5 minutes, the tissue sections were incubated with hematoxylin (1:1 ratio concentration, Sigma, Cat no. H9627) for 20 minutes. The sections were washed once with double-distilled water for 10 minutes, followed by staining with Eosin (1% concentration, Sigma, Cat no. E4009-5G) for 5 minutes, followed by another wash with double-distilled water for 2 minutes. Sections are rehydrated by sequentially exposing to increasing percentage of alcohol: 30%, 50%, 70%, and 90%, for 5 minutes each, and finally with xylene for 5 minutes. The sections were dried by gently pressing on filter paper and mounted with DPX (one small drop or 100% concentration, Sigma, Cat no. 100579).

2.2.42 Immunohistochemistry/IHC:

The blocks for IHC were submerged either on ice or in a refrigerator at a temperature of 4 °C and then sliced into sections with a thickness ranging from 4 to 7 μ m. The sections were air-dried overnight and subsequently placed into an oven for 2 hours, set at 60 °C. The sections are deparaffinized by submerging the slide in xylene three times for 10 minutes each. The sections were subjecting to a series of alcohol rinses viz., 100% twice, followed by 80%, and finally to 70%. This process was repeated 10-15 times, followed by a final rinse with deionized water for 5 minutes.

Antigen retrieval is a method that, by restoring the antigenicity of sectioned tissue, enhances the reactivity between antigens and antibodies. The retrieval of antigenicity was performed by using either a microwave oven or a pressure cooker (decloaking chamber). The deparaffinized and rehydrated sections were immersed in 3% hydrogen peroxide for 5 minutes and rinsed in deionized water for 5 minutes. The slides were immersed into the retrieval buffer (10mM citrate) and subjected to microwave irradiation at 100 °C for 5 to 10 minutes by ensuring that the buffer level remains sufficient during the heating procedure. The slides were allowed to cool for 15 minutes at room temperature. The sections were rinsed in deionized water twice for 5 minutes, and in 1X PBS for 5 minutes. To prevent clogging, a solution of 3% hydrogen peroxide was applied for 5 minutes, followed by washing with 0.1% PBST, three times. 200µl of primary antibody solution was applied to the sections diluted in 1:200 ratio and incubated at room temperature for 8 minutes, followed by overnight, at 4°C. The slides were washed with 0.1% PBST three times, followed by incubation with secondary antibody, for 1 hour at room temperature. The sections were washed with 0.1% PBST for three times. Chromogenic substrate DAB chromagen, (Acam Cat no. ab64238) was added to the sections, incubated for 6 minutes, followed by washing the slide with deionized water for 3 minutes. The slides were immersed in a hematoxylin solution for 30 seconds; thoroughly washed with distilled water for 2 minutes. The sections were incubated in Tacha's bluing solution (BIO CARE MEDICALS Cat no. HTBLU-MX) for 1.5 minutes. The slide was washed with distilled water for 2 minutes and dried in oven for 10 to 15 minutes. The section was submerged in xylene for 5 minutes, for 3 times and mounted with a coverslip.

2.2.43 Immuno-precipitation and LC/MS analysis

Immuno-precipitation was performed using the pierce crosslink IP kit (Thermo scientific, cat. no-26147) as per the manufacturer's protocol. Briefly, *Pb*RON6-HA tag parasites were used for in vitro schizont culture. Enriched schizonts were purified using Histodenz (Sigma, cat. no-D2158) gradient. Parasites were lysed by incubating in 0.15% saponin (Sigma, cat no-47036-50G-F) for 10 minutes on ice followed by two washes in cold PBS. Parasite lysate for immuno-precipitation was prepared in IP lysis buffer. Rabbit monoclonal anti-HA antibody (Abcam, ab236632) was cross linked to protein A/G plus agarose beads and subsequently incubated with parasite lysate (>1mg) overnight at 4°C. After overnight incubation the protein A/G beads were washed in IP lysis buffer and the bead bound proteins were eluted in elution buffer (Tris-glycine, pH-2.8) provided with the kit. Simultaneously a purified rabbit IgG mediated pulldown was done for control. The successful immune-precipitation was confirmed by western blotting using anti HA rabbit monoclonal antibody.

For LC/MS analysis the proteins present in elution fraction after immuno-precipitation were digested by in solution trypsin digestion method. The samples were reduced using 20mM DTT (Sigma, Cat no. D9779-1G) for one hour at 57°C, 700rpm on a thermo mixer and followed by alkylation of protein with 40mM iodoacetamide (sigma, cat. No-1149) for one hour at room temperature in dark. For in solution trypsin digestion 1:50 (W/W) trypsin to protein ratio was used. Proteins in each elution sample were digested by trypsin (NEB, cat no. P8101S) and incubated at 37°C for 16 hours on a thermo mixer with 1000rpm. After trypsin digestion, the sample was acidified with 2µl of formic acid to final concentration 0.1% (Thermo scientific, cat. no-28905). The acidified peptides were desalted using pierce C-18 spin column (Thermo scientific, cat. no-89870). In brief, the C18 columns were activated with 1ml of 2X acetonitrile (ACN) (Merck, cat no AX0156) prepared in LCMS grade water. The columns were equilibrated in 0.5% trifluoroacetic acid (TFA) (Merck, cat. no-80457) and 0.5% acetonitrile solution. The acidified peptides were bound to the equilibrated columns and washed twice with 1ml of 0.5% ACN and 0.5% TFA solution. The peptide elution was done in 50 µl of elution buffer (70% ACN and 0.1% TFA) in LCMS grade water (Thermo scientific, cat. no-W6-212). The eluted peptide samples were dried in speed Vac and stored in -80°C till further use.

The LC/MS analysis was executed on Orbitrap Q-Exactive HF mass spectrometer, coupled with Nano LC 1000 instrument (Thermo Fisher Scientific, USA) supported with thermoscientific Xcalibur software. The eluted peptides were reconstituted with 0.1% formic acid and approximately $2\mu g$ of peptide sample was resolved on a PepMapTM RSLC C18 column ($2\mu m$ particle size, 100 A° pore size,

and 75 μ m X 50 cm). The raw data files from Orbitrap Q-Exactive HF were acquired on proteome discoverer, version 2.2 using SEQUEST algorithm. The predicted peptides were searched against the uniprot database *Plasmodium berghei*. The data was normalized with peptides detected in control IgG immuno-precipitation. The GO term analysis was carried out via plasmodb GO term analysis tool. The data was clustered according to the fold enrichment and the number of proteins involved in a particular pathway detected in IP/MS results.

2.2.44 RBC invasion assay

To quantify merozoite invasion of RBC, invitro cultures *Pbron6* KO mutant and WT *P. berghei* asexual stages were set up and enrichment of schizonts were done as described in earlier sections. The purified schizonts were quantified by using hemocytometer and nearly 10° parasites of WT and *Pbron6* KO were injected intravenously into two groups of Swiss Albino mice (n=5/group). To capture the early snapshots of merozoites invasion and propagation, blood smears were done on a 4 hourly basis for 48 hours and parasitemia was determined by Giemsa staining.

2.3 Results

2.3.1 Bioinformatics analysis revealed that the RON6 is extracellular in nature

To examine the presence of functional domains in *Plasmodium* RON6 protein in *P. berghei* and *P. falciparum*, the amino acid sequences were retrieved from the PlasmoDB and were analysed using the DTU/Deep TMHMM online tool. The analysis predicted both orthologues to be extracellular. However, the tool did not predict the transmembrane domain in *P. berghei*, though the analysis was suggestive of a globular nature of the protein. In *P. falciparum* 1 to 15 amino acids were detected as signal peptides and 16 to 950 amino acids were detected as extracellular domain.

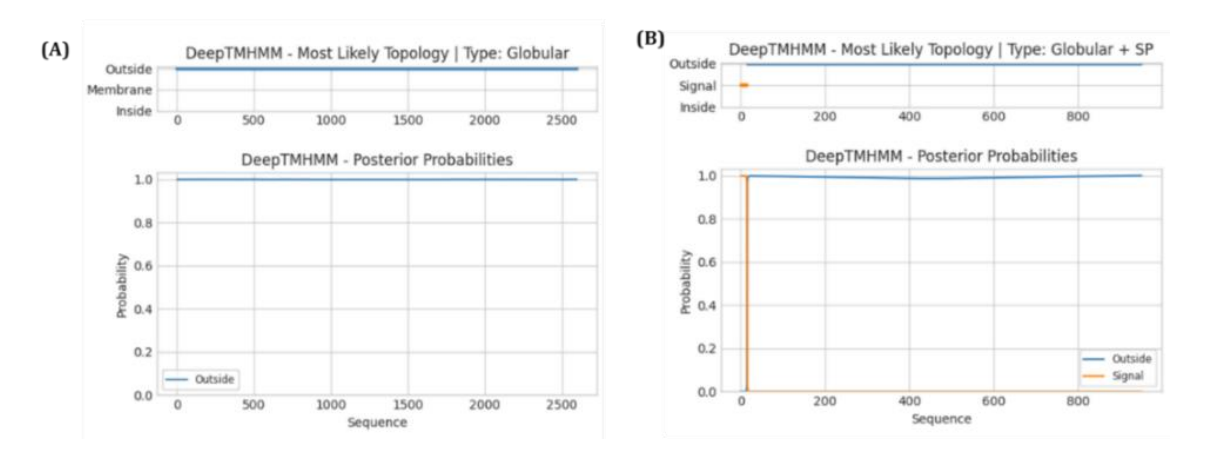


Figure:8 The bioinformatics approach towards prediction of functional motifs in *Pb*RON6 and *Pf*RON6. Deep TMHMM-Posterior Probabilities of (A) *P. berghei* and (B) *P. falciparum.* The predictions show both proteins to be globular in nature, with only *Pf* having an SP domain between aa 1-15.

In a similar manner, the amino acid sequence was analysed using Phobious web server. The RON6 proteins from both *P. berghei* and *P. falciparum* were predicted to be non-cytosolic in nature.

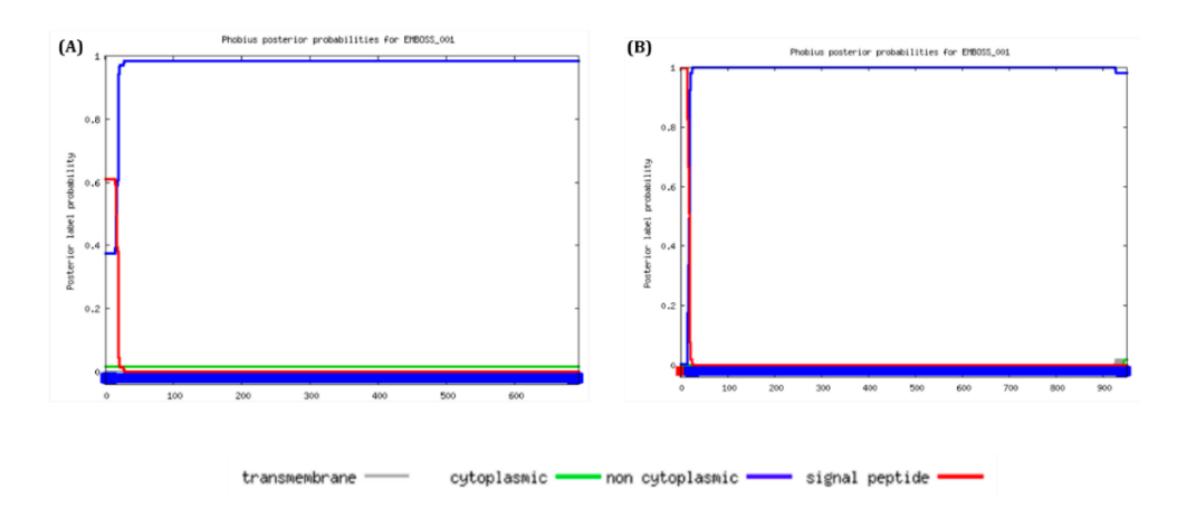


Figure: 9 Phobious web server predicted the *Pb*RON6 as a non-cytosolic protein both in (A) *P. berghei* and (B) *P. falciparum*.

The Signal P-4.1 tool was additionally used to independently validate the earlier predictions of a signal peptide. Signal P-4.1 identified a signal sequence in *P. falciparum*, between amino acids 1 and 15. However, no signal sequence was detected in *P. berghei*. Shown in the figure are the C, S, and Y scores. The C score represents the unprocessed cleavage site, whereas the S score indicates the presence of a signal peptide site. The Y score is the combination of the C and S scores. A cut-off value greater than 0.45 is indicative of the presence of a signal peptide in the protein sequence.

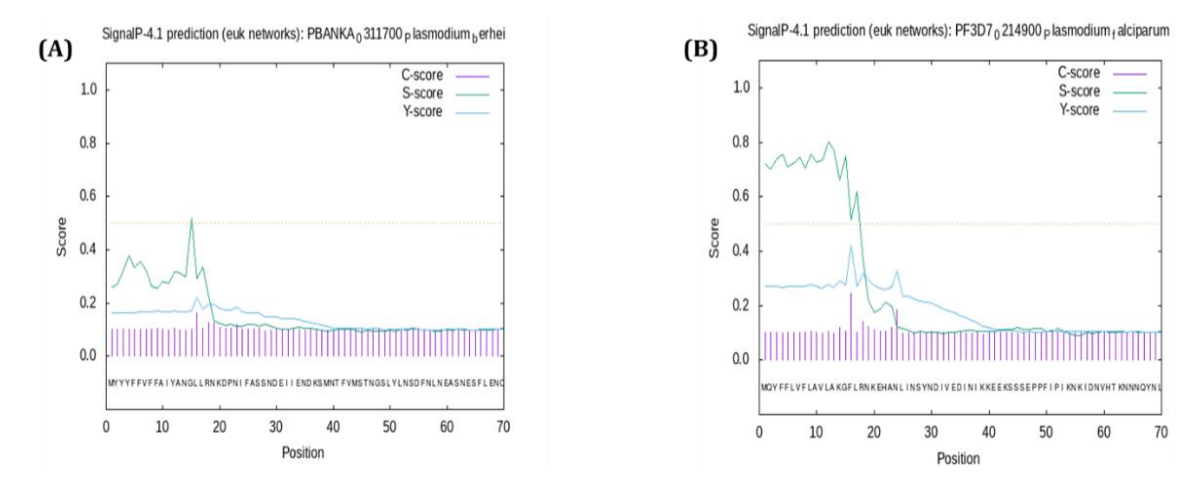
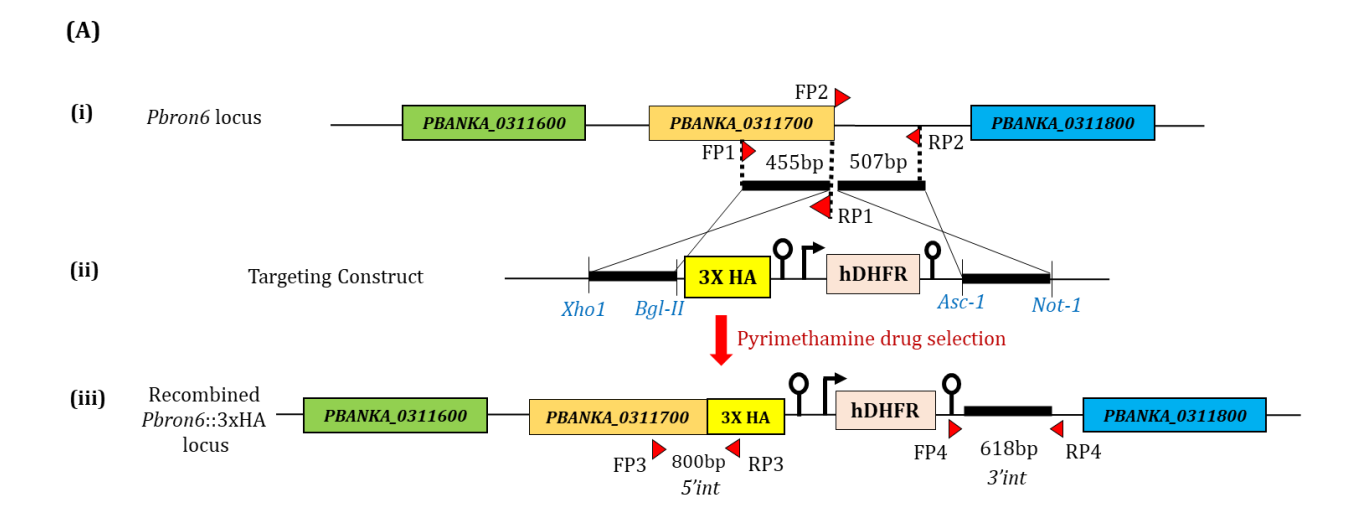


Figure 10: Signal P-4.1 did not predict SP in (A) *P. berghei* however in (B) *P. falciparum,* SP was detected between 1-15 amino acids.

2.3.2 Analysing the cellular localization of *Pb*RON6 in *Plasmodium berghei* across the life cycle

To study the cellular localization of *Pb*RON6 expression throughout the life cycle of *Plasmodium berghei*, a 3XHA (3X hemagglutinin) tag was translationally fused inframe with the *Pb*RON6 ORF by excluding the stop codon. The transgenic *P. berghei* RON6-HA reporter line was confirmed by PCR employing diagnostic primer pairs and the recombined locus was sequenced to confirm the presence of an inframe 3XHA tag. The transgenic parasites were intended for analysing the expression pattern of *Pb*RON6 by indirect immunofluorescence assay at multiple life cycle stages like blood-stage schizonts, gametocytes, ookinetes, oocyst sporozoites, salivary-gland sporozoites, and liver stages. Towards this end, transgenic parasites were propagated in BALB/c mice, and schizonts and gametocytes were enriched. The transgenic parasites were next transmitted to female *Anopheles* mosquitoes to produce mosquito stages of *Plasmodium* viz., ookinetes (18h post-infective blood meal), oocyst sporozoites (D14 post-infective blood meal), and salivary gland sporozoites (D18/20 post-infective blood meal). Sporozoites were further added to HepG2 cultures to produce different developmental stages of EEFs (axenic, 12h, 24h, 36h, 48h and 62h). All aforementioned stages were fixed and HA expression was detected by IFA using anti-HA antibodies in combination with stage-specific markers.



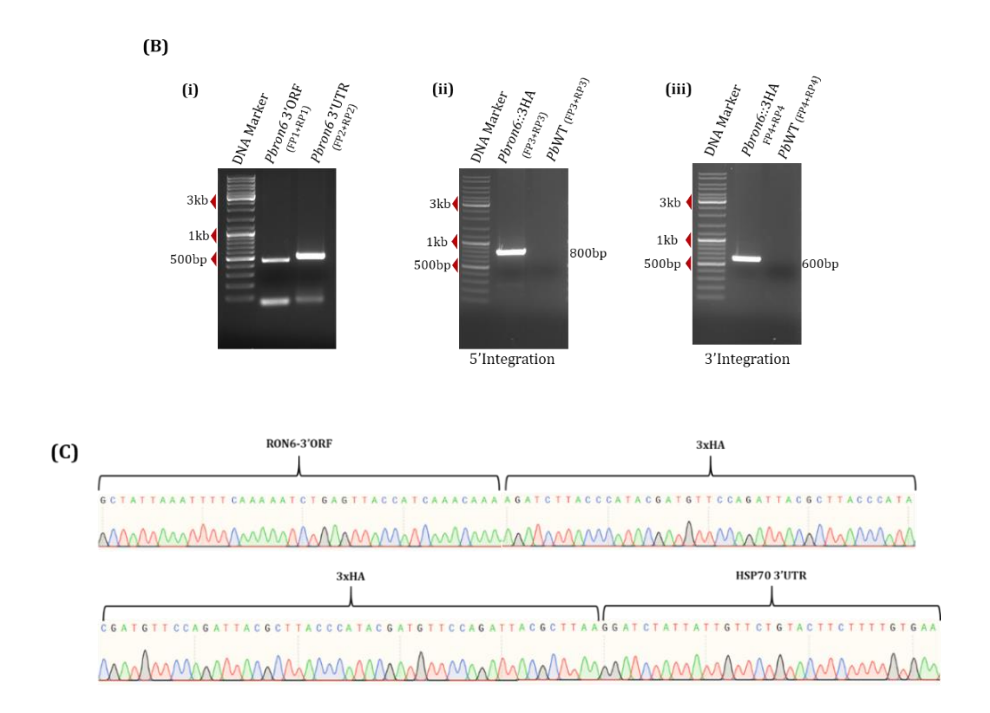


Figure: 11 *Pb*RON6-HA reporter line generation and investigating the expression and localization in all life cycle stages of *Plasmodium berghei*. The schematic representation for generating the *Pb*RON6-HA transgenic line. The 3'ORF of *RON6* and the 3'UTR were amplified and cloned at the MCS I and MCS II regions of the localization plasmid bearing 3XHA and hDHFR selection marker. In Fig **(A)** the top panel corresponds to the genomic locus of *Pbron6* (*PBANKA_0311700*), the middle panel shows the localization construct for fusion into the *Pb*RON6 locus and the lower panel shows the recombined locus in the transgenic line, where *Pbron6* locus is inframe with 3XHA parasite **(B)** PCR products of the 3'ORF and 3'UTR of the *Pbron6* used for cloning into the 3XHA-hDHFR plasmid and 5' and 3' clone. The transgenic line was confirmed by PCR using diagnostic primers that only amplified products from the transgenic line and not WT. **(C)** The sequence of recombinant locus confirming 3XHA tag inframe with RON6 ORF excluding the stop codon.

The HA expression was investigated in enriched schizonts and gametocytes. We noted punctate staining of HA in the schizont stage, likely suggestive of a signal from the rhoptry compartment of individual merozoites. In gametocytes, we noted discrete patches of HA expression only towards one side of the cell. The schizonts and gametocytes were counter-stained respectively with anti-PhL-IP5 and anti-SIMP antibodies, used as a stage-specific marker.

The rhoptries are not found in the ookinete stage, despite these being the invasive forms, that cross midgut epithelium. However, the ookinetes showed HA immunoreactivity both in cytoplasmic and membrane compartments. The midgut sporozoites showed immunoreactivity in the apical

region, indicative of a rhoptry localization of PbRON6. In the salivary gland sporozoites, we noted expression of HA both in the rhoptry and on the sporozoite membrane.

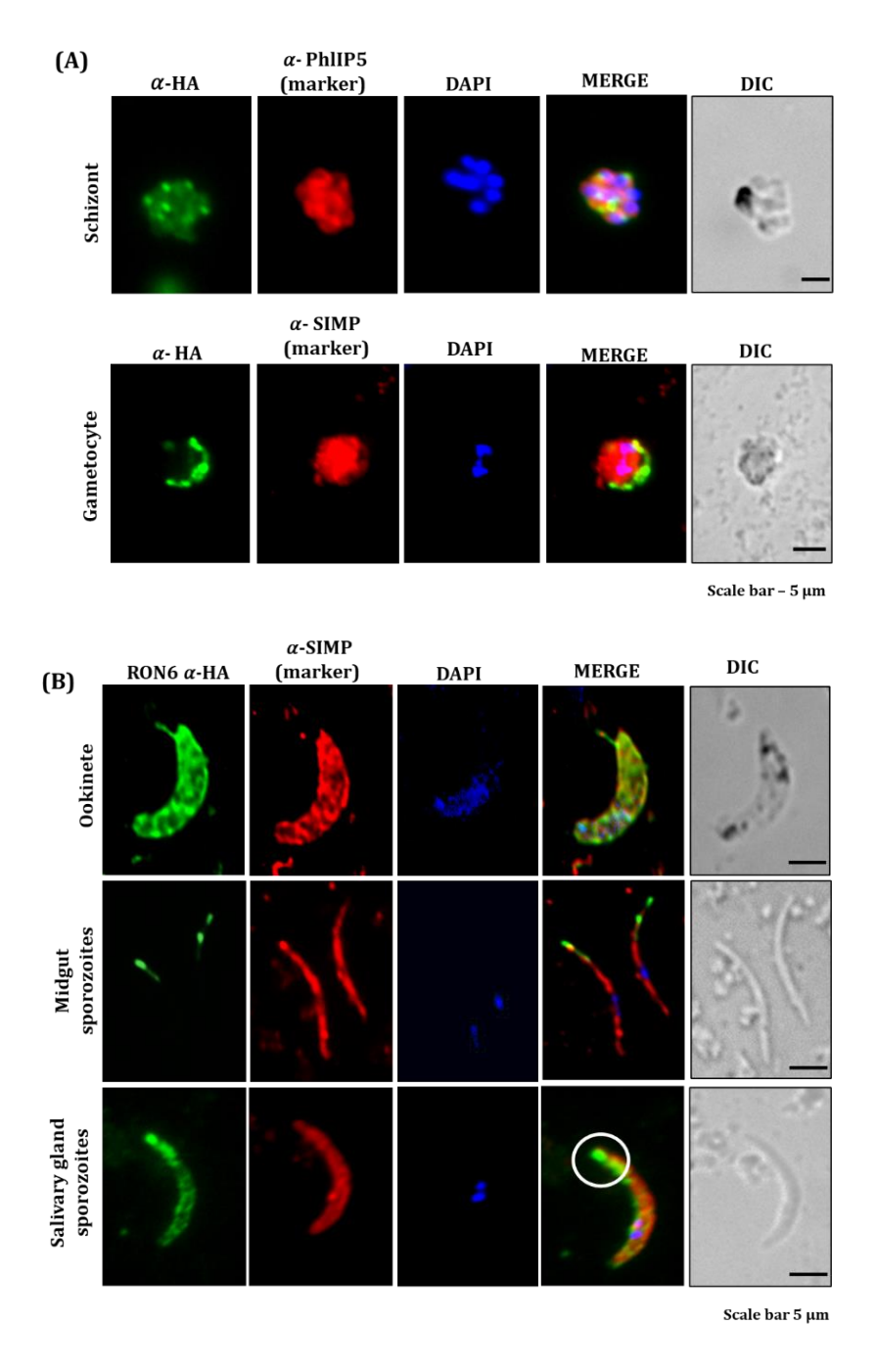


Figure: 12 Analysing the localization of *Pb*RON6 3XHA during asexual, gametocyte, and mosquito stages (ookinetes, midgut, and salivary gland sporozoites). (A) The blood stage schizonts were stained with antimouse HA monoclonal antibody and with anti-*Pb*PhIP, a marker for asexual stages. The immunoreactivity was revealed with anti-mouse Alexa Fluor 488 and anti-rabbit Alexa Fluor 594 secondary antibodies. Similarly, the gametocytes were stained with anti-mouse HA and anti-SIMP (marker) primary antibodies and revealed by

Alexa Fluor 488 and 594 secondary antibodies respectively. **(B)** The mosquito stages viz. the ookinete, midgut, and salivary gland sporozoites were stained with anti-mouse HA antibody and anti-SIMP (marker) antibodies and revealed with anti-mouse Alexa Fluor 488 secondary antibody and anti-rabbit Alexa Fluor 594 secondary antibody. Nuclei were stained with DAPI.

2.3.3 PbRON6 localization during the development of P. berghei in the hepatocytes

During the process of hepatocytic development, the sporozoite undergoes a transformation from an elongated structure to a spherical shape. These spherical forms of the parasite are commonly referred to as exoerythrocytic forms (EEF), which are obligate intermediary stages of parasites, serving as a transitional phase between the mosquito and the blood-stage parasites [231]. The sporozoites undergo a morphological transformation, transitioning into a bulbous structure characterized by a singular nucleus. The bulbous structure undergoes a gradual process of enlargement until the elongated sporozoite is entirely assimilated. Subsequently, the early exoerythrocytic forms (EEF) experience multiple cycles of nuclear division and subsequently differentiate into a multitude of initial merozoites, numbering in the thousands [232].

To investigate the subcellular distribution of *Pb*RON6 during the hepatic stage of development, the transgenic sporozoites were added to HepG2 cultures, a human hepatoma cell line. These HepG2 cells facilitate the growth and complete development of *Plasmodium berghei* sporozoites allowing continuous monitoring of their developmental progress up to 65 hours. We noted HA expression in the 6h axenic (cell-free) cultures, that continued in all other stages of EEF development corresponding to 12h, 26h, 36h, 48h, and 62h. Interestingly, at 26h and other later stages of EEF development, we noted the HA staining the periphery of the EEF body, reminiscent of a typical staining pattern of PVM. The EEFs were stained with 3d11 monoclonal antibody, that detects CSP, which is abundantly expressed in all developmental stages. Our observations likely suggest the localization of RON6-3XHA to PVM, a niche that encloses the developing liver stages. We further investigated the 65h HepG2 cultures, a point when hepatic merozomes are generated, that contains several thousand hepatic merozoites. We noted HA signals from individual hepatic merozoites, that may likely point to the rhoptry localization of RON6-3XHA. Taken together, sporozoites and liver stages showed high expression of RON6-3XHA, which may hint to its role in maintaining the infectivity status of both stages.

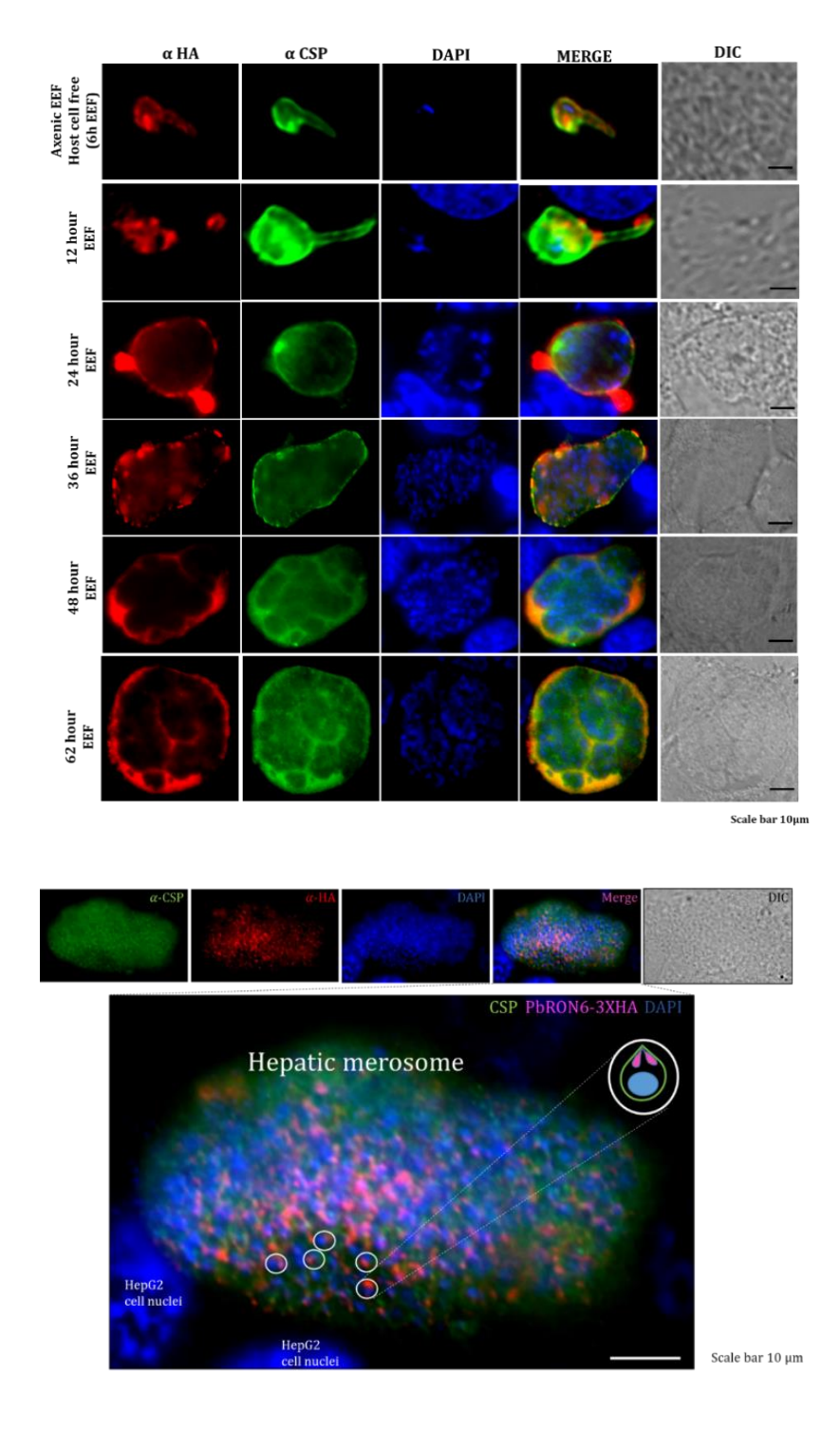


Figure: 13 The *invitro* **development of** *Pb***RON6-HA transgenic parasites.** Localization of *Pb*RON6 during liver stage development. Approximately $2x10^4$ partially purified *Pb*RON6 salivary gland sporozoites were cocultured with HepG2 cells. The cultures were fixed at 6 hours (axenic EEFF) 12 hours, 24 hours, 36 hours, 48 hours, 62 hours, and 72 hours and stained with anti-HA (rabbit monoclonal) antibody and anti-CSP (3D11)

(mouse monoclonal) antibody. The fluorescence was detected by anti-mouse Alexa fluor 488 and anti-rabbit Alexa fluor 596 secondary antibodies. The host and parasite nuclei were stained with DAPI.

PbRON6 co-localizes with Parasitophorous Vacuolar Membrane (PVM)

The proteins of rhoptry compartment are utilized for two purposes: one for making a moving junction, a bridge established between the parasite and host cell membrane, that allows invasion, and a second cohort of sequentially released proteins, facilitate the formation of PVM. To investigate if RON6 localises to PVM, we stained 36h EEF stage, with anti-HA antibody and anti-UIS4, a marker for PVM. The immunoreactivity was detected by Alexa fluor 488 anti-mouse and Alexa fluor 596 anti-rabbit secondary antibodies and the nucleus was stained with DAPI. We noted the colocalization of *Pb*RON6 at multiple foci, overlapping the PVM marker, suggesting the recruitment of RON6 to this membrane. These studies concur with the peripheral localization of HA signals covering the EEF body, during all developmental stages.

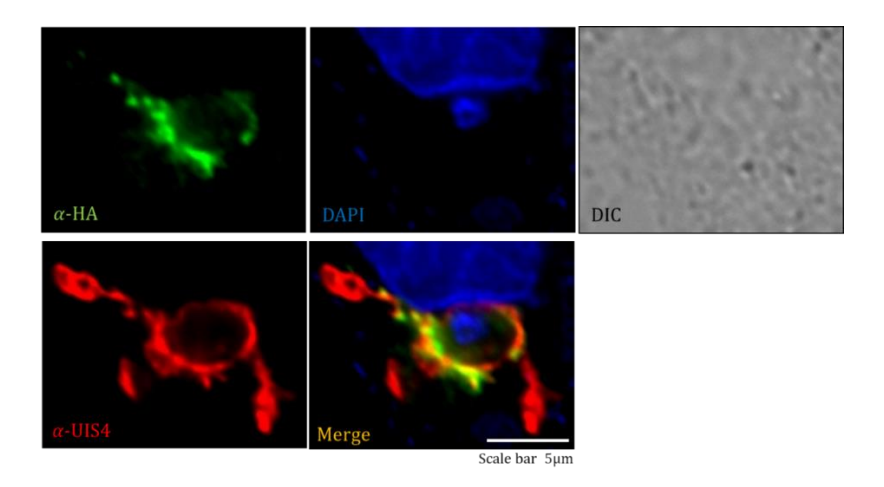


Figure:14 *Pb*RON6-3xHA is colocalizing with parasitophorous vacuolar membrane. The liver stage development and co-localization of *Pb*RON6. Approximately 2 x 10⁴ isolated *Pb*RON6 salivary gland sporozoites were co-cultured with HepG2 cells. The cultures were fixed at 36 hours and stained with anti-HA (mouse monoclonal) and anti-UIS4 (rabbit) primary antibodies, and immunoreactivity was detected using Alexa fluor 488 anti-mouse and Alexa fluor 596 anti-rabbit antibodies. The nucleus was stained with DAPI.

The C-terminus of *Pb*RON6 is extracellular

Our IFA studies showed an association of *Pb*RON6 with the membrane and the apical end of salivary gland sporozoites. We further tested the possible orientation of the C- terminal HA tag, by performing IFA without permeabilization. Towards this, we performed IFA using two different commercial anti-HA antibodies. Co-staining of sporozoite was done with 3d11, (sporozoite membrane marker) and anti-HA antibodies under non-permeabilisation conditions. The immunoreactivity of 3d11 and HA was revealed respectively using Alexa fluor 488 anti-mouse and Alexa fluor 596 anti-rabbit secondary antibodies. This observation provided compelling evidence that the membrane-associated *Pb*RON6 has a C-terminal domain, that is extracellular, though the precise amino acid sequence of this domain is not known.

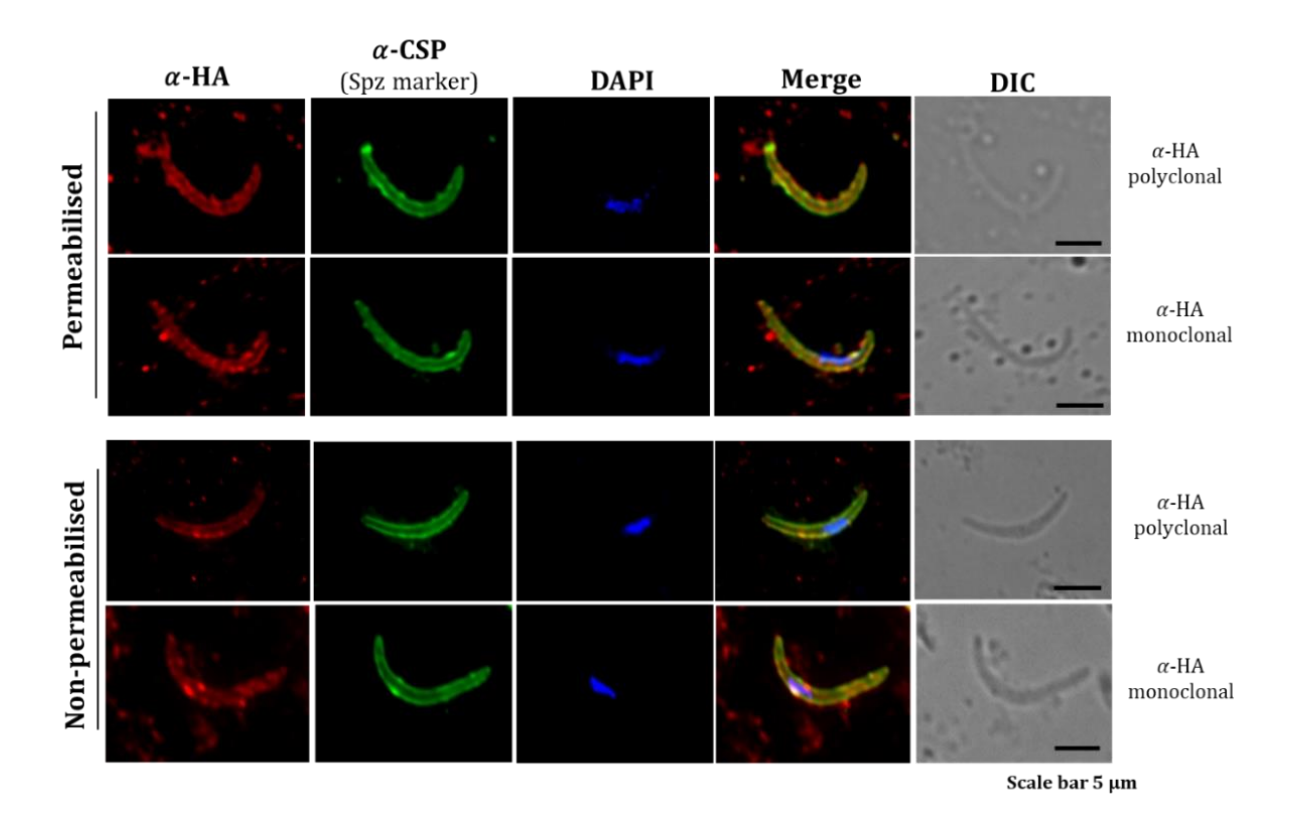


Figure 15: The sporozoite membrane localized *Pb*RON6 has a C-terminal domain that is likely extracellular. The co-localization studies using sporozoite membrane marker- 3d11 and anti-HA antibodies under non-permeabilised conditions revealed that the C- terminal HA tag is extracellular. The nucleus was stained with DAPI.

The *Pb*RON6-3xHA sporozoites are targets for anti-HA antibodies as evident by delayed pre-patency and enhanced the survival rate of mice

Having shown that the PbRON6 is associated with sporozoite membrane and the C- terminal HA tag to be extracellular, we next tested if the extracellular domain can be targeted with commercial anti-HA antibodies, to achieve sporozoite neutralization. Sporozoite neutralization assay was carried out at room temperature by incubating $5X10^3$ sporozoites for 35 minutes, with either two commercial anti-HA antibodies viz., rabbit monoclonal (#Cat. No. ab236632) and rabbit polyclonal (#Cat. No. ab9110) or 3D11, which targets CSP, that served as a positive control. Sporozoite neutralization assays were performed at two concentrations- 2.5 µg and 5 µg. A similar number of untreated sporozoites, and iso-type specific IgG-treated sporozoites served as negative control. After neutralization, the sporozoites were injected intravenously into C57Bl6 mice (5 per group) and infectivity was assessed from day 3 onwards, by observing Giemsa-stained smears. All mice that received sporozoites neutralized with anti-rabbit HA polyclonal antibody (Cat. No. ab9110) developed prepatency by day 4.5. In the group of mice that received sporozoites neutralized with anti-rabbit HA monoclonal antibody (Cat. No. ab236632), one developed prepatency by day 6.5, and remaining 4 developed blood-stage infection by day 10. The group of mice that received sporozoites neutralized with 3D11 antibody, developed prepatency on day 10. All mice that received untreated sporozoites or treated with isotype-specific IgG developed an infection around day 3.5-4. Sporozoite neutralization assays with 2.5µg of antibody concentration for all aforementioned groups showed a prepatency of 3.5 days. Taken together, our observations suggest a neutralization potency of antirabbit HA monoclonal antibody, on par with 3d11, at a concentration of 5 µg concentration. The observations also suggest the feasibility of targeting the C- terminus of native RON6 protein on sporozoite surface, as a means to reduce the incidence of sporozoite infection to hepatocytes.

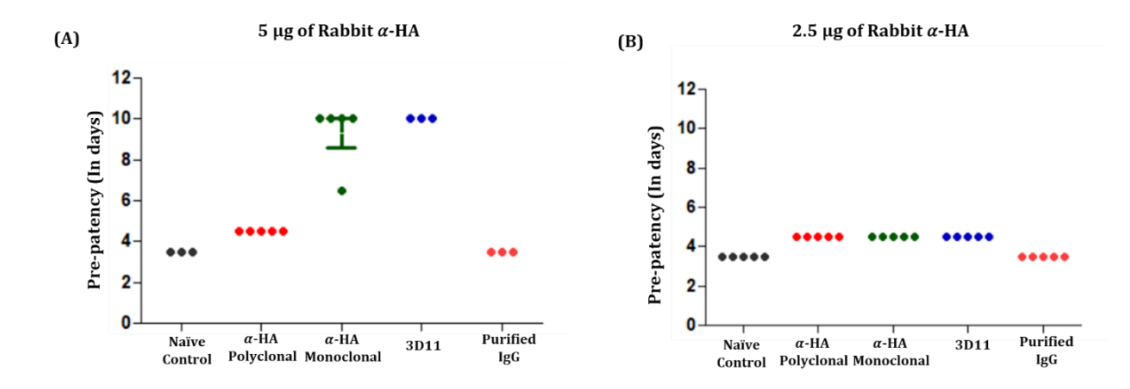


Figure:16 Prepatency in mice receiving i.v., sporozoites neutralized with anti-HA antibodies at 5 μ g and 2.5 μ g concentrations (A) Sporozoites neutralized with rabbit polyclonal HA antibody-initiated blood-stage infection in all five mice in 4.5 days whereas sporozoites neutralized with rabbit monoclonal HA antibody-initiated blood stage infection on day 10 in 4/5 mice while one mouse, developed infection on day 6. Furthermore, we observed that the anti-CSP-neutralized sporozoites resulted in a blood-stage infection on day 10. The untreated sporozoites and iso-type specific treated IgG sporozoites yielded infection on day 3.5. (B) The sporozoite neutralization assay was repeated with 2.5 μ g concentration antibody, that showed no delay in prepatency, in all tested groups.

Since the rabbit anti-HA monoclonal clonal antibody effectively delayed prepatency, we next measured the duration of mice survival in different groups exposed to neuralised sporozoites. We generated Kaplan-Meier survival plots for all groups of mice under study. We noted 19-20 days of survival in mice that manifested delayed prepatency i.e., sporozoites—treated with 5µg antibody of either anti-rabbit HA monoclonal antibody and 3D11. Interestingly, the mice that received anti-rabbit HA poly antibody, though showed pre-patency on day 4.5, yet survived for 16-18 days. The survival of mice that received 2.5 µg antibody treatments from all groups was similar to the non-treated group or isotype IgG-control group. Taken together, following exposure of RON6-3XHA sporozoites to anti-HA antibodies significantly delayed the prepatency, who duration matched the 3d11 treated sporozoites. A likely explanation for the enhanced survival of mice may be a reduction in sporozoite infectivity following exposure to anti-HA treatment.

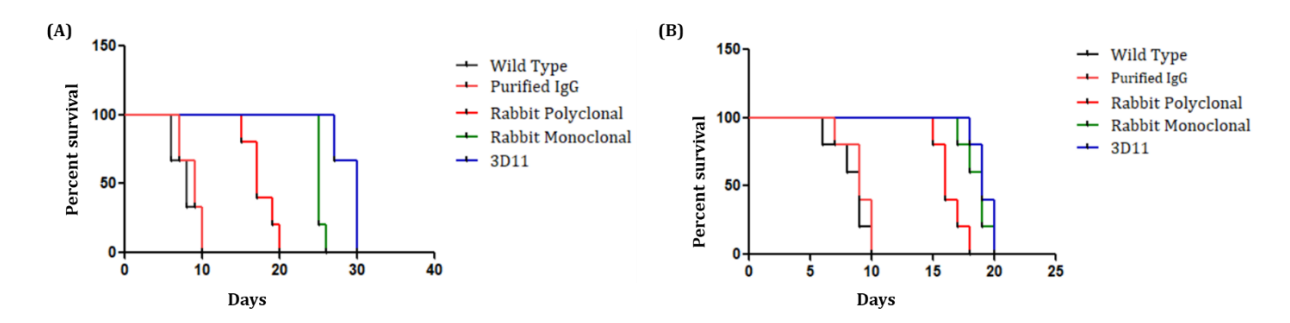


Figure 17: Kaplan-Meier survival plots for mice receiving neutralised sporozoites: The survival rate of mice that received (A) 5μ g antibody-neutralized sporozoites and (B) 2.5μ g of antibody-neutralized sporozoites. Mice that have received HA polyclonal-treated sporozoites have survived up to 16-18 days, and mice that have received untreated sporozoites have survived a maximum of 8.5- days.

Both 3d11 and anti-HA antibodies neutralize RON6-3xHA sporozoites using a distant mechanism

Owing to the delay in prepatency, we next wanted to investigate the fate of RON6-3XHA tagged sporozoites, following their exposure to anti-HA antibodies. A well-known mechanism of sporozoite inactivation is achieved when sporozoites are exposed to 3d11, which results in binding to CSP, a major sporozoite surface antigen. The CSP-antibody complex is shed from the posterior end of the parasite in a "precipitin reaction, that can be visualized under a microscope, as the complex gets slouged off during sporozoite gliding movement [233], finally leading to their immobilization [234]. The shedding of the CSP-antibody complex is due to the exocytosis of CSP, following its proteolytic cleavage by another sporozoite membrane resident cysteine protease [28]. Since we demonstrated that RON6 is localized on sporozoite membrane, we next asked if RON6 is also secreted through exocytosis. To this end, we incubated 5X10³ PbRON6-3XHA sporozoites with 1µg of anti-HA-rabbit monoclonal or 3d11 (as a positive control) at 37°C for 30 min and visualized under phase contrast microscope. Sporozoites treated with 3D11, as expected, exhibited precipitin reaction, however, no such activity was noted with the RON6-HA sporozoites. In fact, antibody treatment did not arrest the motility of the transgenic sporozoites. To rule out the possibility of low or undetectable levels of PbRON6 constitutive exocytosis, we also next analysed if RON6 can be detected in supernatant collected from sporozoite incubated medium. For this, we incubated 3X10⁵ RON6HA transgenic sporozoites in 20ul complete medium and 10ul aliquot of sporozoite incubation media was collected at 30 min and 60 min time points. Supernatants and pellets generated from both time points were

subjected to Western blotting to analyse the levels of CSP and RON6HA. We noted a dose-dependent release of CSP in the supernatants, while RON6HA was not released. However, in the pellet fraction, we noted RON6HA expression, whose levels were much lower as compared to CSP. We conclude that no detectable processing of *Pb*RON6 likely happens on the surface of sporozoite.

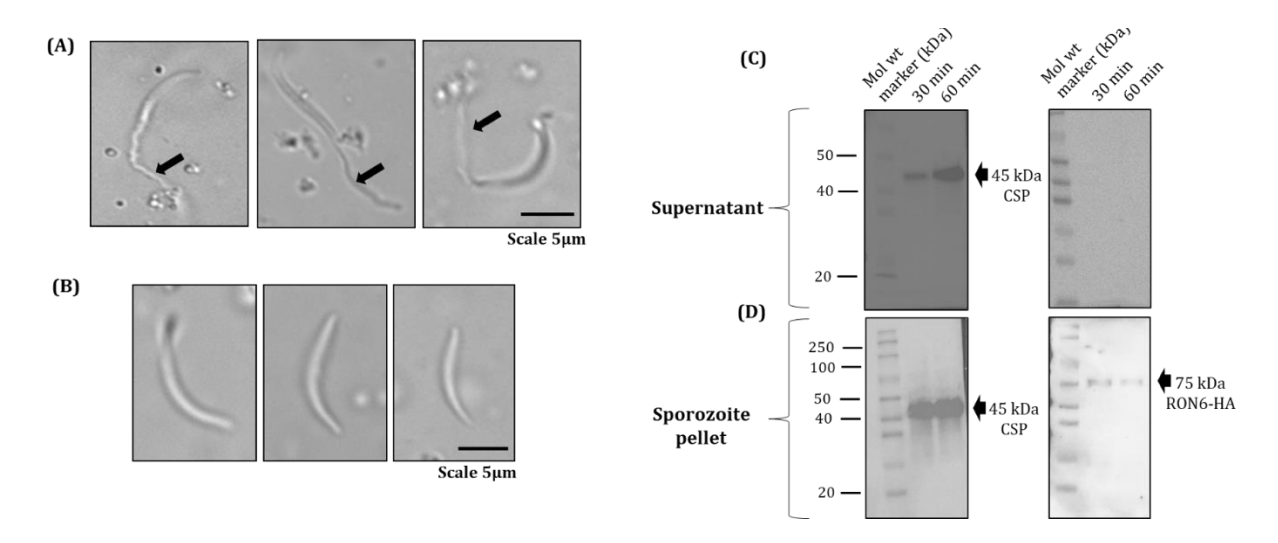


Figure: 11 During sporozoite exocytosis, CSP is released *Pb***RON6 is secreted from the sporozoite surface. (A)** 3D11 (anti-CSP) antibody-treated sporozoites showing precipitin reaction; **(B)** anti-HA-treated sporozoites don't show any reaction **(C)** western blot analysis reveals that the CSP was present in the supernatant but the RON6 is not present in the supernatant **(D)** the RON6 was identified in the pelletm, however the expression levels but the size of pellet is smaller than the CSP in the pellet.

What explains the delay in prepatency, of anti-HA treated sporozoites, at levels comparable to 3d11? Opsonisation is the most common outcome of antibody (ab) coating the pathogens and is mediated by a variety of Fc and complement receptors present on phagocytic cells (monocytes, neutrophils, natural killer (NK) cells, and dendritic cells). We reasoned the possibility of sporozoite bound HA-antibodies to be phagocytosed through Fc receptors. To test this, we added anti-HA or 3d11 incubated sporozoites to RAW cells, a murine macrophage cell line. As expected, majority of 3D11 coated sporozoites were taken up by the RAW cells as observed at 7h post addition of sporozoites. Interestingly we noted none of the internalized sporozoites were intact. We noted remnants of sporozoites, highly disintegrated, in vesicle-like structures following staining the CSP. Interestingly the CSP staining colocalized with Rab5- an early endosomal marker. However, the anti-HA treated RON6-HA sporozoites were predominantly extracellular, indicating their lack of opsonization.

Currently, we are investigating if anti-HA treated sporozoites can be targeted by complement proteins- to account for delay in prepatency.

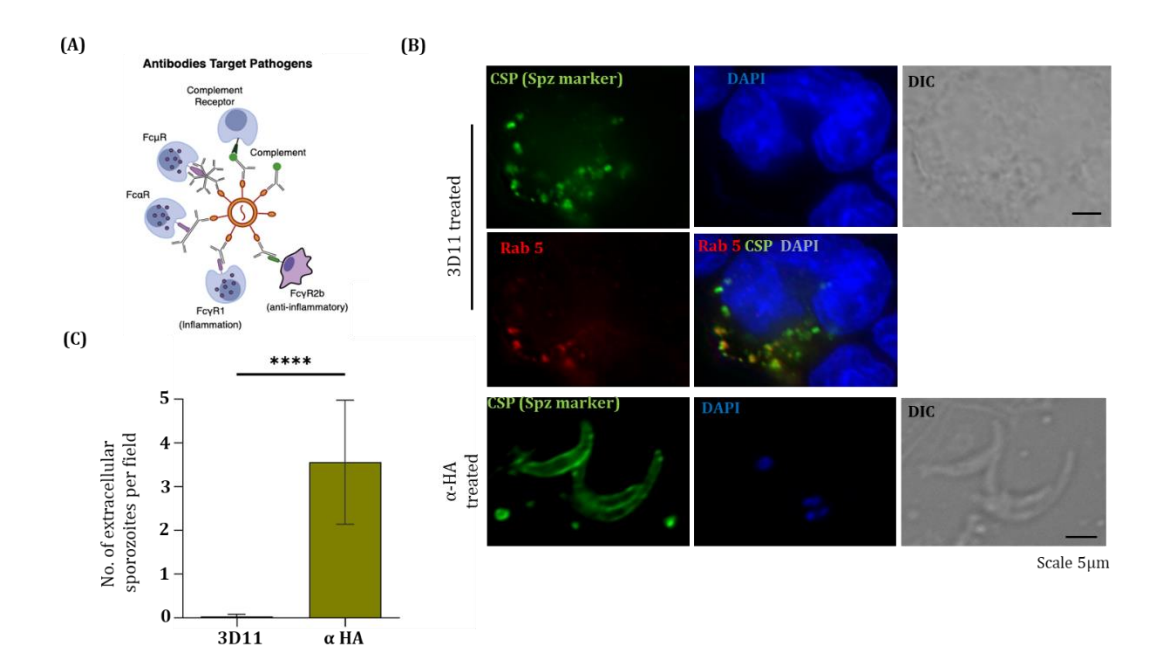


Figure 12: Fate of 3D11 and anti-HA rabbit monoclonal treated *Pb*RON6-3xHA transgenic sporozoites in mouse macrophage (RAW) cell line (A) Diagrammatic representation of antibody-mediated opsonization. (B) *Pb*RON6-3xHA sporozoites incubated with either 3D11 or anti-HA rabbit monoclonal antibodies for 30 min at room temperature and added to RAW cell line. After 7 h, indirect immunofluorescence assay was performed using 3D11 to visualize sporozoites and rabbit anti-Rab5 was used to stain macrophage endosomes. The immunoreactivity was revealed with Alexa Fluor 488 conjugated anti-mouse and Alexa Fluor 594 conjugated anti-rabbit secondary antibodies. Nuclei were stained with DAPI. Scale bar -5 μ m. (C) Bar graph showing 3D11 or anti-HA treated *Pb*RON6-3xHA transgenic sporozoites that were extracellular quantified at 7 hpi. Error bars represent mean with standard deviation (**** = p<0.0001, Mann–Whitney test).

*Pb*RON6-3XHA appear as discrete speckles on sporozoite membrane following exposure to 37°C and host cells

The proteins of the rhoptry compartment have been implicated in both the formation of MJ and later, as a sieve to form the PVM to harbor EEF inside the hepatocytes [235]. For the formation of MJ, the rhoptry protein accumulates at the apical end of the zoite, is translocated onto the host membrane, and establish connection with a preformed RON2- AMA-1 complex [236]. As these are the events associated with invasion of sporozoites into HepG2 cells, we reasoned whether

temperature shift and HepG2 cell contact upregulate sporozoite-specific expression of *Pb*RON6-3XHA. To this end, we analysed *Pb*RON6-3XHA expression on sporozoites under three conditions, viz., immediately after isolation from salivary glands, 30 min after exposure to 37°C, and 30 min after exposure to 37°C in the presence of HepG2 cells. The HA levels were analysed visually by IFA, and the sporozoite was counter-stained with 3d11. The parasite and host cell nuclei were stained with DAPI. We noted very meager levels of RON6-HA levels in immediately dissected sporozoites, while sporozoites exposed to 37°C had some appreciable levels of protein appearing on sporozoite membrane. However, we noted a dramatic accumulation of RON6 at several foci, as discrete spots on the sporozoite membrane when incubated with host cells. We conclude that RON6 levels induced during host cell contact may prepare the sporozoites for hepatocyte invasion.

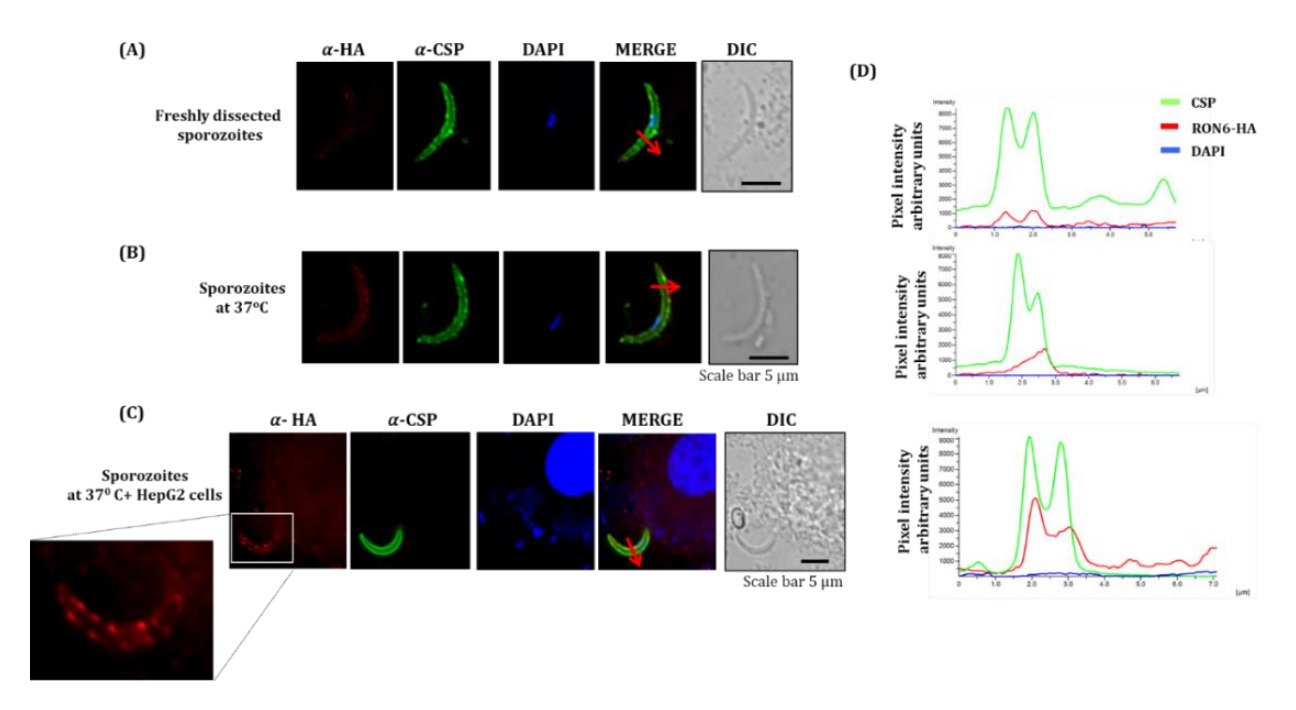


Figure: 13 The levels of *Pb*RON6-3xHA associated with sporozoite membrane were assessed in three different conditions. (A) Immediately after isolation from salivary glands. (B) After incubation of sporozoites at 37° C for 30 min and (C) after incubation of sporozoites at 37° C for 30 min in the presence of HepG2 cells. The sporozoites were stained with anti-HA rabbit and anti-CSP mouse monoclonal antibodies. Immunoreactivity was revealed respectively with Alexa Fluor 594 conjugated goat anti-rabbit and Alexa Fluor 488 conjugated chicken anti mouse secondary antibodies. Nuclei were stained with DAPI. Enlarged inset from bottom panel shows accumulation of RON6-3xHA at discrete foci on sporozoite membrane. The right panels show the pixel intensity profile and colocalisation of HA and CSP for all three conditions measured by cross sectional imaging using NIS-element AR software. Scale bar – 5 μ m.

Identification of potential interacting partners of PbRON6 by Immunoprecipitation/IP

To investigate the interacting partners of *Pb*RON6, we performed immunoprecipitation (IP), followed by LC/MS-based protein identification. The anti-HA antibody was conjugated to protein A/G bead and the lysates were incubated overnight at 4C with gentle agitation. The purified IgG was used as a negative control. The eluate was analysed on a western blot that revealed the presence of RON6-3xHA tagged protein in IP samples using an anti-HA antibody, and no band was detected in IP using isotype-specific IgG. Table B summarizes the most probable interacting partners for which >2 peptides were detected in LC/MS analysis.

The interactome study allowed the identification of discovered new partners that interact with *Pb*RON6 and are crucial for the invasion of merozoites during the asexual stage. These partners include apical complex proteins such as RON6, RON3, ROP14, and apical merozoite protein. The inner membrane complex protein consists of RON6 and CLAG, whereas the merozoite surface proteins comprise RON6, MSP1, MSP, and MSRP2. Previously identified interacting partners of the merozoite invasion of RBC include apical proteins such as RON2, AMA1, RON4, RON5, RAMA, and RHop2 [237], [238]. The inner membrane complex proteins contain GAP45, GAP50, and MSP1 [239], and the merozoite surface proteins contain MSP1, MSP9, MSP2, MSP3, PVP2, and PVP5 [69, 240].

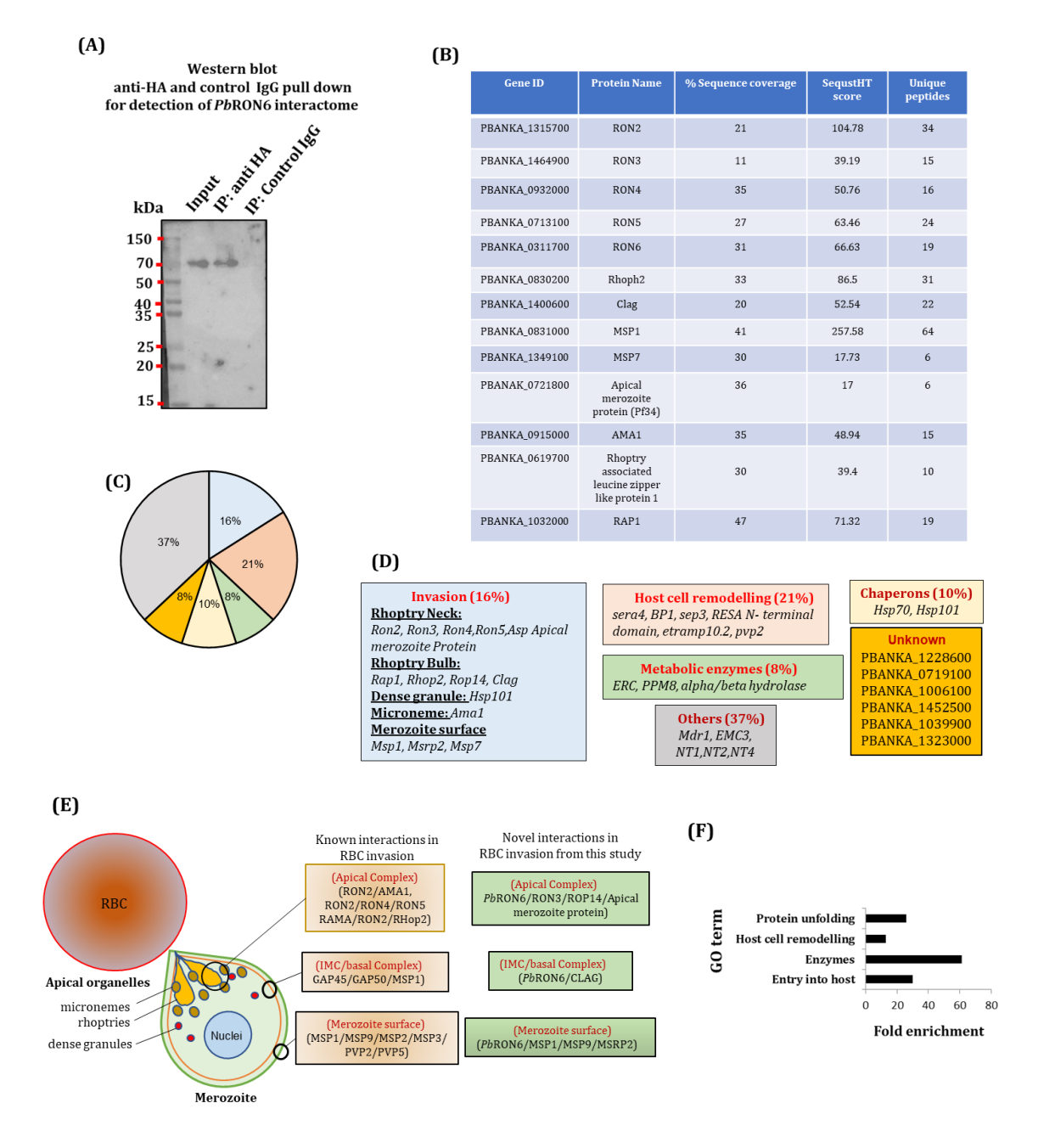


Figure: 14 Identification of *Pb***RON6 interactome by LC/MS analysis. (A)** Western blot showing the presence of *Pb*RON6 both in the schizont lysate (input) and proteins pulled down using anti-HA antibody. *Pb*RON6 was not detected in immunoprecipitation (IP) performed with pre-immune IgG (negative control). **(B)** List of *Pb*RON6 interacting partners identified by LC/MS analysis with significant sequestHT score. **(C)** Pie diagram showing the percentage of genes categorized in individual clusters identified by functional gene ontology (GO). **(D)** Functional clusters showing the list of proteins interacting with RON6 detected in LC/MS analysis by co-immunoprecipitation using HA antibody. **(E)** Schematic showing probable novel invasion-related complex identified in this study. **(F)** Validation of GO term ID for each cluster with fold enrichment >10 and p<0.05 identified in co-immunoprecipitation of *Pb*RON6::3xHA schizont lysate using rabbit anti-HA monoclonal antibody.

Quantitative expression profiling of Pbron6 gene

To investigate the expression of *Pbron6* throughout all the life cycle stages of *Plasmodium berghei*, we performed quantitative real-time PCR (qRT-PCR) by absolute quantification method. cDNA was synthesized from all the stages of *Plasmodium* and qRT-PCR was performed by amplifying *Pbron6* or *Pb*18s rRNA transcripts from cDNA template. The gene-specific standards were generated both for *Pbron6* or *Pb*18s rRNA that was used in a log dilution to set up a dynamic range of standards. The copy number of *Pbron6* or *Pb*18s rRNA was deduced from gene-specific standards. We have observed the maximum transcripts of *Pbron6* mid-gut sporozoites, followed by mixed blood-stage, and low early liver stage 13h post-infection. The transcripts were calculated from the lowest level of transcripts was observed in the early liver stage.

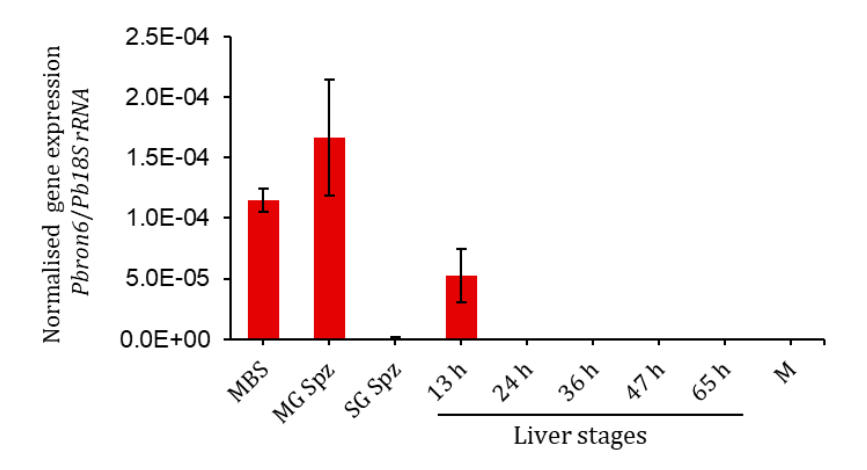
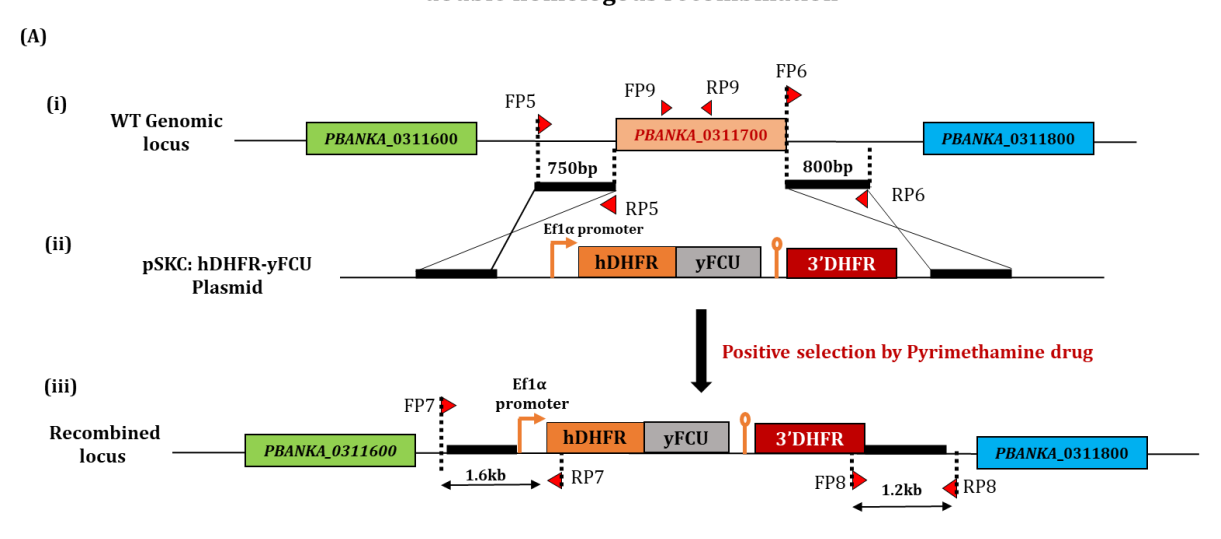


Figure 16: Gene expression analysis of *Pbron6* **from different life cycle stages by quantitative real time PCR.** The cDNAs generated from different stages are as indicated - MBS: mixed blood stages; Mg Spz: midgut sporozoites; SG Spz: salivary gland sporozoites; Liver stages at 13 h, 24 h, 36 h, 47 h, and 65 h post infection of HepG2 cells with sporozoites and M: merosomes collected from the supernatants of liver stage cultures. Data normalisation was performed by taking ratio of absolute copy numbers of *Pbron6* and *Pb18s rRNA*.

Generation of *Pbron6* KO by double homologous recombination with hDHFR-yFCU cassette:

To investigate the functional role of *Pbron6* across all the life cycle stages of *Plasmodium*, *Pbron6* KO parasites were generated by double homologous recombination. In this approach, the endogenous *Pbron6* locus was replaced by a targeting construct carrying hDHFR-yFCU dual selection cassette, that allowed respectively the positive selection of KO transfectants, and enrichment of complemented parasites by negative selection, following targeting KO locus. After transfection, the stably integrated hDHFR enabled a positive selection of KO mutants under the cover of pyrimethamine, an anti-malarial drug (Figure: 17 A). The KO parasites were confirmed by diagnostic PCR, where the recombined locus was confirmed by amplifying products from 5' and 3' regions using a primer that flanked beyond the sites and recombination and within the stably integrated KO locus. cassette. An expected 1.5kb size of PCR product was amplified by using FP3 and RP3-specific primers from 5' integration. Similarly, 3' integration was confirmed by 1.1 kb product size using FP4 and RP4 primers. The KO parasites were further subjected to limiting dilution and two independent *Pbron6* KO isogenic lines were isolated for further phenotypic characterization. The clonal population was confirmed by the complete absence of wild-type locus in PCR performed with the two independent *Pbron6* KO isogenic lines (Figure: 17 B).

Strategy to generate *Pbron6* (*PBANKA_0311700*) KO by double homologous recombination



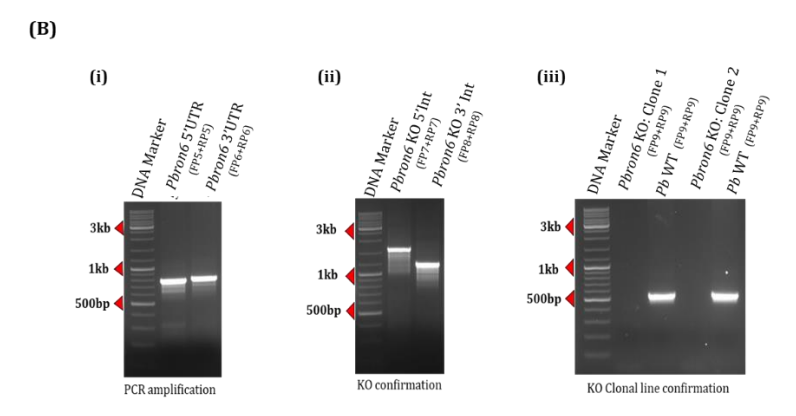


Figure 17: (A) Strategy for generating *Pbron6* KO line by double homologous recombination (i)Organization of the *Pbron6* genomic locus. Two PCR products of 750bp and 800bp were amplified from the 5' and 3' regions of *Pbron6* using primer pairs FP5/RP5 and FP6/RP6. The products were cloned respectively into MCS-I and MCS-II regions of the transfection vector. (ii) The targeting construct carrying hDHFR-yFCU dual selection marker and 5' and 3' homology arms of *Pbron6* at its termini. (iii) Recombined locus after successful double cross-over recombination. (B) KO line confirmation by genotyping (i) Agarose gel showing the amplification of 5' and 3' regions of *Pbron6* amplified from genomic DNA of WT parasites. (ii) Diagnostic PCR showing correct integration of KO construct at *Pbron6* locus as confirmed by PCR product sizes of 1.5kb and 1.2kb amplified with primer sets FP7/RP7 and FP8/RP8. (iii) PCR product of 500bp amplified within *Pbron6* locus of WT line and not *Pbron6* KO line (FP9+RP9).

The *Pbron6* mutant parasites exhibits slow asexual growth and decreased the virulence

To investigate the functional role of *Pb*RON6 across all the life cycle stages of *Plasmodium*, knockout mutant (*Pbron6* KO) was generated by double homologous recombination. The *Pbron6 orf* was replaced with hDHFR-yFCU dual selectable marker cassette and correct integration was confirmed by integration specific diagnostic PCRs that showed expected products of 1.6 kb and 1.2 kb that confirmed the 5' and 3' integrations respectively. The null mutants were cloned by limiting dilution and clones from two independent transfections were isolated for further phenotypic characterization. Genotyping of clonal population by PCRs confirmed the absence of *Pbron6 orf* in clonal lines. Asexual propagation of *Pbron6* KO line in mice was determined by delivering 1x10³ mutant parasites intravenously. A similar number of WT parasites were injected that served as control. We observed a gradual increase in parasitemia of WT line from approximately 4.5% to 17% during days 5-8, while the parasitemia of mice harbouring *Pbron6* KO mutants did not exceed more than 1% during the same duration. The slow growth phenotype of mutant was manifested identically, in two null mutant clones derived from independent transfections. The data provided compelling evidence for the requirement of *Pbron6* in normal propagation of asexual stages. Considering that

Pbron6 showed high expression in the mixed blood stage, lack of expression may impact either growth of the parasite or reinvasion of freshly egressed merozoites, thus slowing down the parasitemia. To test this hypothesis, we injected intravenously $1x10^9$ synchronised schizonts of *Pbron6* KO and WT line into Swiss mice. Parasitemia was monitored every 6 h for a duration of 48 h, which allowed capturing reinvasion of freshly egressed merozoites into RBC, thus enabling the analysis of any defect in this process. We noted a progressive increase in parasitemia from 0.4 to 1.5% in WT. During this time, the parasitemia of mutant line increased only in an incremental manner from 0.2% to 0.5%. Our observation reiterated that the reduced asexual propagation noted in earlier experiments was indeed associated with reduced invasion efficiency of erythrocytic merozoites. A likely explanation for the observed phenotype is that *Pb*RON6 may be required for the formation of moving junction, and its altered composition in the absence of *Pb*RON6 may dramatically impact, but not totally abrogate invasion.

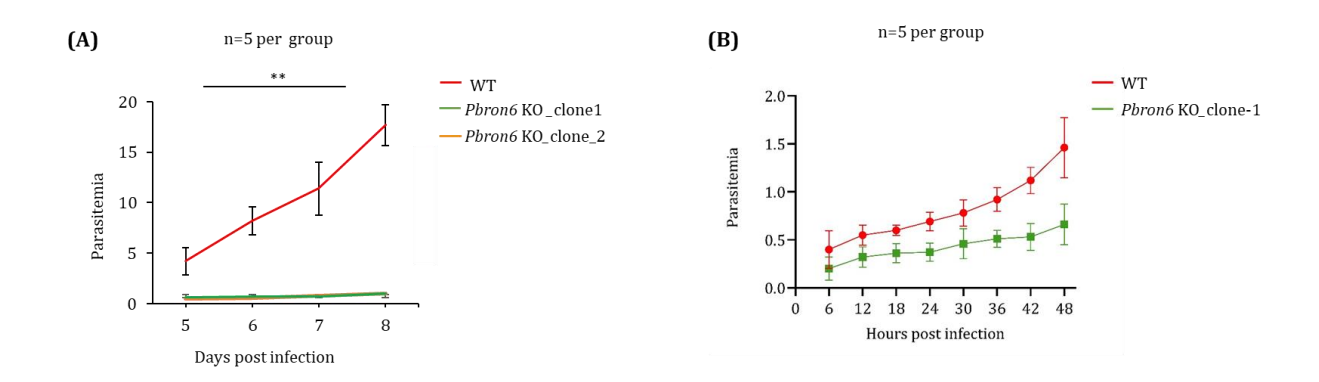


Figure 18: Asexual propagation of Pbron6 KO mutant parasites. (A) Asexual growth propagation of **Pbron6** KO clone-1 and clone-2 in BALB/c mice. $1x10^3$ infected RBCs of WT, **Pbron6** KO clone-1 and clone-2 were injected intravenously in all three groups of BALB/c mice (n=5/group). Parasitemia was monitored by reading the Giemsa-stained blood smears. Error bars represent the mean with standard deviation (**p<0.005, one-way ANOVA with Tukey's multiple comparison test). **(B)** Reinvasion assay was performed *in vivo* by intravenous injection of $1x10^9$ purified schizonts of WT and **Pbron6** KO clone-1 into two groups of BALB/c mice (n=5). Parasitemia was monitored every 6 hours post infection by reading the Giemsa-stained blood smears. Error bars represent the mean with standard deviation (**p=0.0045, Mann-Whitney test).

As mutant parasites lagged in asexual propagation, we next assessed the survival rate of mice harbouring the mutants. To this end, we injected by an i.v., route approximately 1X10³ *Pbron6* KO parasites and wild-type parasites in female C57BL/6 mice (n=10 per group). We generated Kaplan-

Meier plots to represent the survival rate of both groups of mice. We noted mortality in mice infected with WT parasites during days 8-16, while the survival of mice harbouring mutants, were significantly prolonged, with mortality occurring on day 22-32 post infection. Taken together, *Pbron6* depletion affected both the reinvasion capacity and overall virulence of mutant parasite.

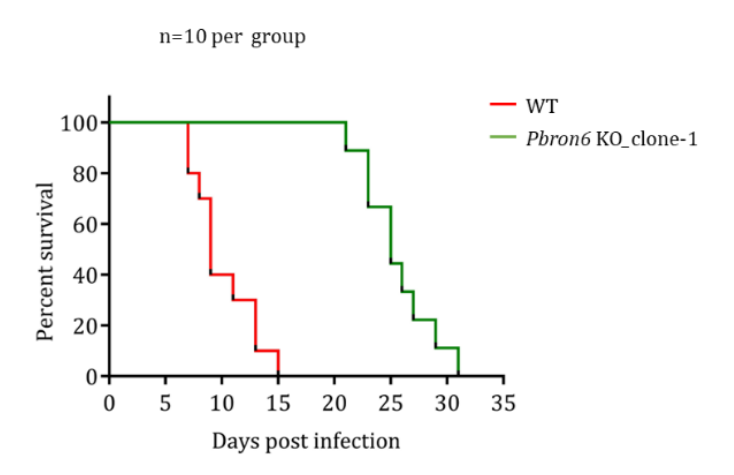


Figure 19: Kaplan-Meier plots, representing the duration of C57BL/6 mice survival, following infection with WT and *Pbron6* KO clone-1 (n=10, ***p<0.0001, Mantel-Cox test).

The Pbron6 knockout parasites exhibit normal development in the mosquito vector

To investigate the effect of the *Pbron6* depletion in the sexual stage of the parasite life cycle, female *Anopheles stephensii* mosquitoes were allowed to take a blood meal from gametocyte-positive mice, harbouring either WT or mutants. On day 14th post blood meal, the mosquito mid-guts were dissected and observed for the presence of oocyst. We noted that the mutants produced oocysts, with a pattern of sporulation that was indistinguishable from WT. In fact, the oocyst burden and the oocyst sporozoite numbers were similar to that of WT parasites. Since oocysts are derived from ookinetes, that breach the midgut epithelium and settle on the hemocoel side, we conclude that RON6 depletion also did not affect the formation of ookinetes. This observation concurs with the general notion that ookinetes that do not have rhoptries [241], remain unaffected when the composition of the rhoptry compartment is altered.

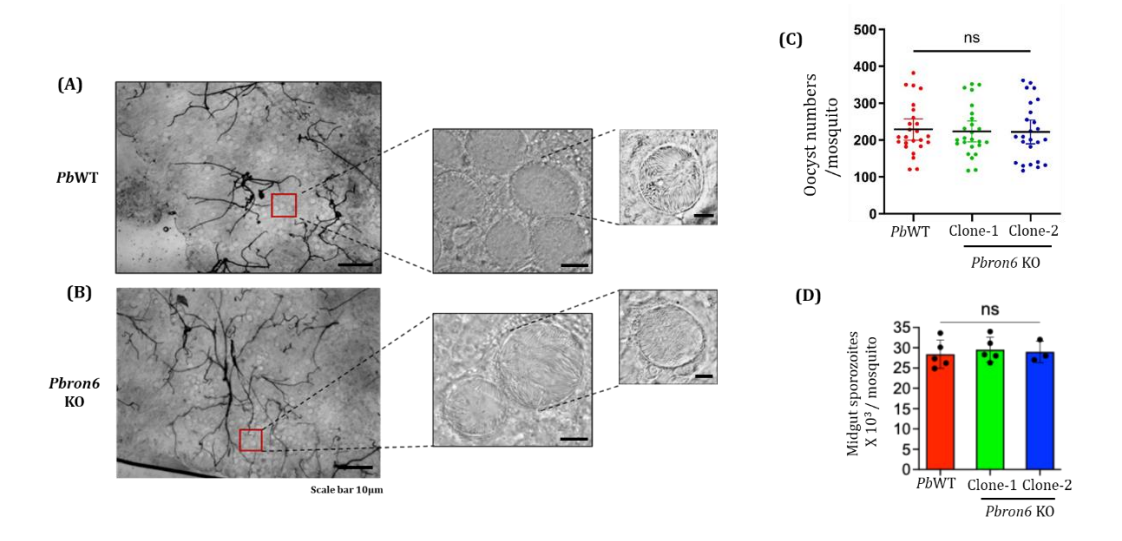


Figure 20: The deletion of *Pbron6* does not affect sexual reproduction, formation of oocyst and midgut sporozoites. Dissected mosquito mid-gut infected with **(A)** wild-type and **(B)** *Pbron6* KO parasites. The red insets show oocysts, that reveal sporulation **(C)** Quantification of oocyst numbers in mosquitoes (n=25) infected with WT and *Pbron6* KO. Data has shown as mean \pm SD. No significance difference (p=0.9857, one-way Anova). **(D)** The quantification of mid-gut sporozoites in mosquitoes (n=25) infected with WT and *Pbron6* KO. Data has shown as mean \pm SD. No significance difference (p=9918, one-way Anova).

We next analysed the ability of the mutant sporozoites to colonise the salivary glands. We dissected salivary glands on day 19 post-blood meal and analysed them under a light microscope. We noted the presence of *Pbron6* depleted sporozoites in glands, whose morphology and numbers were also indistinguishable from WT. Taken together, the mosquito stages of *Pbron6* KO manifested no alteration in phenotype, implicating a dispensable role in ookinete, oocyst, and salivary gland stages.

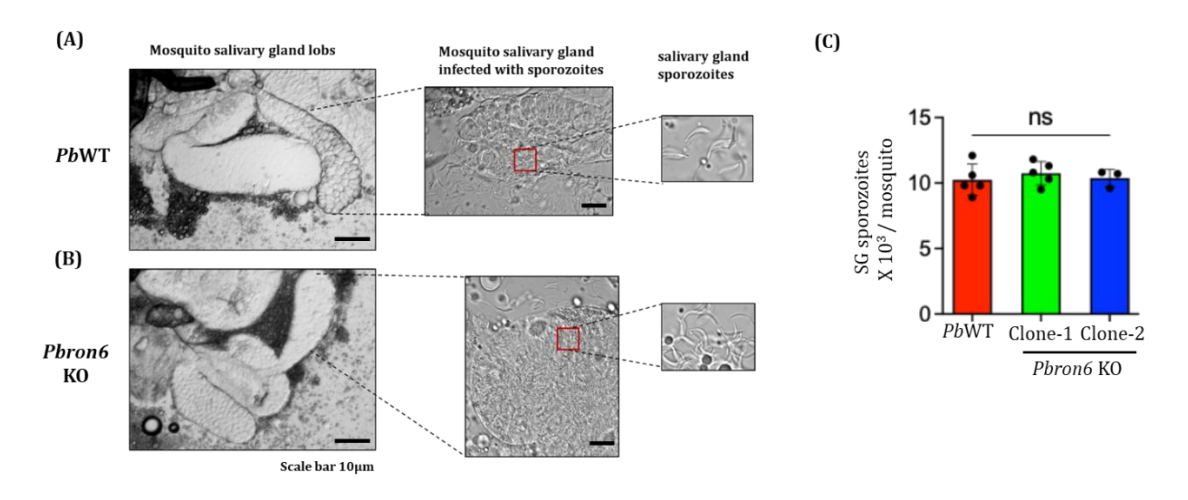
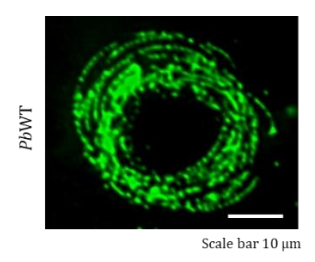


Figure 21: *Pbron6* **KO mutant successfully colonise the mosquito salivary gland: (A & B)** DIC images of intact salivary gland sporozoites harbouring wild type and *Pbron6* mutant line. The red outlined insets show individual sporozoites. The salivary glands that have been infected with both wild-type (WT) and *Pbron6* sporozoites. **(C)** The quantification of the sporozoites in the salivary glands harbouring WT and two independent clones of *Pbron6* KO (clone-1 and clone-2). The number of mosquitoes dissected per group was 25. The data has represented as mean ± SD. No significance difference (*p*=0.9918, one-way Anova).

The Pbron6 mutant sporozoites are not defective in gliding motility

Plasmodium sporozoites count on substrate-dependent, actin-based gliding motility to penetrate host cells and traverse cellular barriers. The motility of *Pbron6* mutant sporozoites was studied on glass slides precoated with 3d11 antibody. During process of sporozoite gliding, the shed CSP binds to the coated antibody. The antibody captured CSP was, in turn, detected by using biotin-conjugated 3d11 and revealed with FITC conjugated streptavidin. This approach revealed that both WT and *Pbron6* sporozoites displayed similar patterns of CSP trails, as well as normal gliding motility.



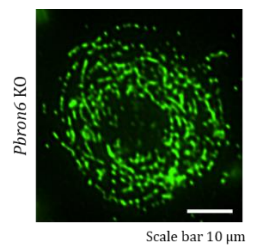


Figure 22: *Pbron6* **knockout sporozoites exhibit normal gliding motility.** Shown are the representative immunofluorescence images of CSP trails released by WT and *Pbron6* KO sporozoites. Scale bars = $10 \mu m$.

Pbron6 is required for the host cell invasion

Since erythrocytic merozoites were compromised to invade RBC under conditions of *Pbron6* depletion, we next investigated if other invasive stages like the salivary gland sporozoites had any discernible deficiency in hepatocyte invasion. We tested this hypothesis using a human liver carcinoma cell line (HepG2), that favors invasion and complete intrahepatic development of rodent *P. berghie* line. After addition of 2X10⁴ sporozoites of either WT or *Pbron6* KO mutants, the cultures were maintained for 1 hour at 37°C and fixed. A dual sporozoite staining assay called the "inside-out"

assay" was performed [242], which allowed quantification of the total sporozoites versus the non-invaded or extracellular sporozoites per field by staining these two populations with 3d11 antibody, receptively under non-permeabilised and permeabilised condition. The immunoreactivity was revealed with secondary antibodies conjugated to Alexa 488 under non-permeabilised conditions and with Alexa 596 after permeabilization. The data was recorded from 20 fields and the infectivity was expressed as average of the percentage of sporozoites inside the cells/ field. This approach revealed a 60% invasion for the WT sporozoites, while the mutant's invasion efficiency was nearly 20%. We conclude that mutant sporozoites, fail to efficiently invade HepG2 cells, in the absence of *Pbron6*.

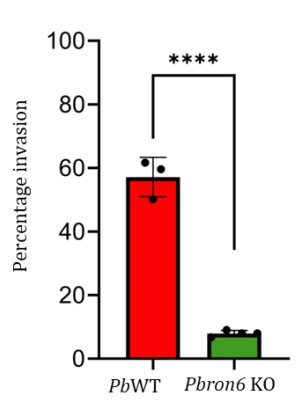


Figure 23: Inside-out assay for quantification of sporozoite invasion in HepG2 cells. PbWT and Pbron6 KO sporozoites were added to monolayers of HepG2 cells and cultures were fixed at 1h. The cultures were stained with 3d11 before permeabilization, and immunoreactivity was revealed with anti-mouse Alexafluor 488. Subsequently, after permeabilization, the cells were again stained with 3d11, and the immunoreactivity was revealed with anti-mouse Alexafluor 596. A total of 20 observed fields were viewed under a fluorescent microscope to count green and red sporozoites, which represented, respectively, the extracellular and total number of sporozoites respectively. The data has represented as mean \pm SD (****p<0.0001, Mann Whitney test).

The *Pbron6* knockout parasites exhibit delay in the pre-patency

We next tested the effect of compromised sporozoite infectivity on pre-patency, which is defined as the time required for detection of blood stages following delivery of infectious sporozoites. In two independent experiments, female C57BL/6 mice were infected intravenously with $5x10^3$ sporozoites of either Pb @ron6 or WT parasites. Parasitemia was monitored in all the animals from day 3 post-infection by making Giemsa-stained tail blood smears. Animals exposed to WT sporozoites

exhibited blood stage infection by day 3.5, whereas in mice infected with *Pbron6* KO mutant sporozoites, the pre-patency was day 8 (Table 2). When the experiment was repeated with 1x10⁴ sporozoites, we noted a pre-patency of 7.5 days in *Pbron6* KO mutant whereas WT infected mice showed 3.5 days. Given the already reduced invasion phenotype of the sporozoites, a delayed prepotency may simply be explained as the inability of mutant sporozoites to commit to hepatocytes, as efficiently as WT parasites. However, the possibility of any developmental arrest additionally contributing to the delayed prepatency cannot be ruled out.

Experiment Number	Parasite strain	Number of Animas	Number of sporozoites injected per animal	Number of animals positive for blood stage infection	Prepatent period (in days)
1	Wild Type	6	5X10 ³	6	3.5 days
	Pbron6 KO	6	5X10 ³	6	8 days
2	Wild Type	7	5X10 ³	7	3.5 days
	Pbron6 KO	7	5X10 ³	7	8 days
3	Wild Type	3	1X10 ⁴	3	3.5 days
	Pbron6 KO	3	$1X10^{4}$	3	7.5 days

Table 2: Table showing prepatency in mice exposed to two different doses of *Pbron6* KO and WT sporozoites viz., $5X10^3$ and $1X10^4$. The prepatency was detected by Giemsa-stained blood smears. The table shows details of parasite strain, sporozoites doses, number of animals used per experiment, number of animals positive for blood stage infection and prepatency period.

The *Pbron6* knockout parasites exhibit a reduced hepatocyte invasion and likely manifest a developmental delay in EEF development *in vivo*

To investigate the *in vivo* hepatocyte invasion efficiency, the parasite liver burden was estimated in mice infected with Pbron6 and WT parasites. C57BL/6 mice were injected with $5x10^3$ sporozoites intravenously and livers were isolated at 12 h and 48 h post infection. Total RNA was isolated from the livers, and approximately 2 μ g was reverse transcribed. cDNA samples were used to quantify the expression of Pb18S rRNA at 12 h and msp1 at 48 h by quantitative real-time PCR. Mouse gapdh was used as an internal control. The mutants manifested nearly 5-fold reduction in sporozoite commitment to hepatocytes as inferred from the Pb18S rRNA quantification at 12 h. We also noted a 65-fold reduction in liver burden quantified from msp1 expression at 48 h post infection. Taken together, Pbron6 depletion resulted in reduced efficiency of sporozoite invasion and also developmental arrest in mutant EEFs. The developmental arrest in liver may likely be implicated to the lack of association of PbRON6 with PVM in the developing EEFs in mutants.

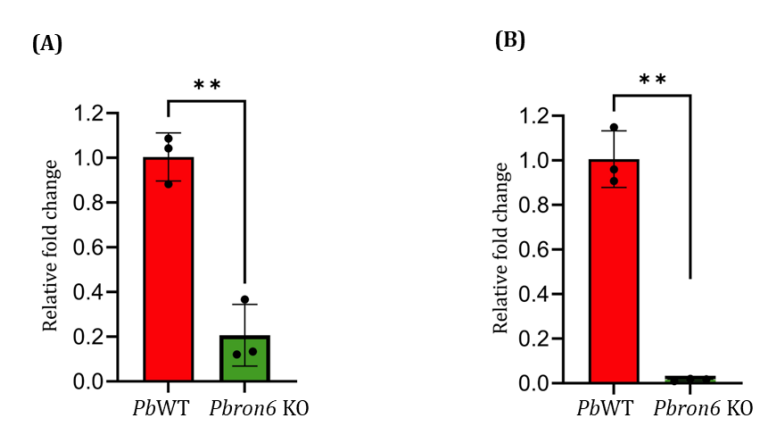
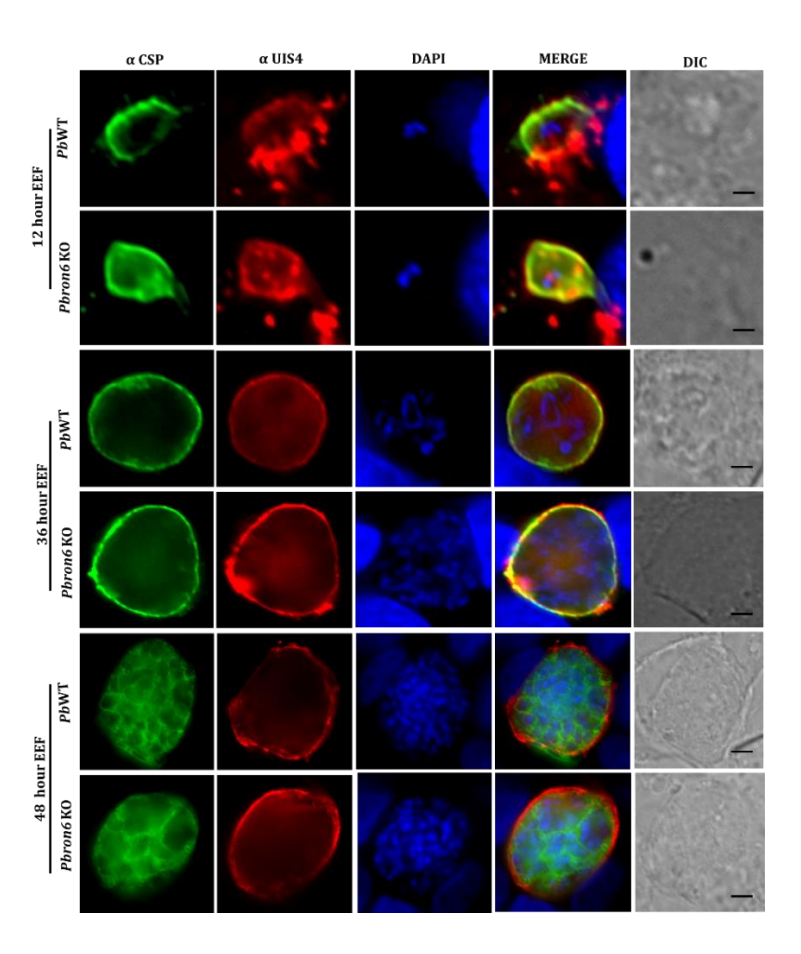


Figure 24: The quantification of liver burden of *Pbron6* KO and WT parasites by analyzing Ct values associated with 18SrRNA and MSP-1 markers at 12h and 48h respectively. (A) The graph representing the liver burden of *Pb*WT and *Pbron6* KO at 12 hours by measuring the Ct values of 18srRNA and mouse gapdh. We have observed low parasite burden in *Pbron6* KO with a statistically significant difference from *Pb*WT (p=0.0018, Mann Whitney test). (B) Graph representing KO sporozoite invasion efficiency measuring at 48 hours with *Pbmsp-1*. We observed reduced invasion efficiency in *Pbron6* KO with a statistical difference from *Pb*WT (p=0.0054, Mann Whitney test).

Pbron6 KO parasites exhibit developmental defect during EEF maturation in HepG2 cells.

Owing to the delay in prepatency in mice exposed to mutant sporozoites, we next analysed, if there was any developmental defect associated with EEF maturation. To test this, the HepG2 cells were exposed to 1.5×10^4 sporozoites of WT and *Pbron6* KO sporozoites, and the cultures were fixed at different time points of EEF maturation viz., 12h, 36h, 48h, 60h, and 65h. The 12h, 36h, and 48h parasites were stained with PVM marker, UIS4 and EEF marker CSP. The 60h and 65h were stained with MSP1 and UIS4. While no detectable size difference was observed in 12h EEF between WT and mutant, in all other developmental stages, we found that EEFs derived from mutant sporozoites were smaller that WT. We also observed a notable reduction in hepatic schizogony in 48h and beyond time point. This confirmed a developmental defect in mutant EEFs that was also reflected in the size of the cytomeres, that were much smaller in WT parasites as compared to mutants at 48h.



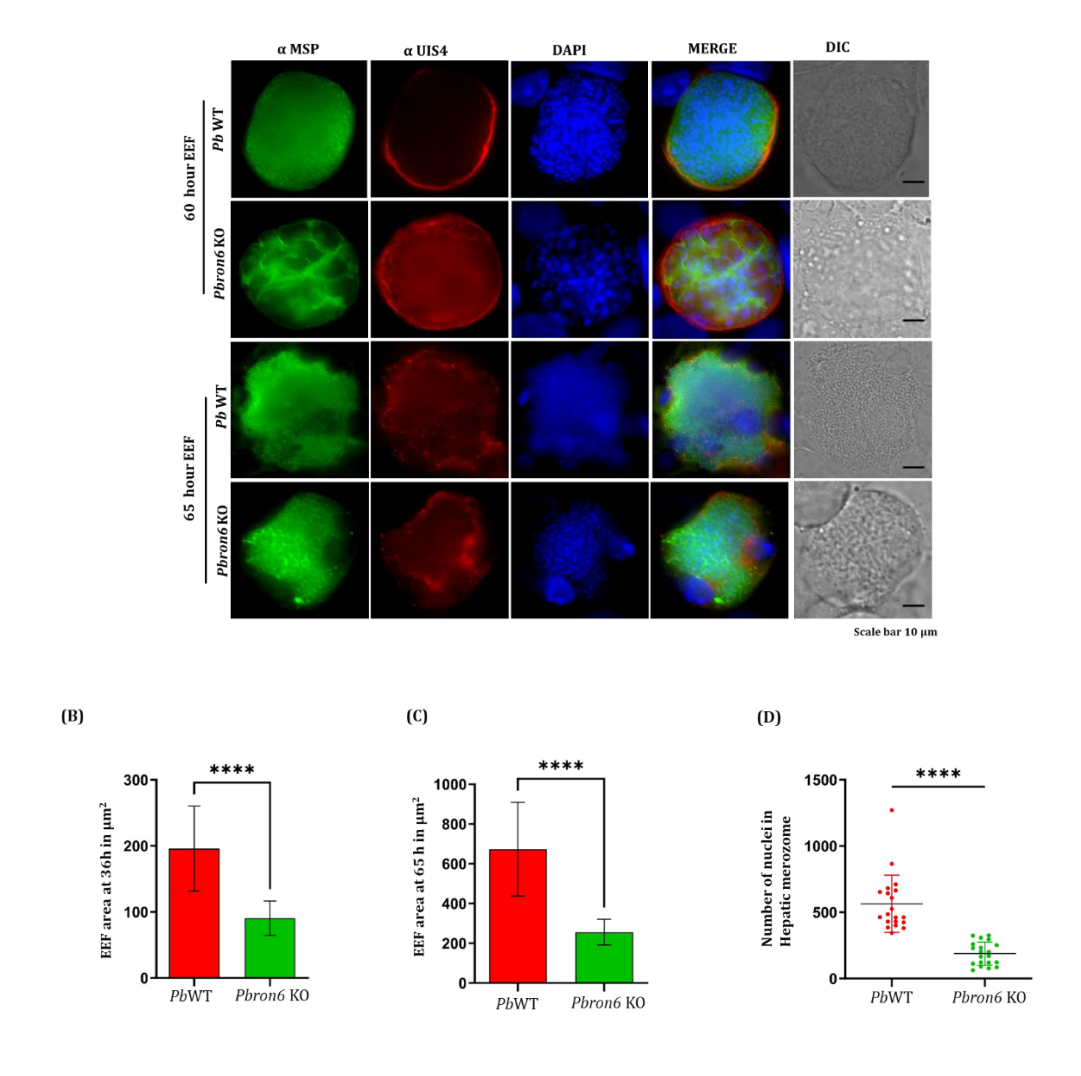


Figure 25: EEF development of sporozoites derived from *Pbron6* **KO** in **HepG2** cells **(A)** HepG2 cells were exposed to WT and *Pbron6* KO sporozoites and incubated for 65 hours. The EEF stained with 3d11, an EEF marker and with UIS4, PVM marker. The later liver stages were stained with MSP1. The loss of PVM boundary was very distinct in 60h and 65h time points. The CSP and MSP-1 immunoreactivity was revealed with Alexaflour 488 anti-mouse secondary antibody and UIS4 immunoreactivity was revealed with Alexaflour 596 anti-rabbit secondary antibody. **(B)**, **(C)** Graphs showing mean area EEFs (n=20). We have observed the EEF size as low in *Pbron6* KO with a statistical difference from *Pb*WT in 36 hours and 65 hours (****p<0.0001, Mann Whitney test). **(D)**. The scattered dot plot showing quantification of hepatic schizogony (n=20). We have noted the low number of hepatic nuclei in 65-hour merozome of *Pbron6* KO with a statistical difference from *Pb*WT (****p<0.0001, Mann Whitney test).

Restoration of the phenotype by complementing the *Pbron6* locus

To demonstrate that the observed phenotype in mutant was indeed due to lack of *PbRON6* expression, we complemented the *Pbron6* KO locus with *Pbron6* ORF. *To generate a complementation* construct, we replaced the hDHFR-yFCU marker in *Pbron6* KO construct with *Pbron6* ORF, that resulted in 5'UTR and 3'UTR flanking the *Pbron6* ORF, that were initially cloned at MCS-I and MCS-II to generate the *Pbron6* KO construct. Enriched schizonts cultures of *Pbron6* KO parasites were electroporated with linearized complementation constructs and the transfected parasites were subjected to negative selection by 5 flurouracil to eliminate non-recombinants. Following the negative section by the yFCU cassette, the complemented line was confirmed by diagnostic PCR using the gene-specific primers listed in Table 1.1

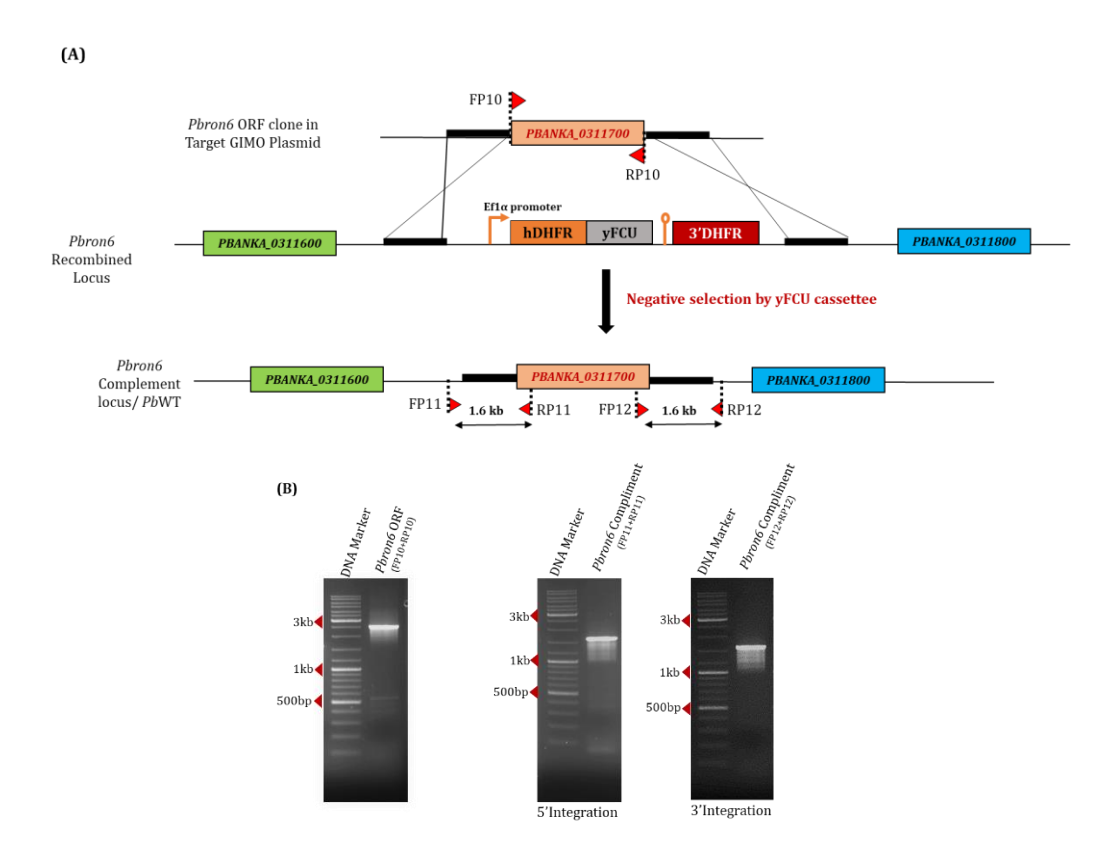


Figure 26: Schematic representation of complementing the *Pbron6* KO locus with *Pbron6* ORF. **(A)**. The GIMO (hDHER-yFCU) cassette in the genome of the KO line was replaced by the *Pbron6* ORF by double-crossover homologous recombination. **(B)**. The amplification of the *Pbron6* ORF and the genotypic characterization of *Pbron6* complement parasites were conducted using diagnostic PCR using specific primers, as shown in the image. The confirmation of integration at the 5' and 3' ends was accomplished using primer combinations FP11+RP11 and FP12+RP12, respectively. The replaced GIMO cassette was confirmed by gene-specific primers.

Restoration of asexual propagation rate in complemented parasites reduces the survival rate of mice

With the complemented parasites, we analysed the possibility of reversing the delayed asexual growth propagation noted in mutants. We injected by intravenous route, 1X10³ asexual parasites of WT or two clones of complemented line in three groups of Swiss mice (n=5) and monitored parasitemia from day 5 to 8 by Giemsa staining. We noted that both complemented clones propagated at rates comparable to the WT parasite. We also monitored the survival rate of mice in one of the complemented lines. We noted that all 5 mice succumbed to mortality during day 8-12, that was comparable to WT line. Thus, restoration of RON6 ORF in KO line, resulted in restoring the infectivity and virulence of the parasite.

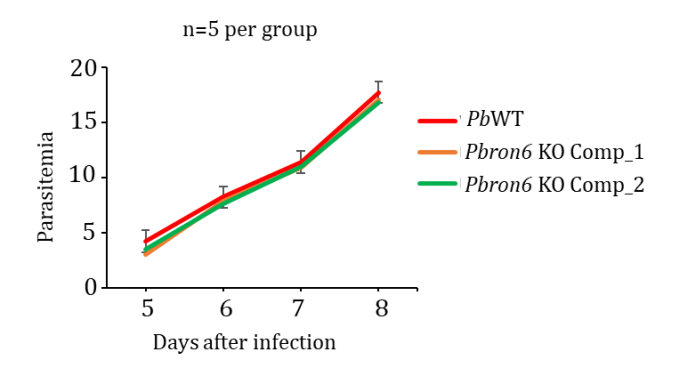


Figure 27: *Pbron6* complemented parasites (clone-1 and clone-2) showing similar asexual propagation compared to WT (p=0.9910, one-way ANOVA with Dunnett's multiple comparison test).

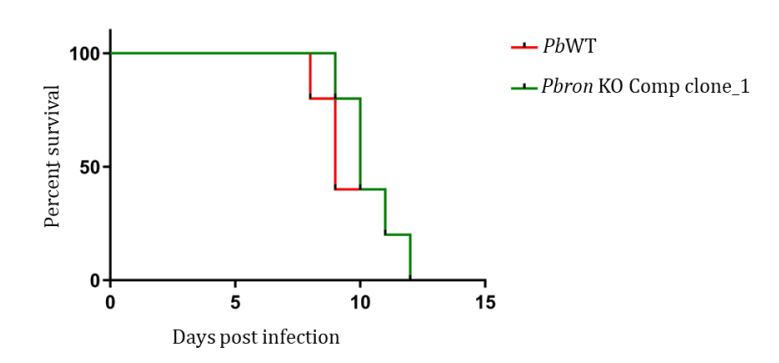


Figure 28: Kaplan-Meier plots, representing the duration of C57BL/6 mice survival, following infection with WT and *Pbron6* KO complement line clone-1 (n=10, non-significance, *p*=0.6825, Mantel-Cox test).

The *Pbron6* compliment parasites and their development inside the mosquito life cycle stage:

While no discernible phenotype was noted in the *Pbron6* mutants in all stages of *Plasmodium* occurring in the mosquitoes, we still monitored the fitness of the complimented line by transmitting malaria to mosquito. We noted that the complemented parasites produced oocyst in numbers comparable to WT and KO, and had distinct sporulation. The sporozoites from the complimented line also colonized mosquito salivary glands, and their numbers were comparable to WT and KO.

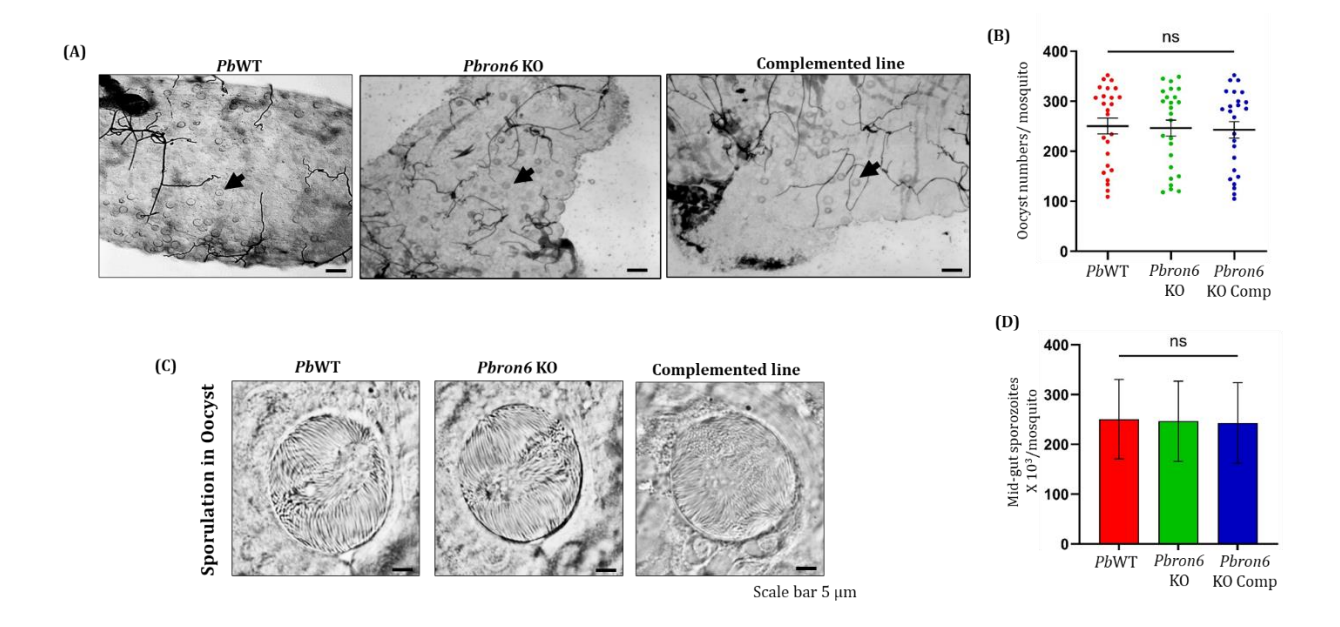


Figure 29: (A) Representative images of mosquito mid-guts infected with wild-type, *Pbron6* KO and *Pbron6* complemented line. **(B)** Quantification of oocyst numbers in mosquito (n=25) infected with *PbWT*, *Pbron6* KO and *Pbron6* complemented lines. Data has shown as mean \pm SD. No significance difference (p=9461, one-way Anova). **(C)** The sporulation of mid-guts of mosquitoes infected with wild-type and *Pbron6* KO and *Pbron6* complemented line. **(D)** Quantification of mid-gut sporozoites in mosquitoes (n=25) infected with WT, *Pbron6* KO and *Pbron6* complemented lines. Data has shown as mean \pm SD. No significance difference (p=0.9999, one-way Anova).

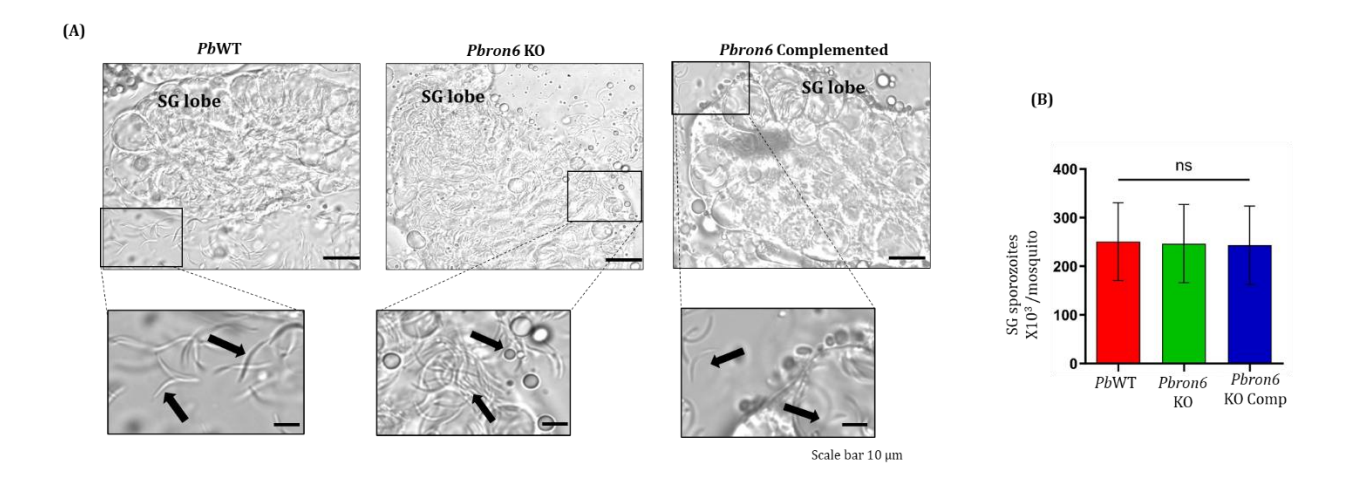


Figure 30: (A) Representative images of sporozoite colonization of salivary glands of mosquitoes infected with WT, *Pbron6* KO and *Pbron6* complemented lines. **(B)** Quantification salivary gland load of sporozoite in mosquitoes (n=25) infected with WT, *Pbron6* KO and *Pbron6* complemented lines. Data has shown as mean \pm SD. No significance difference (p=0.9999, one-way Anova).

The Pbron6 complement parasites exhibited normal prepatency

Approximately 5x10³ sporozoites derived from *Pbron6* complemented line and WT line were injected intravenously into two group of female C57BL/6 mice (n=5/group). The preparent period for all mice infected with complemented line was day 3.5, as comparable to WT.

Experiment number	Parasite strain	Number of Animals	Number of sporozoites injected per animal	Number of animals positive for blood stage infection	Pre-patent period
1	Wild type	5	5X10 ⁴	5	3.5 days
2	Pbron6 complement	5	5X10 ⁴	5	3.5 days

Table 3: Determination of preparency in *Pbron6* complimented line. The table shows the parasite line used, the animals used per group, a dose of sporozoites introduced by i.v., route, the animal positive for an infection, and the pre-patent period. The parasites were detected by Giemsa staining.

Phron6 KO parasites induce hyperactive splenomegaly in mice that did not dependent on the dose of sporozoite exposure:

Malaria disease often presents with splenomegaly, which is a frequent clinical manifestation and is characterized by an enlarged spleen [243]. Chronic malaria infections may often initiate a prolonged stimulation of the spleen, resulting in splenomegaly. However, hyper-reactive malarial splenomegaly is a medical condition that sporadically appears in humans, whose cause is not completely known. However, during hyper-reactive malarial splenomegaly, the spleen becomes significantly enlarged as a result of an excessive immune response to recurrent malaria infections. We surprisingly noted a scenario comparable to hyperactive splenomegaly in mice that were exposed to *Pbron6* mutants by noting the size and weight of spleens taken from uninfected mice infected with WT or *Pbron6* KO. The average weight of the uninfected spleen was nearly 105 mg as compared to the wild-type infected spleen, that weighed nearly 238 mg. Interestingly, the spleen from mice infected with *Pbron6* mutant weighed approximately 980 mg to 1 gram. We also noted that all mutant parasites were able to induce hyperactive splenomegaly in C57Bl6 mice, and the condition was independent of the sporozoite inoculum used to induce infection.

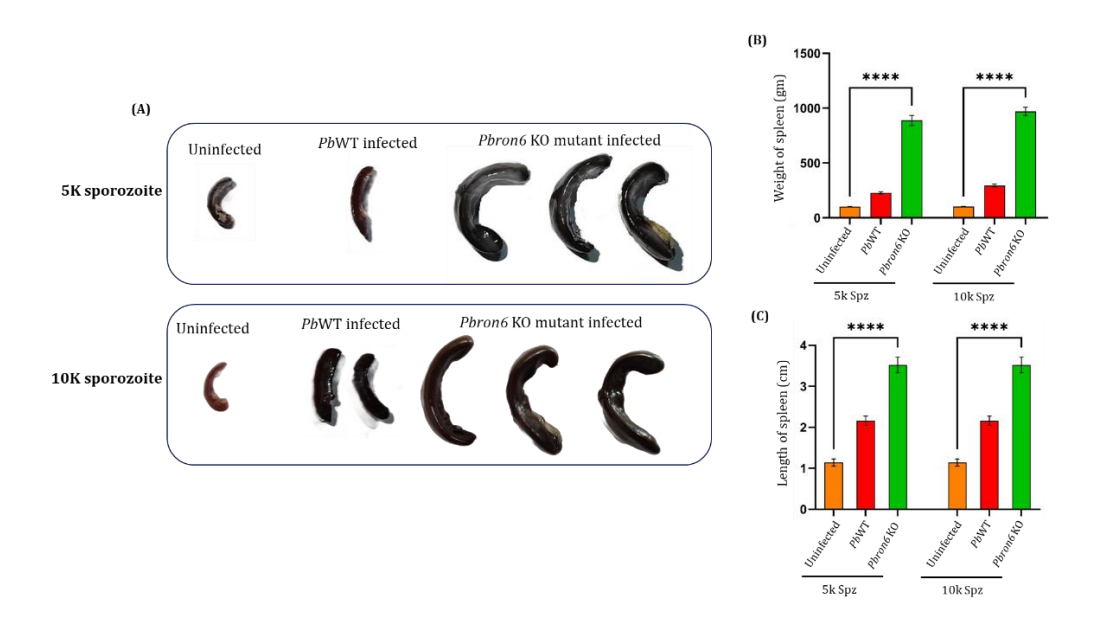


Figure 31: Hyper active splenomegaly in *Pbron6* KO infected mice. (A) Representative images of spleens isolated from uninfected, *P. berghei* wild type, and *Pbron6* KO infected mice. The upper panel and lower panel show images of spleens taken from C57BL/6 mice exposed to an intravenous dose of $5x10^3$ and $1X10^4$ sporozoites, respectively. (B) Bar graph showing weight of spleens measured in grams from uninfected, *P. berghei* wild type and *Pbron6* KO infected mice. Statistical differences were determined by one-way ANOVA with Tukey's multiple comparisons test. (n=5). (C) Bar graph showing length of spleens measured in cm from

uninfected *P. berghei* wild type (WT) and *Pbron6* KO infected mice. Statistical differences were determined by Krushal-Wallis test with Dunn's multiple comparisons test. (n=5).

Hematoxylin and Eosin staining of spleen tissues (H&E):

The spleen plays a crucial role in erythropoiesis, removal of infected erythrocytes (iRBCs), and the activation of the immune system in response to malaria parasites in RBC. As mice exhibited hyperactive splenomegaly in response to *Pbron6*KO parasite infection, we performed histological analysis of the spleen tissue. We noted a clear differentiation between the white pulp and red pulp, prominent marginal zones, and resting follicles, as observed in the spleen of control mice (uninfected). Enhance cellularity in red pulp and increased size of white pulp was observed in wild-type infected mice. In the *Pbron6* mutant parasite-infected mice, white pulp disappeared, the cellularity of red pulp is increased, and the distinct marginal zones around follicles also were seen to be disappeared. Over-destruction of iRBC was evident by an increased number of hemosiderophages.

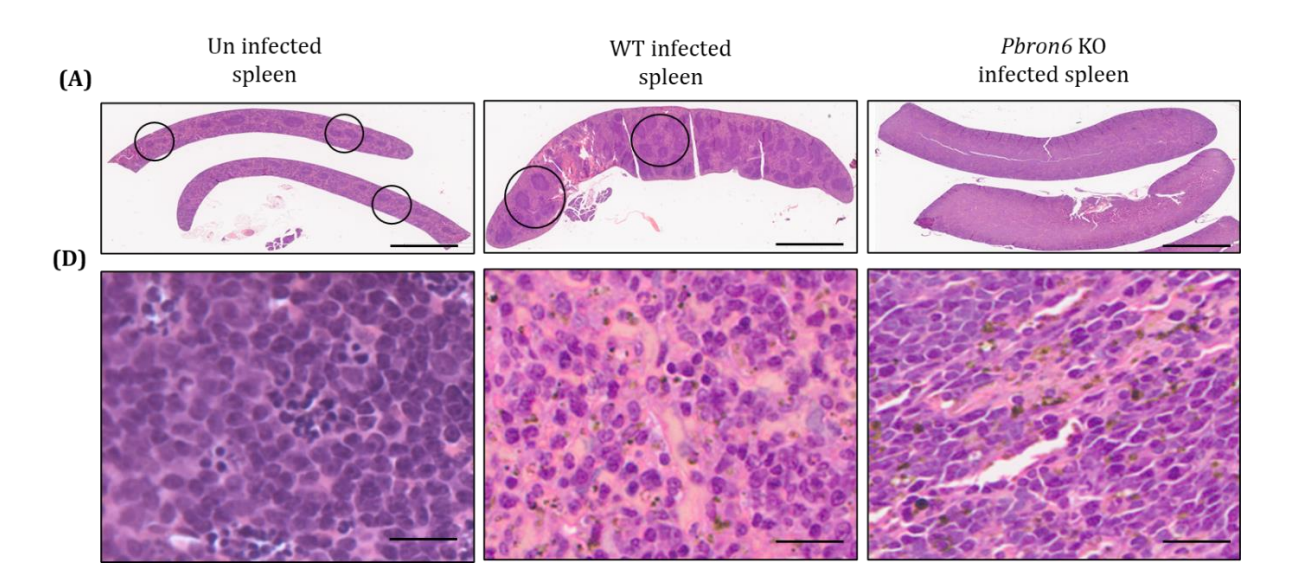
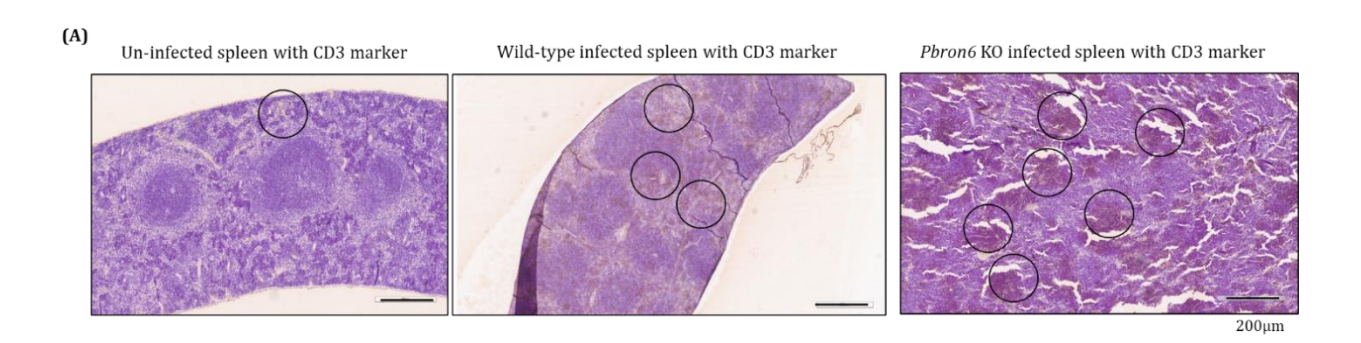


Figure 32: H&E staining of spleen: (A) H&E staining of spleen sections from uninfected, *P. berghei* wild type (WT) and *Pbron6* KO infected mice. The black circles indicate intact lymphoid follicles in the spleens. No lymphoid follicles were noted in spleens of *Pbron6* KO infected mice. Scale bar – 2 mm. **(B)** Sections of spleen showing hemosiderophages in uninfected, *P. berghei* wild type (WT) and *Pbron6* KO infected mice. Scale bar – 30 μm.

Obliteration of B-lymphoid follicular pattern during hyperactive splenomegaly:

In an attempt to grossly immunophenotype the changes associated with hyperactive splenomegaly, we resorted to histopathological analysis of spleen sections using T-cell marker CD3 and B-cell marker CD20. In uninfected (control) spleen, we noted normal sinusoidal proliferation and lymphoid follicle pattern with minimal CD3 expression. In wild-type infected spleen diffused expression of CD3 was observed along with sinusoidal proliferation and lymphoid follicle. Whereas in KO infected spleen intense and diffused expression of CD3 was observed in addition to absence of sinusoidal proliferation and loss of lymphoid follicle. Similarly, following CD20 staining of spleen tissue, we noted nearly 10 to 20 percent of lymphocytes and marina zone of lymphatic nodules expressed the marker in uninfected spleen. However, in infected spleen, we noted 80 to 90 percent of lymphocytes overexpressing CD20 in marginal zone of lymphatic nodules. Interestingly, in KO infected spleen, there was a significant reduction in CD20 expression was observed. Taken together, hyperactive splenomegaly induced by *Pbron6* mutants dramatically altered the expression of T and B cell markers in spleen, which likely hints to an altered immunological niche of the spleen.



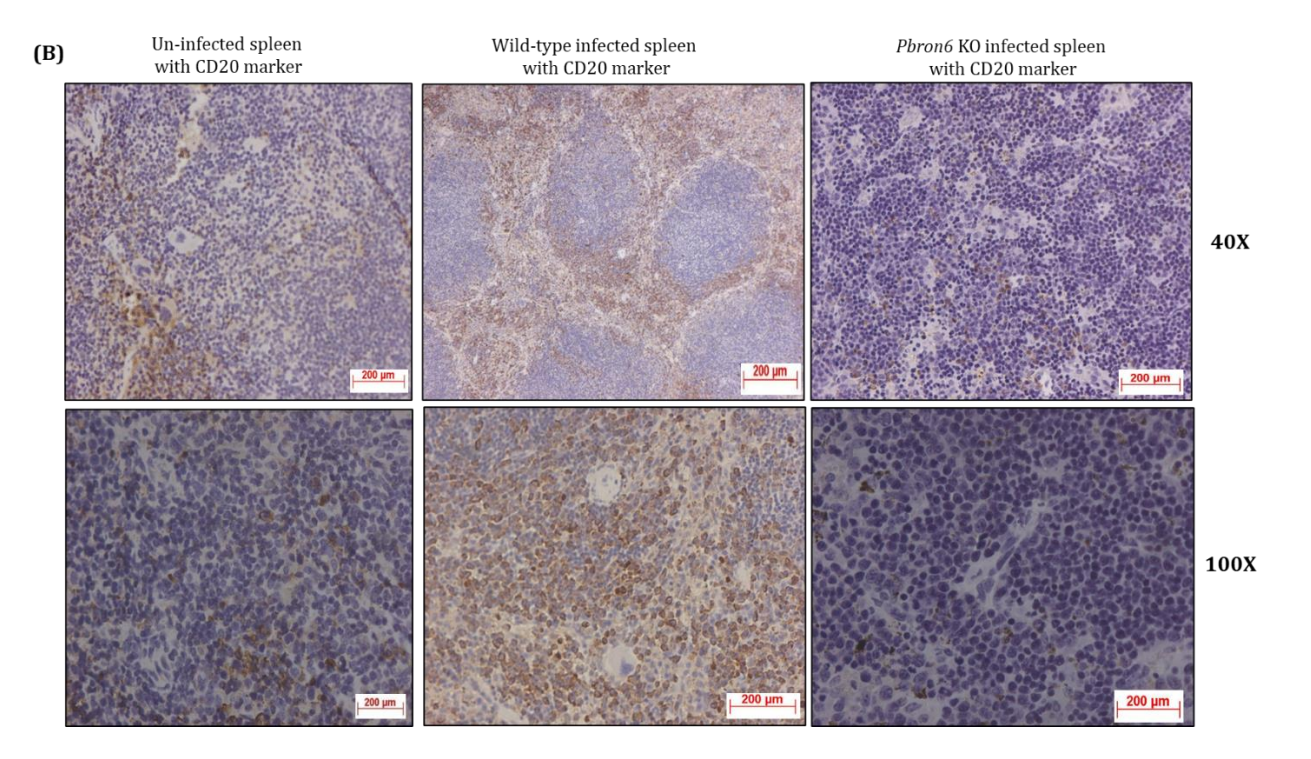


Figure 33: IHC Staining of spleen tissue: (A) Immunohistochemistry of spleens showing expression of CD3 (T cell marker) from uninfected, *P. berghei* wild type (WT) and *Pbron6* KO infected mice. Scale bar - 200 μ m. (B) Immunohistochemistry of spleen sections showing expression of CD20 (B cell marker) at 40X and 100X magnifications, respectively, from uninfected, *P. berghei* wild type (WT) and *Pbron6* KO infected mice. Loss of lymphoid follicular pattern coincided with loss of CD20 expression in spleens obtained from *Pbron6* KO infected mice.

Discussion

In the current study, an in-depth functional investigation of *Pb*RON6, a putative orthologue of *P. falciparum* RON6, was performed across all life cycle stages using a genetic approach. These studies revealed novel and previously unappreciated roles of *Pb*RON6 in cellular redistribution, host cell invasion and maintenance of virulence. Structurally, *Pb*RON6 lacks the C terminal Cys rich domain, previously implicated in host cell invasion and correct protein trafficking in *P. falciparum* [224]. Further, in striking contrast to the indispensable nature of the *Pfron6* locus and its C terminal cys rich domain [224], we demonstrate the feasibility of successfully targeting the *Pbron6* locus.

Bioinformatics and biochemical approaches revealed localization of PfRON6 to rhoptries in schizonts and rings and to PVM in maturing intra-erythrocytic forms [224]. However, not much is known about the localisation in the sporozoite and exoerythrocytic forms of *P. falciparum*. The only studies available for RON6 localisation, are from the rodent malaria model of P. berghei, using an immuno EM approach, where it was shown to reside in rhoptries of sporozoite [244]. However, the functional domains within the *Pb*RON6 and its cellular distribution, especially in the developing liver stages and merosomes, are yet to be characterised. We used several online prediction tools to first assess the cellular probability of PbRON6. DTU/Deep TMHMM predicted both Pfalciparum and P.berghei RON6, as globular proteins, lacking TM and having large extracellular domain while Phobious predicted both PbRON6 and PfRON6 a non-cytosolic proteins. Consistent with these predictions, we noted an association of PbRON6-HA with the sporozoite membrane, colocalizing with CSP and in PVM of developing EEFs, colocalizing with UIS-4. Interestingly, the extracellular domain of PbRON6 could also be confirmed by HA immunoreactivity on sporozoites under non-permeabilised condition. Previous studies reported the immunoreactivity of malarial antisera from Vietnam and PNG to the N, C and cys-rich repeat regions of recombinantly expressed PfRON6 [224]. This likely implies a possible shedding of the PfRON6 antigen by the merozoites. Indeed, this prediction is likely to be true, as *Pf*RON6 has a signal peptide that can allow its trafficking to the secretory compartment, as demonstrated earlier [224]. A clear lack of SP in P.berghei as predicted by Signal P-4.1 was also reiterated by lack of exocytosis in sporozoite stages, though *Pb*RON6 is associated with membrane. Interestingly however, the antisera from N- terminal PbRON6 (110-281 aa) did not show sporozoite membrane localization, under non-permeabilised condition. Rather, we noted an intracellular localization, most prominently in proximity to the nucleus, likely implicating an ER association, that

needs further confirmation. It is very likely that *Pb*RON6 targets ER and only processed form translocate to membrane of sporozoite, with a possible extracellular C-terminus part.

The sporozoite membrane association of PbRON6, bearing extracellular domain is a novel finding with important therapeutic implications for blocking the invasion in hepatocytes. Indeed, transgenic sporozoites expressing PbRON6-HA were sensitive to HA antibodies, as judged by delay in prepatency. Further, the mice receiving HA antibody treated sporozoites showed enhanced longevity, and at a concentration of $5\mu g$, the delay in onset of infection was comparable to 3d11 treated sporozoites. The HA antibody treated sporozoites apparently had a fate distinct from the 3d11 treatment and a possibility of sporozoite inhibition via complement mechanism cannot be ruled out and awaits further investigation.

The punctate staining pattern of *Pb*RON6 in daughter cells of schizonts and hepatic merozoites, characteristic of the apical organelle, is by large, expected. This may explain the lack of optimal invasion of *Pbron6* mutants into rbc, given that rhoptry neck proteins have been implicated in the formation of MJ [245], though a definitive role of *Pb*RON6 in the complex awaits further investigation. Our current study also provides added evidence for the role of *Pb*RON6 in invasion of hepatocytes both under *invitro* and *invitro* conditions. Following sporozoite inoculation into mammalian host, and prior to its hepatocyte entry, several transcripts implicated in invasion and subsequent intrahepatic development are upregulated, as demonstrated in a model of co-culture of *P. falciparum* sporozoites with primary human hepatocytes [246]. This concurs with the "just in time" model of gene expression, preparing invasive stages for host cell entry, characterised by enhanced synthesis of apical secretory and parasite surface proteins [247]. The maximal gene expression of *PbRON6* in mixed blood stages and midgut salivary gland sporozoite stage, may imply two bursts of transcriptional activities, coinciding with the need to invade RBC and hepatocytes.

Interestingly, we noted aggregates of PbRON6-HA at multiple foci over the membrane when sporozoites contacted with host cells maintained at $37^{\circ}C$. This hinted to a role in hepatocyte commitment, though no secreted form of PbRON6-HA was detected in sporozoite incubated supernatants. In comparison to the rhoptry discharge that occurs only once during the RBC invasion of merozoites, sporozoites may have to release the rhoptry contents, possibly during SG invasion, hepatocyte invasion and also export to EEF membrane, in the case of PbRON6. Therefore, RON6 secretion may be programed for release in multiple bouts, to meet the aforementioned invasion functions.

A conditional depletion of RON 2, 4 and 5 complex affects normal substrate attachment, resulting in reduced gliding [220] A similar function was also noted for PbRON11 [248]. Contrastingly, however, we noted no effect of *Pb*RON6 depletion on the colonization of mutants to the salivary gland, ruling out a role of *Pb*RON6 in substrate attachment and gliding. However, mutant sporozoites showed a threefold reduction in HepG2 cell invasion as compared to WT. Further, the liver loads of *Pb18S* rRNA at 12h post infection, were significantly lower than WT. Based on these observations, we propose a role of *Pb*RON6, primarily in hepatocyte invasion.

A reduction in hepatic schizogony was another important observation we noted in mutants lacking *Pb*RON6 expression. It in only speculative, if this is due to lack of recruitment of *Pb*RON6 on PVM. In fact, other proteins like RAP2/3 that localise to rhoptries of midgut and salivary gland sporozoites, are known to be secreted into the PVM during the EEF stage [249]. Another rhoptry protein, ICP localising to rhoptries of *P. yoelli* sporozoites, continues to be expressed in parasite cytoplasm and in PV of *P.yoelli* and *P.falciparum* and has a role in the inhibition of host proteases and egress of hepatic merozoites [250]. While the precise role of *Pb*RON6 in PVM maintenance is yet to be deciphered, decreased schizogony, reduction in the MSP-1 expression at 48h and delay in prepatency reiterated a growth defect during late EEF development.

The IP and MS analysis with C terminus HA tagged *Pb*RON6 parasites revealed a diverse range of putative proteins involved in erythrocyte invasion and host cell remodelling. This may likely explain for the significant delay in asexual propagation and RBC reinvasion, associated with the mutant. Of particular interest were proteins like MSP1, MSP9, RON3, RAP1 and Apical merozoite protein, an orthologue of *Pf*34, that were detected uniquely, only in pulldown with HA tagged parasite lysates. Additionally, we also detected RON2 and RON5 coprecipitating with HA tagged parasite lysates, with 34 and 24 unique peptides. However, owing to these clients also being detected in negative control (with 5 and 4 peptide hits respectively), we excluded them as authentic clients of *Pb*RON6. MSP-1 forms complex with other merozoite surface proteins such as MSP3, MSP6, MSP7, MSP9 [251] to facilitate anchoring to erythrocyte membrane via band3 protein [252]. Paradoxically however, merozoites lacking MSP-1 expression can still invade rbc [253], and a likely mechanism may be by utilising peripheral invasins, that may mediate tight attachment to rbc surface. Though not demonstrated in merozoites, our study shows an association of C terminal extracellular domain associated with sporozoite membrane, that may act as invasin in the invasion complex. Another novel rhoptry bulb protein detected in LC/MS analysis with high confidence score is RON3. A recent work

claimed that knockdown of PfRON3 C-terminal fragment in the early schizont stage resulted in defect in erythrocyte invasion subsequently showed developmental arrest at ring stage [214, 254]. We observed a similar phenotype where reinvasion was compromised in PbRON6 mutants. Therefore, we suspect both RON3 and RON6 might function concurrently along with other rhoptry invasive complex proteins. Further, two independent research observations elucidated that PfRON6 colocalized with Pf34 in rhoptry neck [224] and C-terminus of PfRON6 interaction with Pf34 [255] which aligns with our LC/MS based interactome findings.

A massive increase in spleen size during malaria infection, referred to as hyper-active splenomegaly (HMS) [256] occurs due to chronic antigenic stimulation in subjects having long term exposure to malaria parasites [257]. Though a triad of symptoms characterised by enlarged spleen, raised IgM levels and presence of malaria antigens are hall marks of HMS, the condition is highly variable [258]. The *PbRON6* mutant induces HGM and offers a model to investigate the pathological insights of the condition. Our preliminary studies reveal an enhanced expression of T cell marker and down regulation of B cell marker, together with increased frequency of hemosiderophages. While the probable cause of altered T and B cell markers are under investigation, it is speculative if the excess hemozoin associated with hemosiderophages alters the expression of MHC class II, costimulatory, adhesion molecules together with inhibition of maturation of dendritic cells. [259-261]. This may explain why the parasites fail to get cleared, in spite of their slow progression in mice.

Two independent studies employing conditional silencing of PfRON6 have shown their role in asexual propagation [255, 262], mirroring our current observations. In the first study, a knock-sideways approach was successfully used to inactivate PfRON6 within ER through fusion of KDEL-ER retrieval sequence [262]. In a second independent study, an AVEXIS assay was employed to characterize the interactions of human and Pfalciparum proteins, involved in host cell invasion, expressed in the human fibroblast cell line [255]. This study reiterated the interaction of C-terminus of PfRON6 with Pf34, that concurs with earlier demonstration, of their coloclisation in rhoptry neck [224]. Interestingly no interaction of Pf34 was noted with N the terminal domain [255]. This coincides with our observation where we recorded HA immunoreactivity on sporozoite membrane under non-permeabilising condition, while the N- terminal antisera showed only intracellular localization around the nucleus, likely in the ER compartment. Based on this observation, it may be possible that PbRON6 may be processed intracellularly, with the C-terminal domain being recruited to membrane via rhoptry neck.

An invasion and developmental defect associated with PbRON6 depletion was indeed a locus-specific effect, as complementation restored both asexual propagation and restoration of a timely prepatency, following inoculation of sporozoites. With the advancement in our understanding of the secretory pathways and invasion mechanisms of apicomplexan parasites, it is become clear that some components of the invasion machinery are conserved among erythrocytic asexual and transmissive stage parasites. Given that rhoptry protein secretion critically regulates cell traversal, host cell invasion, PVM formation and proliferation of parasites within the PV, targeting the secretory effectors may prevent malaria transmission, at multiple life cycle stages. In line with this idea, we demonstrate the role of PbRON6 in the parasite invasion of rbc, hepatocytes and its association with sporozoite and PV membrane. Thus, targeting PbRON6 may enhance the breath of beating the parasite at multiple stages for efficient control of malaria.

References

References:

- 1. Crutcher, J.M. and S.L. Hoffman, *Malaria*, in *Medical Microbiology*, S. Baron, Editor. 1996, University of Texas Medical Branch at Galveston Copyright © 1996, The University of Texas Medical Branch at Galveston.: Galveston (TX).
- 2. Carter, R. and K.N. Mendis, *Evolutionary and historical aspects of the burden of malaria.* Clin Microbiol Rev, 2002. **15**(4): p. 564-94.
- 3. Cox, F.E., *History of the discovery of the malaria parasites and their vectors.* Parasit Vectors, 2010. **3**(1): p. 5.
- 4. Talapko, J., et al., *Malaria: The Past and the Present.* Microorganisms, 2019. **7**(6).
- 5. Boualam, M.A., et al., *Malaria in Europe: A Historical Perspective.* Front Med (Lausanne), 2021. **8**: p. 691095.
- 6. *<WHO.pdf>.*
- 7. Bassat, Q., et al., *Key Knowledge Gaps for Plasmodium vivax Control and Elimination.* Am J Trop Med Hyg, 2016. **95**(6 Suppl): p. 62-71.
- 8. Sato, S., *Plasmodium-a brief introduction to the parasites causing human malaria and their basic biology.* J Physiol Anthropol, 2021. **40**(1): p. 1.
- 9. Amino, R., et al., *Quantitative imaging of Plasmodium transmission from mosquito to mammal.* Nat Med, 2006. **12**(2): p. 220-4.
- 10. Soulard, V., et al., *Plasmodium falciparum full life cycle and Plasmodium ovale liver stages in humanized mice.* Nat Commun, 2015. **6**: p. 7690.
- 11. Aly, A.S., A.M. Vaughan, and S.H. Kappe, *Malaria parasite development in the mosquito and infection of the mammalian host.* Annu Rev Microbiol, 2009. **63**: p. 195-221.
- 12. Bannister, L.H. and I.W. Sherman, *Plasmodium*, in *Encyclopedia of Life Sciences*. 2009.
- 13. Yamauchi, L.M., et al., *Plasmodium sporozoites trickle out of the injection site.* Cell Microbiol, 2007. **9**(5): p. 1215-22.
- 14. Ribeiro, J.M. and I.M. Francischetti, *Role of arthropod saliva in blood feeding: sialome and post-sialome perspectives.* Annu Rev Entomol, 2003. **48**: p. 73-88.
- 15. Kappe, S.H., et al., *Apicomplexan gliding motility and host cell invasion: overhauling the motor model.* Trends Parasitol, 2004. **20**(1): p. 13-6.
- 16. Vanderberg, J.P. and U. Frevert, *Intravital microscopy demonstrating antibody-mediated immobilisation of Plasmodium berghei sporozoites injected into skin by mosquitoes.* Int J Parasitol, 2004. **34**(9): p. 991-6.
- 17. Prudencio, M., A. Rodriguez, and M.M. Mota, *The silent path to thousands of merozoites: the Plasmodium liver stage.* Nat Rev Microbiol, 2006. **4**(11): p. 849-56.
- 18. Menard, R., et al., *Looking under the skin: the first steps in malarial infection and immunity.* Nat Rev Microbiol, 2013. **11**(10): p. 701-12.
- 19. Matuschewski, K., et al., *Plasmodium sporozoite invasion into insect and mammalian cells is directed by the same dual binding system.* Embo j, 2002. **21**(7): p. 1597-606.
- 20. Sultan, A.A., et al., *TRAP* is necessary for gliding motility and infectivity of plasmodium sporozoites. Cell, 1997. **90**(3): p. 511-22.
- 21. Myung, J.M., P. Marshall, and P. Sinnis, *The Plasmodium circumsporozoite protein is involved in mosquito salivary gland invasion by sporozoites.* Mol Biochem Parasitol, 2004. **133**(1): p. 53-9.
- 22. Ishino, T., Y. Chinzei, and M. Yuda, *A Plasmodium sporozoite protein with a membrane attack complex domain is required for breaching the liver sinusoidal cell layer prior to hepatocyte infection.* Cell Microbiol, 2005. **7**(2): p. 199-208.

- 23. Ishino, T., et al., *Cell-passage activity is required for the malarial parasite to cross the liver sinusoidal cell layer.* PLoS Biol, 2004. **2**(1): p. E4.
- 24. Kaiser, K., et al., *A member of a conserved Plasmodium protein family with membrane-attack complex/perforin (MACPF)-like domains localizes to the micronemes of sporozoites.* Mol Biochem Parasitol, 2004. **133**(1): p. 15-26.
- 25. Bhanot, P., et al., *A surface phospholipase is involved in the migration of plasmodium sporozoites through cells.* J Biol Chem, 2005. **280**(8): p. 6752-60.
- 26. Mota, M.M., et al., *Migration of Plasmodium sporozoites through cells before infection.* Science, 2001. **291**(5501): p. 141-4.
- 27. Vaughan, A.M. and S.H.I. Kappe, *Malaria Parasite Liver Infection and Exoerythrocytic Biology.* Cold Spring Harb Perspect Med, 2017. **7**(6).
- 28. Coppi, A., et al., *The malaria circumsporozoite protein has two functional domains, each with distinct roles as sporozoites journey from mosquito to mammalian host.* J Exp Med, 2011. **208**(2): p. 341-56.
- 29. Kappe, S., et al., *Conservation of a gliding motility and cell invasion machinery in Apicomplexan parasites.* J Cell Biol, 1999. **147**(5): p. 937-44.
- 30. VanBuskirk, K.M., et al., *Preerythrocytic, live-attenuated Plasmodium falciparum vaccine candidates by design.* Proc Natl Acad Sci U S A, 2009. **106**(31): p. 13004-9.
- 31. Kaushansky, A., et al., *Malaria parasites target the hepatocyte receptor EphA2 for successful host infection*. Science, 2015. **350**(6264): p. 1089-92.
- 32. Silvie, O., et al., *Hepatocyte CD81 is required for Plasmodium falciparum and Plasmodium yoelii sporozoite infectivity.* Nat Med, 2003. **9**(1): p. 93-6.
- 33. Silvie, O., et al., *Cholesterol contributes to the organization of tetraspanin-enriched microdomains and to CD81-dependent infection by malaria sporozoites.* J Cell Sci, 2006. **119**(Pt 10): p. 1992-2002.
- 34. Yalaoui, S., et al., *Scavenger receptor BI boosts hepatocyte permissiveness to Plasmodium infection.* Cell Host Microbe, 2008. **4**(3): p. 283-92.
- 35. Mueller, A.K., et al., *Plasmodium liver stage developmental arrest by depletion of a protein at the parasite-host interface.* Proc Natl Acad Sci U S A, 2005. **102**(8): p. 3022-7.
- 36. Mikolajczak, S.A., et al., *L-FABP is a critical host factor for successful malaria liver stage development.* Int J Parasitol, 2007. **37**(5): p. 483-9.
- 37. Rijpma, S.R., et al., *Multidrug ATP-binding cassette transporters are essential for hepatic development of Plasmodium sporozoites.* Cell Microbiol, 2016. **18**(3): p. 369-83.
- 38. Hiller, N.L., et al., *A host-targeting signal in virulence proteins reveals a secretome in malarial infection.* Science, 2004. **306**(5703): p. 1934-7.
- 39. Marti, M., et al., *Targeting malaria virulence and remodeling proteins to the host erythrocyte.* Science, 2004. **306**(5703): p. 1930-3.
- 40. Boddey, J.A., et al., *An aspartyl protease directs malaria effector proteins to the host cell.* Nature, 2010. **463**(7281): p. 627-31.
- 41. Russo, I., et al., *Plasmepsin V licenses Plasmodium proteins for export into the host erythrocyte.* Nature, 2010. **463**(7281): p. 632-6.
- 42. Ho, C.M., et al., *Malaria parasite translocon structure and mechanism of effector export.* Nature, 2018. **561**(7721): p. 70-75.
- 43. Heiber, A., et al., *Identification of new PNEPs indicates a substantial non-PEXEL exportome and underpins common features in Plasmodium falciparum protein export.* PLoS Pathog, 2013. **9**(8): p. e1003546.
- 44. Plassmeyer, M.L., et al., *Structure of the Plasmodium falciparum circumsporozoite protein, a leading malaria vaccine candidate.* J Biol Chem, 2009. **284**(39): p. 26951-63.

- 45. Ingmundson, A., et al., *The exported Plasmodium berghei protein IBIS1 delineates membranous structures in infected red blood cells.* Mol Microbiol, 2012. **83**(6): p. 1229-43.
- 46. Jaijyan, D.K., H. Singh, and A.P. Singh, *A Sporozoite- and Liver Stage-expressed Tryptophan-rich Protein Plays an Auxiliary Role in Plasmodium Liver Stage Development and Is a Potential Vaccine Candidate.* J Biol Chem, 2015. **290**(32): p. 19496-511.
- 47. Ishino, T., et al., *LISP1* is important for the egress of Plasmodium berghei parasites from liver cells. Cell Microbiol, 2009. **11**(9): p. 1329-39.
- 48. Bano, N., et al., *Cellular interactions of Plasmodium liver stage with its host mammalian cell.* Int J Parasitol, 2007. **37**(12): p. 1329-41.
- 49. Sturm, A., et al., *Manipulation of host hepatocytes by the malaria parasite for delivery into liver sinusoids.* Science, 2006. **313**(5791): p. 1287-90.
- 50. Blackman, M.J., *Malarial proteases and host cell egress: an 'emerging' cascade.* Cell Microbiol, 2008. **10**(10): p. 1925-34.
- 51. Putrianti, E.D., et al., *The Plasmodium serine-type SERA proteases display distinct expression patterns and non-essential in vivo roles during life cycle progression of the malaria parasite.* Cell Microbiol, 2010. **12**(6): p. 725-39.
- 52. Agarwal, S., et al., Ca(2+) -mediated exocytosis of subtilisin-like protease 1: a key step in egress of Plasmodium falciparum merozoites. Cell Microbiol, 2013. **15**(6): p. 910-21.
- Tawk, L., et al., *A key role for Plasmodium subtilisin-like SUB1 protease in egress of malaria parasites from host hepatocytes.* J Biol Chem, 2013. **288**(46): p. 33336-46.
- 54. Falae, A., et al., *Role of Plasmodium berghei cGMP-dependent protein kinase in late liver stage development.* J Biol Chem, 2010. **285**(5): p. 3282-8.
- 55. Collins, C.R., et al., *Malaria parasite cGMP-dependent protein kinase regulates blood stage merozoite secretory organelle discharge and egress.* PLoS Pathog, 2013. **9**(5): p. e1003344.
- 56. Schmidt-Christensen, A., et al., *Expression and processing of Plasmodium berghei SERA3 during liver stages.* Cell Microbiol, 2008. **10**(8): p. 1723-34.
- 57. Suarez, C., et al., *The malarial serine protease SUB1 plays an essential role in parasite liver stage development.* PLoS Pathog, 2013. **9**(12): p. e1003811.
- Tarun, A.S., et al., *Quantitative isolation and in vivo imaging of malaria parasite liver stages.* Int I Parasitol, 2006. **36**(12): p. 1283-93.
- 59. Belachew, E.B., *Immune Response and Evasion Mechanisms of Plasmodium falciparum Parasites.* J Immunol Res, 2018. **2018**: p. 6529681.
- 60. Cowman, A.F., et al., *The Molecular Basis of Erythrocyte Invasion by Malaria Parasites.* Cell Host Microbe, 2017. **22**(2): p. 232-245.
- Mayer, D.C., et al., *The glycophorin C N-linked glycan is a critical component of the ligand for the Plasmodium falciparum erythrocyte receptor BAEBL.* Proc Natl Acad Sci U S A, 2006. **103**(7): p. 2358-62.
- 62. Cowman, A.F. and B.S. Crabb, *Invasion of red blood cells by malaria parasites.* Cell, 2006. **124**(4): p. 755-66.
- 63. Goel, V.K., et al., Band 3 is a host receptor binding merozoite surface protein 1 during the Plasmodium falciparum invasion of erythrocytes. Proc Natl Acad Sci U S A, 2003. **100**(9): p. 5164-9.
- 64. Mitchell, G.H., et al., *Apical membrane antigen 1, a major malaria vaccine candidate, mediates the close attachment of invasive merozoites to host red blood cells.* Infect Immun, 2004. **72**(1): p. 154-8.
- 65. Pinder, J.C., et al., *Actomyosin motor in the merozoite of the malaria parasite, Plasmodium falciparum: implications for red cell invasion.* J Cell Sci, 1998. **111 (Pt 13)**: p. 1831-9.

- 66. Keeley, A. and D. Soldati, *The glideosome: a molecular machine powering motility and host-cell invasion by Apicomplexa*. Trends Cell Biol, 2004. **14**(10): p. 528-32.
- 67. Haynes, J.D., et al., *Receptor-like specificity of a Plasmodium knowlesi malarial protein that binds to Duffy antigen ligands on erythrocytes.* J Exp Med, 1988. **167**(6): p. 1873-81.
- 68. Crosnier, C., et al., *Basigin is a receptor essential for erythrocyte invasion by Plasmodium falciparum.* Nature, 2011. **480**(7378): p. 534-7.
- 69. Boyle, M.J., et al., *Sequential processing of merozoite surface proteins during and after erythrocyte invasion by Plasmodium falciparum*. Infect Immun, 2014. **82**(3): p. 924-36.
- 70. de Koning-Ward, T.F., et al., *Plasmodium species: master renovators of their host cells.* Nat Rev Microbiol, 2016. **14**(8): p. 494-507.
- 71. Sargeant, T.J., et al., *Lineage-specific expansion of proteins exported to erythrocytes in malaria parasites.* Genome Biol, 2006. **7**(2): p. R12.
- 72. Spielmann, T. and T.W. Gilberger, *Critical Steps in Protein Export of Plasmodium falciparum Blood Stages.* Trends Parasitol, 2015. **31**(10): p. 514-525.
- 73. Rug, M., et al., *Export of virulence proteins by malaria-infected erythrocytes involves remodeling of host actin cytoskeleton.* Blood, 2014. **124**(23): p. 3459-68.
- 74. Scherf, A., J.J. Lopez-Rubio, and L. Riviere, *Antigenic variation in Plasmodium falciparum*. Annu Rev Microbiol, 2008. **62**: p. 445-70.
- 75. Papakrivos, J., C.I. Newbold, and K. Lingelbach, *A potential novel mechanism for the insertion of a membrane protein revealed by a biochemical analysis of the Plasmodium falciparum cytoadherence molecule PfEMP-1.* Mol Microbiol, 2005. **55**(4): p. 1272-84.
- 76. Baruch, D.I., et al., Cloning the P. falciparum gene encoding PfEMP1, a malarial variant antigen and adherence receptor on the surface of parasitized human erythrocytes. Cell, 1995. **82**(1): p. 77-87.
- 77. Egan, T.J., Recent advances in understanding the mechanism of hemozoin (malaria pigment) formation. J Inorg Biochem, 2008. **102**(5-6): p. 1288-99.
- 78. Foley, M. and L. Tilley, *Quinoline antimalarials: mechanisms of action and resistance and prospects for new agents.* Pharmacol Ther, 1998. **79**(1): p. 55-87.
- 79. Vaughan, A.M., R. Wang, and S.H. Kappe, *Genetically engineered, attenuated whole-cell vaccine approaches for malaria.* Hum Vaccin, 2010. **6**(1): p. 107-13.
- 80. McCoubrie, J.E., et al., Evidence for a common role for the serine-type Plasmodium falciparum serine repeat antigen proteases: implications for vaccine and drug design. Infect Immun, 2007. **75**(12): p. 5565-74.
- 81. Miller, S.K., et al., A subset of Plasmodium falciparum SERA genes are expressed and appear to play an important role in the erythrocytic cycle. J Biol Chem, 2002. **277**(49): p. 47524-32.
- 82. Harris, P.K., et al., *Molecular identification of a malaria merozoite surface sheddase.* PLoS Pathog, 2005. **1**(3): p. 241-51.
- 83. Hale, V.L., et al., *Parasitophorous vacuole poration precedes its rupture and rapid host erythrocyte cytoskeleton collapse in Plasmodium falciparum egress.* Proc Natl Acad Sci U S A, 2017. **114**(13): p. 3439-3444.
- 84. Glushakova, S., et al., *New stages in the program of malaria parasite egress imaged in normal and sickle erythrocytes.* Curr Biol, 2010. **20**(12): p. 1117-21.
- 85. Gardiner, D.L., et al., *Implication of a Plasmodium falciparum gene in the switch between asexual reproduction and gametocytogenesis.* Mol Biochem Parasitol, 2005. **140**(2): p. 153-60.
- 86. Kafsack, B.F., et al., *A transcriptional switch underlies commitment to sexual development in malaria parasites.* Nature, 2014. **507**(7491): p. 248-52.
- 87. Sinha, A., et al., *A cascade of DNA-binding proteins for sexual commitment and development in Plasmodium.* Nature, 2014. **507**(7491): p. 253-257.

- 88. Campbell, T.L., et al., *Identification and genome-wide prediction of DNA binding specificities for the ApiAP2 family of regulators from the malaria parasite.* PLoS Pathog, 2010. **6**(10): p. e1001165.
- 89. Filarsky, M., et al., *GDV1 induces sexual commitment of malaria parasites by antagonizing HP1-dependent gene silencing.* Science, 2018. **359**(6381): p. 1259-1263.
- 90. Harding, C.R. and M. Meissner, *The inner membrane complex through development of Toxoplasma gondii and Plasmodium.* Cell Microbiol, 2014. **16**(5): p. 632-41.
- 91. Naissant, B., et al., *Plasmodium falciparum STEVOR phosphorylation regulates host erythrocyte deformability enabling malaria parasite transmission.* Blood, 2016. **127**(24): p. e42-53.
- 92. Mair, G.R., et al., *Regulation of sexual development of Plasmodium by translational repression.* Science, 2006. **313**(5787): p. 667-9.
- 93. White, N.J., *Primaquine to prevent transmission of falciparum malaria.* Lancet Infect Dis, 2013. **13**(2): p. 175-81.
- 94. Kuehn, A. and G. Pradel, *The coming-out of malaria gametocytes.* J Biomed Biotechnol, 2010. **2010**: p. 976827.
- 95. Silvestrini, F., P. Alano, and J.L. Williams, *Commitment to the production of male and female gametocytes in the human malaria parasite Plasmodium falciparum.* Parasitology, 2000. **121 Pt 5**: p. 465-71.
- 96. Bennink, S., M.J. Kiesow, and G. Pradel, *The development of malaria parasites in the mosquito midgut*. Cell Microbiol, 2016. **18**(7): p. 905-18.
- 97. Billker, O., et al., *The roles of temperature, pH and mosquito factors as triggers of male and female gametogenesis of Plasmodium berghei in vitro.* Parasitology, 1997. **115 (Pt 1)**: p. 1-7.
- 98. Billker, O., et al., *Identification of xanthurenic acid as the putative inducer of malaria development in the mosquito.* Nature, 1998. **392**(6673): p. 289-92.
- 99. Raabe, A.C., et al., Multiple roles for Plasmodium berghei phosphoinositide-specific phospholipase C in regulating gametocyte activation and differentiation. Cell Microbiol, 2011. **13**(7): p. 955-66.
- 100. Hirai, M., et al., *PbGCbeta is essential for Plasmodium ookinete motility to invade midgut cell and for successful completion of parasite life cycle in mosquitoes.* J Biochem, 2006. **140**(5): p. 747-57.
- 101. Billker, O., et al., *Calcium and a calcium-dependent protein kinase regulate gamete formation and mosquito transmission in a malaria parasite.* Cell, 2004. **117**(4): p. 503-14.
- 102. Nofal, S.D., et al., *Plasmodium falciparum Guanylyl Cyclase-Alpha and the Activity of Its Appended P4-ATPase Domain Are Essential for cGMP Synthesis and Blood-Stage Egress.* mBio, 2021. **12**(1).
- 103. Ponzi, M., et al., *Egress of Plasmodium berghei gametes from their host erythrocyte is mediated by the MDV-1/PEG3 protein.* Cell Microbiol, 2009. **11**(8): p. 1272-88.
- Rangarajan, R., et al., *A mitogen-activated protein kinase regulates male gametogenesis and transmission of the malaria parasite Plasmodium berghei.* EMBO Rep, 2005. **6**(5): p. 464-9.
- 105. Straschil, U., et al., *The Armadillo repeat protein PF16 is essential for flagellar structure and function in Plasmodium male gametes.* PLoS One, 2010. **5**(9): p. e12901.
- 106. Deligianni, E., et al., *Critical role for a stage-specific actin in male exflagellation of the malaria parasite.* Cell Microbiol, 2011. **13**(11): p. 1714-30.
- 107. Shahabuddin, M., et al., *Transmission-blocking activity of a chitinase inhibitor and activation of malarial parasite chitinase by mosquito protease.* Proc Natl Acad Sci U S A, 1993. **90**(9): p. 4266-70.
- 108. Janse, C.J., et al., *DNA synthesis in Plasmodium berghei during asexual and sexual development.* Mol Biochem Parasitol, 1986. **20**(2): p. 173-82.

- 109. Reininger, L., et al., *A NIMA-related protein kinase is essential for completion of the sexual cycle of malaria parasites.* J Biol Chem, 2005. **280**(36): p. 31957-64.
- 110. Reininger, L., et al., *An essential role for the Plasmodium Nek-2 Nima-related protein kinase in the sexual development of malaria parasites.* J Biol Chem, 2009. **284**(31): p. 20858-68.
- 111. Guttery, D.S., et al., *Commit and Transmit: Molecular Players in Plasmodium Sexual Development and Zygote Differentiation.* Trends Parasitol, 2015. **31**(12): p. 676-685.
- Huber, M., E. Cabib, and L.H. Miller, *Malaria parasite chitinase and penetration of the mosquito peritrophic membrane.* Proc Natl Acad Sci U S A, 1991. **88**(7): p. 2807-10.
- 113. Pradel, G., *Proteins of the malaria parasite sexual stages: expression, function and potential for transmission blocking strategies.* Parasitology, 2007. **134**(Pt.14): p. 1911-29.
- 114. Yuda, M., H. Sakaida, and Y. Chinzei, *Targeted disruption of the plasmodium berghei CTRP gene reveals its essential role in malaria infection of the vector mosquito.* J Exp Med, 1999. **190**(11): p. 1711-6.
- 115. Ishino, T., et al., *A calcium-dependent protein kinase regulates Plasmodium ookinete access to the midgut epithelial cell.* Mol Microbiol, 2006. **59**(4): p. 1175-84.
- 116. Siden-Kiamos, I., et al., *Plasmodium berghei calcium-dependent protein kinase 3 is required for ookinete gliding motility and mosquito midgut invasion.* Mol Microbiol, 2006. **60**(6): p. 1355-63.
- 117. Tremp, A.Z., E.I. Khater, and J.T. Dessens, *IMC1b* is a putative membrane skeleton protein involved in cell shape, mechanical strength, motility, and infectivity of malaria ookinetes. J Biol Chem, 2008. **283**(41): p. 27604-27611.
- 118. Wang, X., et al., *A protein palmitoylation cascade regulates microtubule cytoskeleton integrity in Plasmodium.* Embo j, 2020. **39**(13): p. e104168.
- 119. Dessens, J.T., et al., *SOAP*, a novel malaria ookinete protein involved in mosquito midgut invasion and oocyst development. Mol Microbiol, 2003. **49**(2): p. 319-29.
- 120. Limviroj, W., et al., *Immuno-electron microscopic observation of Plasmodium berghei CTRP localization in the midgut of the vector mosquito Anopheles stephensi.* J Parasitol, 2002. **88**(4): p. 664-72.
- 121. Nacer, A., K. Walker, and H. Hurd, *Localisation of laminin within Plasmodium berghei oocysts and the midgut epithelial cells of Anopheles stephensi.* Parasit Vectors, 2008. **1**(1): p. 33.
- 122. Sinden, R.E., Y. Alavi, and J.D. Raine, *Mosquito--malaria interactions: a reappraisal of the concepts of susceptibility and refractoriness.* Insect Biochem Mol Biol, 2004. **34**(7): p. 625-9.
- 123. Thathy, V., et al., *Levels of circumsporozoite protein in the Plasmodium oocyst determine sporozoite morphology.* Embo j, 2002. **21**(7): p. 1586-96.
- 124. Moran, P. and I.W. Caras, Requirements for glycosylphosphatidylinositol attachment are similar but not identical in mammalian cells and parasitic protozoa. J Cell Biol, 1994. **125**(2): p. 333-43.
- 125. Sinden, R.E., Excystment by sporozoites of malaria parasites. Nature, 1974. 252(5481): p. 314.
- 126. Sinden, R.E. and P.C. Garnham, *A comparative study on the ultrastructure of Plasmodium sporozoites within the oöcyst and salivary glands, with particular reference to the incidence of the micropore.* Trans R Soc Trop Med Hyg, 1973. **67**(5): p. 631-7.
- 127. Ménard, R., et al., *Circumsporozoite protein is required for development of malaria sporozoites in mosquitoes.* Nature, 1997. **385**(6614): p. 336-40.
- 128. Vanderberg, J. and J. Rhodin, *Differentiation of nuclear and cytoplasmic fine structure during sporogonic development of Plasmodium berghei.* J Cell Biol, 1967. **32**(3): p. C7-10.
- 129. Sinden, R.E. and K. Strong, *An ultrastructural study of the sporogonic development of Plasmodium falciparum in Anopheles gambiae.* Trans R Soc Trop Med Hyg, 1978. **72**(5): p. 477-91.

- 130. Khater, E.I., R.E. Sinden, and J.T. Dessens, *A malaria membrane skeletal protein is essential for normal morphogenesis, motility, and infectivity of sporozoites.* J Cell Biol, 2004. **167**(3): p. 425-32.
- 131. Vanderberg, J.P., *Studies on the motility of Plasmodium sporozoites.* J Protozool, 1974. **21**(4): p. 527-37.
- 132. Aly, A.S. and K. Matuschewski, *A malarial cysteine protease is necessary for Plasmodium sporozoite egress from oocysts.* J Exp Med, 2005. **202**(2): p. 225-30.
- 133. Wang, Q., H. Fujioka, and V. Nussenzweig, *Exit of Plasmodium sporozoites from oocysts is an active process that involves the circumsporozoite protein.* PLoS Pathog, 2005. **1**(1): p. e9.
- 134. Lasonder, E., et al., *Proteomic profiling of Plasmodium sporozoite maturation identifies new proteins essential for parasite development and infectivity.* PLoS Pathog, 2008. **4**(10): p. e1000195.
- 135. Sidjanski, S.P., J.P. Vanderberg, and P. Sinnis, *Anopheles stephensi salivary glands bear receptors for region I of the circumsporozoite protein of Plasmodium falciparum.* Mol Biochem Parasitol, 1997. **90**(1): p. 33-41.
- 136. Barreau, C., et al., *Plasmodium gallinaceum: sporozoite invasion of Aedes aegypti salivary glands is inhibited by anti-gland antibodies and by lectins.* Exp Parasitol, 1995. **81**(3): p. 332-43.
- do Rosario, V.E., et al., *Plasmodium falciparum: administration of anti-sporozoite antibodies during sporogony results in production of sporozoites which are not neutralized by human anti-circumsporozoite protein vaccine sera.* Trans R Soc Trop Med Hyg, 1989. **83**(3): p. 305-7.
- 138. Warburg, A., et al., *Plasmodium gallinaceum: antibodies to circumsporozoite protein prevent sporozoites from invading the salivary glands of Aedes aegypti.* Exp Parasitol, 1992. **75**(3): p. 303-7.
- 139. Wengelnik, K., et al., *The A-domain and the thrombospondin-related motif of Plasmodium falciparum TRAP are implicated in the invasion process of mosquito salivary glands.* Embo j, 1999. **18**(19): p. 5195-204.
- 140. Okulate, M.A., et al., *Identification and molecular characterization of a novel protein Saglin as a target of monoclonal antibodies affecting salivary gland infectivity of Plasmodium sporozoites.* Insect Mol Biol, 2007. **16**(6): p. 711-22.
- 141. Combe, A., et al., *TREP, a novel protein necessary for gliding motility of the malaria sporozoite.* Int J Parasitol, 2009. **39**(4): p. 489-96.
- 142. Mikolajczak, S.A., et al., *Distinct malaria parasite sporozoites reveal transcriptional changes that cause differential tissue infection competence in the mosquito vector and mammalian host.* Mol Cell Biol, 2008. **28**(20): p. 6196-207.
- 143. Steinbuechel, M. and K. Matuschewski, *Role for the Plasmodium sporozoite-specific transmembrane protein S6 in parasite motility and efficient malaria transmission.* Cell Microbiol, 2009. **11**(2): p. 279-88.
- 144. Thompson, J., et al., *Plasmodium cysteine repeat modular proteins 1-4: complex proteins with roles throughout the malaria parasite life cycle.* Cell Microbiol, 2007. **9**(6): p. 1466-80.
- 145. Kariu, T., et al., *MAEBL* is essential for malarial sporozoite infection of the mosquito salivary gland. J Exp Med, 2002. **195**(10): p. 1317-23.
- 146. Kappe, S.H., et al., *A family of chimeric erythrocyte binding proteins of malaria parasites.* Proc Natl Acad Sci U S A, 1998. **95**(3): p. 1230-5.
- 147. Singh, N., et al., *Conservation and developmental control of alternative splicing in maebl among malaria parasites.* J Mol Biol, 2004. **343**(3): p. 589-99.
- 148. Preiser, P., et al., *Antibodies against MAEBL ligand domains M1 and M2 inhibit sporozoite development in vitro.* Infect Immun, 2004. **72**(6): p. 3604-8.

- 149. Matuschewski, K., *Getting infectious: formation and maturation of Plasmodium sporozoites in the Anopheles vector.* Cell Microbiol, 2006. **8**(10): p. 1547-56.
- 150. Matuschewski, K., et al., *Infectivity-associated changes in the transcriptional repertoire of the malaria parasite sporozoite stage.* J Biol Chem, 2002. **277**(44): p. 41948-53.
- Thang, M., et al., *The Plasmodium eukaryotic initiation factor-2alpha kinase IK2 controls the latency of sporozoites in the mosquito salivary glands.* J Exp Med, 2010. **207**(7): p. 1465-74.
- 152. Aly, A.S., et al., *Targeted deletion of SAP1 abolishes the expression of infectivity factors necessary for successful malaria parasite liver infection.* Mol Microbiol, 2008. **69**(1): p. 152-63.
- 153. Kumar, K.A., et al., *Conserved protective mechanisms in radiation and genetically attenuated uis3(-) and uis4(-) Plasmodium sporozoites.* PLoS One, 2009. **4**(2): p. e4480.
- 154. Gardner, M.J., et al., *Genome sequence of the human malaria parasite Plasmodium falciparum.* Nature, 2002. **419**(6906): p. 498-511.
- 155. Steffen, R. and R.H. Behrens, *Travellers' malaria*. Parasitol Today, 1992. **8**(2): p. 61-6.
- 156. Kokwaro, G., *Ongoing challenges in the management of malaria.* Malar J, 2009. **8 Suppl 1**(Suppl 1): p. S2.
- 157. Struik, S.S. and E.M. Riley, *Does malaria suffer from lack of memory?* Immunol Rev, 2004. **201**: p. 268-90.
- 158. Singh, N., et al., *Malaria control using indoor residual spraying and larvivorous fish: a case study in Betul, central India.* Trop Med Int Health, 2006. **11**(10): p. 1512-20.
- 159. Pluess, B., et al., *Indoor residual spraying for preventing malaria*. Cochrane Database Syst Rev, 2010. **2010**(4): p. Cd006657.
- 160. Adesanmi, T.A., et al., *Diagnosis of malaria parasitemia in children using a rapid diagnostic test.* Niger J Clin Pract, 2011. **14**(2): p. 195-200.
- 161. Frean, J., et al., *Case management of malaria: diagnosis.* S Afr Med J, 2013. **103**(10 Pt 2): p. 789-93.
- 162. Howard, R.J., et al., *Secretion of a malarial histidine-rich protein (Pf HRP II) from Plasmodium falciparum-infected erythrocytes.* J Cell Biol, 1986. **103**(4): p. 1269-77.
- 163. Hoffman, S.L., et al., *Protection of humans against malaria by immunization with radiation-attenuated Plasmodium falciparum sporozoites.* J Infect Dis, 2002. **185**(8): p. 1155-64.
- 164. Girard, M.P., et al., *A review of human vaccine research and development: malaria.* Vaccine, 2007. **25**(9): p. 1567-80.
- 165. Agnandji, S.T., et al., First results of phase 3 trial of RTS,S/AS01 malaria vaccine in African children. N Engl J Med, 2011. **365**(20): p. 1863-75.
- 166. Mueller, A.K., et al., *Genetically modified Plasmodium parasites as a protective experimental malaria vaccine.* Nature, 2005. **433**(7022): p. 164-7.
- 167. Cowman, A.F., D. Berry, and J. Baum, *The cellular and molecular basis for malaria parasite invasion of the human red blood cell.* J Cell Biol, 2012. **198**(6): p. 961-71.
- 168. Malkin, E.M., et al., *Phase 1 vaccine trial of Pvs25H: a transmission blocking vaccine for Plasmodium vivax malaria.* Vaccine, 2005. **23**(24): p. 3131-8.
- 169. Templeton, T.J. and D.C. Kaslow, *Identification of additional members define a Plasmodium falciparum gene superfamily which includes Pfs48/45 and Pfs230.* Mol Biochem Parasitol, 1999. **101**(1-2): p. 223-7.
- 170. Kain, K.C., G.D. Shanks, and J.S. Keystone, *Malaria chemoprophylaxis in the age of drug resistance*. *I. Currently recommended drug regimens*. Clin Infect Dis, 2001. **33**(2): p. 226-34.
- 171. Ivanescu, B., A. Miron, and A. Corciova, *Sesquiterpene Lactones from Artemisia Genus: Biological Activities and Methods of Analysis.* J Anal Methods Chem, 2015. **2015**: p. 247685.
- 172. White, N.J., *Qinghaosu (artemisinin): the price of success.* Science, 2008. **320**(5874): p. 330-4.

- 173. Prapunwattana, P., W.J. O'Sullivan, and Y. Yuthavong, *Depression of Plasmodium falciparum dihydroorotate dehydrogenase activity in in vitro culture by tetracycline.* Mol Biochem Parasitol, 1988. **27**(2-3): p. 119-24.
- 174. Camps, M., G. Arrizabalaga, and J. Boothroyd, *An rRNA mutation identifies the apicoplast as the target for clindamycin in Toxoplasma gondii.* Mol Microbiol, 2002. **43**(5): p. 1309-18.
- 175. Carlton, J., J. Silva, and N. Hall, *The genome of model malaria parasites, and comparative genomics*. Curr Issues Mol Biol, 2005. **7**(1): p. 23-37.
- 176. Kooij, T.W., et al., *A Plasmodium whole-genome synteny map: indels and synteny breakpoints as foci for species-specific genes.* PLoS Pathog, 2005. **1**(4): p. e44.
- 177. Hall, N., et al., *A comprehensive survey of the Plasmodium life cycle by genomic, transcriptomic, and proteomic analyses.* Science, 2005. **307**(5706): p. 82-6.
- 178. Carvalho, T.G. and R. Ménard, *Manipulating the Plasmodium genome.* Curr Issues Mol Biol, 2005. **7**(1): p. 39-55.
- 179. Balu, B. and J.H. Adams, *Advancements in transfection technologies for Plasmodium*. Int J Parasitol, 2007. **37**(1): p. 1-10.
- 180. Imwong, M., et al., *Association of genetic mutations in Plasmodium vivax dhfr with resistance to sulfadoxine-pyrimethamine: geographical and clinical correlates.* Antimicrob Agents Chemother, 2001. **45**(11): p. 3122-7.
- 181. Bwijo, B., et al., *High prevalence of quintuple mutant dhps/dhfr genes in Plasmodium falciparum infections seven years after introduction of sulfadoxine and pyrimethamine as first line treatment in Malawi.* Acta Trop, 2003. **85**(3): p. 363-73.
- 182. Ashley, E.A., et al., *Spread of artemisinin resistance in Plasmodium falciparum malaria.* N Engl J Med, 2014. **371**(5): p. 411-23.
- 183. Thomson, R., et al., *Prevalence of Plasmodium falciparum lacking histidine-rich proteins 2 and 3: a systematic review.* Bull World Health Organ, 2020. **98**(8): p. 558-568f.
- 184. Hien, A.S., et al., Evidence that agricultural use of pesticides selects pyrethroid resistance within Anopheles gambiae s.l. populations from cotton growing areas in Burkina Faso, West Africa. PLoS One, 2017. **12**(3): p. e0173098.
- 185. Lourenço, C., et al., *Strengthening surveillance systems for malaria elimination: a global landscaping of system performance, 2015-2017.* Malar J. 2019. **18**(1): p. 315.
- 186. Yang, W.Z. and X.N. Zhou, [New challenges of malaria elimination in China]. Zhonghua Yu Fang Yi Xue Za Zhi, 2016. **50**(4): p. 289-91.
- 187. Coppens, I. and K.A. Joiner, *Host but not parasite cholesterol controls Toxoplasma cell entry by modulating organelle discharge.* Mol Biol Cell, 2003. **14**(9): p. 3804-20.
- 188. Foussard, F., M.A. Leriche, and J.F. Dubremetz, *Characterization of the lipid content of Toxoplasma gondii rhoptries.* Parasitology, 1991. **102 Pt 3**: p. 367-70.
- 189. Dluzewski, A.R., et al., *Origins of the parasitophorous vacuole membrane of the malaria parasite: surface area of the parasitized red cell.* Eur J Cell Biol, 1995. **68**(4): p. 446-9.
- 190. Kats, L.M., et al., *Plasmodium rhoptries: how things went pear-shaped.* Trends Parasitol, 2006. **22**(6): p. 269-76.
- 191. Shaw, M.K. and L.G. Tilney, *How individual cells develop from a syncytium: merogony in Theileria parva (Apicomplexa).* J Cell Sci, 1992. **101 (Pt 1)**: p. 109-23.
- 192. Tetley, L., et al., *Ultrastructural analysis of the sporozoite of Cryptosporidium parvum.* Microbiology (Reading), 1998. **144 (Pt 12)**: p. 3249-3255.
- 193. Boothroyd, J.C. and J.F. Dubremetz, *Kiss and spit: the dual roles of Toxoplasma rhoptries.* Nat Rev Microbiol, 2008. **6**(1): p. 79-88.
- 194. Deponte, M., et al., *Wherever I may roam: protein and membrane trafficking in P. falciparum-infected red blood cells.* Mol Biochem Parasitol, 2012. **186**(2): p. 95-116.

- 195. Bannister, L.H., et al., *Ultrastructure of rhoptry development in Plasmodium falciparum erythrocytic schizonts.* Parasitology, 2000. **121 (Pt 3)**: p. 273-87.
- 196. Counihan, N.A., et al., *Plasmodium rhoptry proteins: why order is important.* Trends Parasitol, 2013. **29**(5): p. 228-36.
- 197. Hallée, S., et al., Evidence that the Plasmodium falciparum Protein Sortilin Potentially Acts as an Escorter for the Trafficking of the Rhoptry-Associated Membrane Antigen to the Rhoptries. mSphere, 2018. **3**(1).
- 198. Richard, D., et al., *Identification of rhoptry trafficking determinants and evidence for a novel sorting mechanism in the malaria parasite Plasmodium falciparum.* PLoS Pathog, 2009. **5**(3): p. e1000328.
- 199. Venugopal, K., et al., *Dual role of the Toxoplasma gondii clathrin adaptor AP1 in the sorting of rhoptry and microneme proteins and in parasite division.* PLoS Pathog, 2017. **13**(4): p. e1006331.
- 200. Nasamu, A.S., et al., *Plasmepsins IX and X are essential and druggable mediators of malaria parasite egress and invasion.* Science, 2017. **358**(6362): p. 518-522.
- 201. Pino, P., et al., *A multistage antimalarial targets the plasmepsins IX and X essential for invasion and egress.* Science, 2017. **358**(6362): p. 522-528.
- 202. Breinich, M.S., et al., *A dynamin is required for the biogenesis of secretory organelles in Toxoplasma gondii.* Curr Biol, 2009. **19**(4): p. 277-86.
- 203. Galinski, M.R., et al., *A reticulocyte-binding protein complex of Plasmodium vivax merozoites.* Cell, 1992. **69**(7): p. 1213-26.
- 204. Kerr, J.S. and G.J. Wright, *Avidity-based extracellular interaction screening (AVEXIS) for the scalable detection of low-affinity extracellular receptor-ligand interactions.* J Vis Exp, 2012(61): p. e3881.
- 205. Douglas, A.D., et al., *The blood-stage malaria antigen PfRH5 is susceptible to vaccine-inducible cross-strain neutralizing antibody.* Nat Commun, 2011. **2**: p. 601.
- 206. Baum, J., et al., *Reticulocyte-binding protein homologue 5 an essential adhesin involved in invasion of human erythrocytes by Plasmodium falciparum.* Int J Parasitol, 2009. **39**(3): p. 371-80.
- 207. Harvey, K.L., P.R. Gilson, and B.S. Crabb, *A model for the progression of receptor-ligand interactions during erythrocyte invasion by Plasmodium falciparum.* Int J Parasitol, 2012. **42**(6): p. 567-73.
- 208. Boyle, M.J., et al., *Isolation of viable Plasmodium falciparum merozoites to define erythrocyte invasion events and advance vaccine and drug development.* Proc Natl Acad Sci U S A, 2010. **107**(32): p. 14378-83.
- 209. Zuccala, E.S., et al., Subcompartmentalisation of proteins in the rhoptries correlates with ordered events of erythrocyte invasion by the blood stage malaria parasite. PLoS One, 2012. 7(9): p. e46160.
- 210. Ishino, T., et al., *Rhoptry neck protein 2 expressed in Plasmodium sporozoites plays a crucial role during invasion of mosquito salivary glands.* Cell Microbiol, 2019. **21**(1): p. e12964.
- 211. Besteiro, S., J.F. Dubremetz, and M. Lebrun, *The moving junction of apicomplexan parasites: a key structure for invasion.* Cell Microbiol, 2011. **13**(6): p. 797-805.
- 212. Tyler, J.S. and J.C. Boothroyd, *The C-terminus of Toxoplasma RON2 provides the crucial link between AMA1 and the host-associated invasion complex.* PLoS Pathog, 2011. **7**(2): p. e1001282.
- 213. Ito, D., et al., *Identification of a Novel RAMA/RON3 Rhoptry Protein Complex in Plasmodium falciparum Merozoites.* Front Cell Infect Microbiol, 2020. **10**: p. 605367.

- 214. Low, L.M., et al., *Deletion of Plasmodium falciparum Protein RON3 Affects the Functional Translocation of Exported Proteins and Glucose Uptake.* mBio, 2019. **10**(4).
- 215. Nozaki, M., et al., *Detection of the Rhoptry Neck Protein Complex in Plasmodium Sporozoites and Its Contribution to Sporozoite Invasion of Salivary Glands.* mSphere, 2020. **5**(4).
- 216. Baba, M., et al., *Rhoptry neck protein 4 plays important roles during Plasmodium sporozoite infection of the mammalian liver.* mSphere, 2023. **8**(4): p. e0058722.
- 217. Fernandes, P., et al., *The AMA1-RON complex drives Plasmodium sporozoite invasion in the mosquito and mammalian hosts.* PLoS Pathog, 2022. **18**(6): p. e1010643.
- 218. Tartarelli, I., et al., *During host cell traversal and cell-to-cell passage, Toxoplasma gondii sporozoites inhabit the parasitophorous vacuole and posteriorly release dense granule protein-associated membranous trails.* Int J Parasitol, 2020. **50**(13): p. 1099-1115.
- 219. Hossain, M.E., S. Dhawan, and A. Mohmmed, *The cysteine-rich regions of Plasmodium falciparum RON2 bind with host erythrocyte and AMA1 during merozoite invasion.* Parasitol Res, 2012. **110**(5): p. 1711-21.
- 220. Nozaki, M., et al., *Detection of the Rhoptry Neck Protein Complex in Plasmodium Sporozoites and Its Contribution to Sporozoite Invasion of Salivary Glands.* 2020. **5**(4).
- 221. Bantuchai, S., et al., *Rhoptry neck protein 11 has crucial roles during malaria parasite sporozoite invasion of salivary glands and hepatocytes.* Int J Parasitol, 2019. **49**(9): p. 725-735.
- 222. Anaguano, D., et al., *Plasmodium RON11 triggers biogenesis of the merozoite rhoptry pair and is essential for erythrocyte invasion.* bioRxiv, 2024.
- 223. Knuepfer, E., et al., *RON12*, a novel Plasmodium-specific rhoptry neck protein important for parasite proliferation. Cell Microbiol, 2014. **16**(5): p. 657-72.
- Proellocks, N.I., et al., *Characterisation of PfRON6, a Plasmodium falciparum rhoptry neck protein with a novel cysteine-rich domain.* International Journal for Parasitology, 2009. **39**(6): p. 683-692.
- 225. Segireddy, R.R., et al., A screen for Plasmodium falciparum sporozoite surface protein binding to human hepatocyte surface receptors identifies novel host-pathogen interactions. Malar J, 2024. **23**(1): p. 151.
- 226. Beetsma, A.L., et al., *Plasmodium berghei ANKA: purification of large numbers of infectious gametocytes.* Exp Parasitol, 1998. **88**(1): p. 69-72.
- 227. Singh, D., et al., A conserved Plasmodium structural integrity maintenance protein (SIMP) is associated with sporozoite membrane and is essential for maintaining shape and infectivity. 2022. **117**(6): p. 1324-1339.
- 228. Janse, C.J., J. Ramesar, and A.P. Waters, *High-efficiency transfection and drug selection of genetically transformed blood stages of the rodent malaria parasite Plasmodium berghei.* Nature Protocols, 2006. **1**(1): p. 346-356.
- 229. Rénia, L., et al., *Malaria sporozoite penetration. A new approach by double staining.* J Immunol Methods, 1988. **112**(2): p. 201-5.
- 230. Chomczynski, P. and N. Sacchi, *Single-step method of RNA isolation by acid guanidinium thiocyanate-phenol-chloroform extraction*. Anal Biochem, 1987. **162**(1): p. 156-9.
- 231. Bentley, H.R., R.G. Booth, and et al., *Action of nitrogen trichloride on proteins; production of toxic derivative.* Nature, 1948. **161**(4082): p. 126.
- 232. Meis, J.F., et al., *Transformation of sporozoites of Plasmodium berghei into exoerythrocytic forms in the liver of its mammalian host.* Cell Tissue Res, 1985. **241**(2): p. 353-60.
- 233. Stewart, M.J. and J.P. Vanderberg, *Malaria sporozoites release circumsporozoite protein from their apical end and translocate it along their surface.* J Protozool, 1991. **38**(4): p. 411-21.

- 234. Mishra, S., R.S. Nussenzweig, and V. Nussenzweig, *Antibodies to Plasmodium circumsporozoite protein (CSP) inhibit sporozoite's cell traversal activity.* J Immunol Methods, 2012. **377**(1-2): p. 47-52.
- 235. Arredondo, S.A., et al., *Secretory Organelle Function in the Plasmodium Sporozoite.* Trends Parasitol, 2021. **37**(7): p. 651-663.
- 236. Lamarque, M., et al., *The RON2-AMA1 interaction is a critical step in moving junction-dependent invasion by apicomplexan parasites.* PLoS Pathog, 2011. **7**(2): p. e1001276.
- 237. Sam-Yellowe, T.Y., et al., *Proteome analysis of rhoptry-enriched fractions isolated from Plasmodium merozoites.* J Proteome Res, 2004. **3**(5): p. 995-1001.
- 238. Briquet, S., et al., *Identification of Plasmodium falciparum nuclear proteins by mass spectrometry and proposed protein annotation*. PLoS One, 2018. **13**(10): p. e0205596.
- 239. Santos, J.M., et al., *Red Blood Cell Invasion by the Malaria Parasite Is Coordinated by the PfAP2-I Transcription Factor.* Cell Host Microbe, 2017. **21**(6): p. 731-741.e10.
- 240. Matz, J.M. and K. Matuschewski, *An in silico down-scaling approach uncovers novel constituents of the Plasmodium-containing vacuole.* Sci Rep, 2018. **8**(1): p. 14055.
- 241. Liffner, B., et al., *The Ins and Outs of Plasmodium Rhoptries, Focusing on the Cytosolic Side.* Trends Parasitol, 2021. **37**(7): p. 638-650.
- 242. Srivastava, P.N., P. Paul, and S. Mishra, *Protein O-Fucosyltransferase Is Required for the Efficient Invasion of Hepatocytes by Plasmodium berghei Sporozoites.* ACS Infect Dis, 2024. **10**(4): p. 1116-1125.
- 243. Wang, H., et al., Analysis of spleen histopathology, splenocyte composition and haematological parameters in four strains of mice infected with Plasmodium berghei K173. Malar J, 2021. **20**(1): p. 249.
- 244. Tokunaga, N., et al., *Expression and Localization Profiles of Rhoptry Proteins in Plasmodium berghei Sporozoites.* Frontiers in Cellular and Infection Microbiology, 2019. **9**.
- 245. Richard, D., et al., *Interaction between Plasmodium falciparum Apical Membrane Antigen 1 and the Rhoptry Neck Protein Complex Defines a Key Step in the Erythrocyte Invasion Process of Malaria Parasites*. Journal of Biological Chemistry, 2010. **285**(19): p. 14815-14822.
- 246. Siau, A., et al., Temperature shift and host cell contact up-regulate sporozoite expression of Plasmodium falciparum genes involved in hepatocyte infection. PLoS Pathog, 2008. **4**(8): p. e1000121.
- 247. Bozdech, Z., et al., *The transcriptome of the intraerythrocytic developmental cycle of Plasmodium falciparum.* PLoS Biol, 2003. **1**(1): p. E5.
- 248. Bantuchai, S., et al., *Rhoptry neck protein 11 has crucial roles during malaria parasite sporozoite invasion of salivary glands and hepatocytes.* International Journal for Parasitology, 2019. **49**(9): p. 725-735.
- 249. Risco-Castillo, V., et al., *CD81 is required for rhoptry discharge during host cell invasion byPlasmodium yoeliisporozoites.* Cellular Microbiology, 2014. **16**(10): p. 1533-1548.
- 250. Pei, Y., et al., *Plasmodium yoeliiinhibitor of cysteine proteases is exported to exomembrane structures and interacts with yoelipain-2 during asexual blood-stage development.* Cellular Microbiology, 2013. **15**(9): p. 1508-1526.
- 251. Paul, G., et al., *Protein-protein interaction studies reveal thePlasmodium falciparummerozoite surface protein-1 region involved in a complex formation that binds to human erythrocytes.* Biochemical Journal, 2018. **475**(6): p. 1197-1209.
- 252. Lin, C.S., et al., *The merozoite surface protein 1 complex is a platform for binding to human erythrocytes by Plasmodium falciparum.* J Biol Chem, 2014. **289**(37): p. 25655-69.

- 253. Das, S., et al., *Processing of Plasmodium falciparum Merozoite Surface Protein MSP1 Activates a Spectrin-Binding Function Enabling Parasite Egress from RBCs.* Cell Host Microbe, 2015. **18**(4): p. 433-44.
- 254. Ito, D., et al., Roles of the RON3 C-terminal fragment in erythrocyte invasion and blood-stage parasite proliferation in Plasmodium falciparum. Frontiers in Cellular and Infection Microbiology, 2023. 13.
- 255. Segireddy, R.R., et al., A screen for Plasmodium falciparum sporozoite surface protein binding to human hepatocyte surface receptors identifies novel host–pathogen interactions. Malaria Journal, 2024. **23**(1).
- 256. Bedu-Addo, G. and I. Bates, *Causes of massive tropical splenomegaly in Ghana.* The Lancet, 2002. **360**(9331): p. 449-454.
- 257. Crane, G., Recent studies of hyperreactive malarious splenomegaly (tropical splenomegaly syndrome) in Papua New Guinea. P N G Med J, 1986. **29**(1): p. 35-40.
- 258. Leoni, S., et al., *The hyper-reactive malarial splenomegaly: a systematic review of the literature.* Malaria Journal, 2015. **14**(1).
- 259. Skorokhod, O.A., et al., *Hemozoin (Malarial Pigment) Inhibits Differentiation and Maturation of Human Monocyte-Derived Dendritic Cells: A Peroxisome Proliferator-Activated Receptor-γ-Mediated Effect.* The Journal of Immunology, 2004. **173**(6): p. 4066-4074.
- 260. Schwarzer, E., et al., *Phagocytosis of the malarial pigment, hemozoin, impairs expression of major histocompatibility complex class II antigen, CD54, and CD11c in human monocytes.* Infect Immun, 1998. **66**(4): p. 1601-6.
- 261. Schwarzer, E., et al., *Impairment of macrophage functions after ingestion of Plasmodium falciparum-infected erythrocytes or isolated malarial pigment.* J Exp Med, 1992. **176**(4): p. 1033-41.
- 262. Fierro, M.A., et al., *Knock-sideways by inducible ER retrieval enables a unique approach for studying Plasmodium-secreted proteins.* Proceedings of the National Academy of Sciences, 2023. **120**(33).

Publications

RESEARCH ARTICLE

WILEY

A conserved Plasmodium structural integrity maintenance protein (SIMP) is associated with sporozoite membrane and is essential for maintaining shape and infectivity

Dipti Singh¹ | Smita Patri¹ | Veeda Narahari¹ | Rameswara R. Segireddy¹ | Sandeep Dey¹ | Archi Saurabh² | Macha Vijay³ | N. Prakash Prabhu² | Anand Srivastava³ | Surendra Kumar Kolli o¹ | Kota Arun Kumar o¹

Correspondence

Surendra Kumar Kolli and Kota Arun Kumar, Department of Animal Biology, School of Life Sciences, University of Hyderabad, Gachibowli, Hyderabad, Telangana - 500046, India. Email: skk@uohyd.ac.in and kaksl@uohyd. ac.in

Funding information

Department of Biotechnology, Ministry of Science and Technology, India, Grant/Award Number: BT/PR2495/ BRB/10/950/2011

Abstract

Plasmodium sporozoites are extracellular forms introduced during mosquito bite that selectively invade mammalian hepatocytes. Sporozoites are delimited by a cell membrane that is linked to the underlying acto-myosin molecular motor. While membrane proteins with roles in motility and invasion have been well studied, very little is known about proteins that maintain the sporozoite shape. We demonstrate that in Plasmodium berghei (Pb) a conserved hypothetical gene, PBANKA 1422900 specifies sporozoite structural integrity maintenance protein (SIMP) required for maintaining the sporozoite shape and motility. Sporozoites lacking SIMP exhibited loss of regular shape, extensive membrane blebbing at multiple foci, and membrane detachment. The mutant sporozoites failed to infect hepatocytes, though the altered shape did not affect the organization of cytoskeleton or inner membrane complex (IMC). Interestingly, the components of IMC failed to extend under the membrane blebs likely suggesting that SIMP may assist in anchoring the membrane to IMC. Endogenous C-terminal HA tagging localized SIMP to membrane and revealed the C-terminus of the protein to be extracellular. Since SIMP is highly conserved among Plasmodium species, these findings have important implications for utilizing it as a novel sporozoite-specific vaccine candidate.

KEYWORDS

gliding motility, inner membrane complex, Plasmodium, sporozoites

INTRODUCTION

The life cycle of *Plasmodium* in mammalian host starts with the bite of a female Anopheles mosquito that delivers sporozoites in the skin of the vertebrate host (Gueirard et al., 2010). The sporozoites make their way to the liver, where they transform into exoerythrocytic forms. Following exoerythrocytic schizogony, first-generation merozoites are packaged in membrane-bound structures called merosomes (Sturm et al., 2006) that are extruded into sinusoids. Rupture of merosome releases parasites into the bloodstream, which initiates an erythrocytic cycle. In RBC, the parasites replicate asexually and go through a series of transformations resulting in rings, trophozoites, schizonts, and gametocytes.

Gametocytes are sexual forms and the terminal stages of the parasite in the mammalian host. These forms enter gut of a female Anopheles mosquito during a blood meal. Sexual reproduction occurs in the lumen of gut, resulting in a zygote that transforms into motile ookinete. The ookinete breaches midgut epithelium and settles on

¹Department of Animal Biology, School of Life Sciences, University of Hyderabad, Hvderabad, India

²Department of Biotechnology & Bioinformatics, School of Life Sciences, University of Hyderabad, Hyderabad, India

³National Institute of Animal Biotechnology, Hyderabad, India



Functional insights into Plasmodium berghei rhoptry associated protein RON6(PbRON6)

by Veeda Narahari

Submission date: 08-Oct-2024 12:20PM (UTC+0530)

Submission ID: 2478869009

File name: Veeda Narahari.docx (439.76K)

Word count: 30532

Character count: 173851

Functional insights into Plasmodium berghei rhoptry associated protein RON6(PbRON6)

ass	ociated pr	otein RON6(PbR	ON6)		
ORIGIN	NALITY REPORT				
1 SIMIL	1% ARITY INDEX	8% INTERNET SOURCES	8% PUBLICATIONS	3% STUDENT PAPE	RS
PRIMA	RY SOURCES				
1	dspace. Internet Sour	uohyd.ac.in			2%
2	Submitt Hyderal Student Pape		of Hyderaba	ad,	2%
3	Ramesv Structur associat essentia	ngh, Smita Patri, vara R. Segiredd ral Integrity Main red with sporozo al for maintainin rular Microbiolog	ly et al. " A Contenance Pro Dite membraing shape and	onserved otein () is ne and is infectivity	1 %
4	Babu S. "Plasmo genes- F for the o	ogiri, Rameswar Mastan, Dipti Si dium berghei sp PbS10 and PbS2 development of Molecular and E	ingh et al. porozoite spe 3/SSP3 are re exo-erythroc	ecific equired	Animone sciences Life Sciences Thyderabad Niversity Gachibo Telangana